ISSN Print 0970 - 3268
ISSN Online 2582 - 2020

The Journal of the Indian Association of Sedimentologists

The Indian Association of Sedimentologists

Volume 40 No. 1 Jan - June, 2023

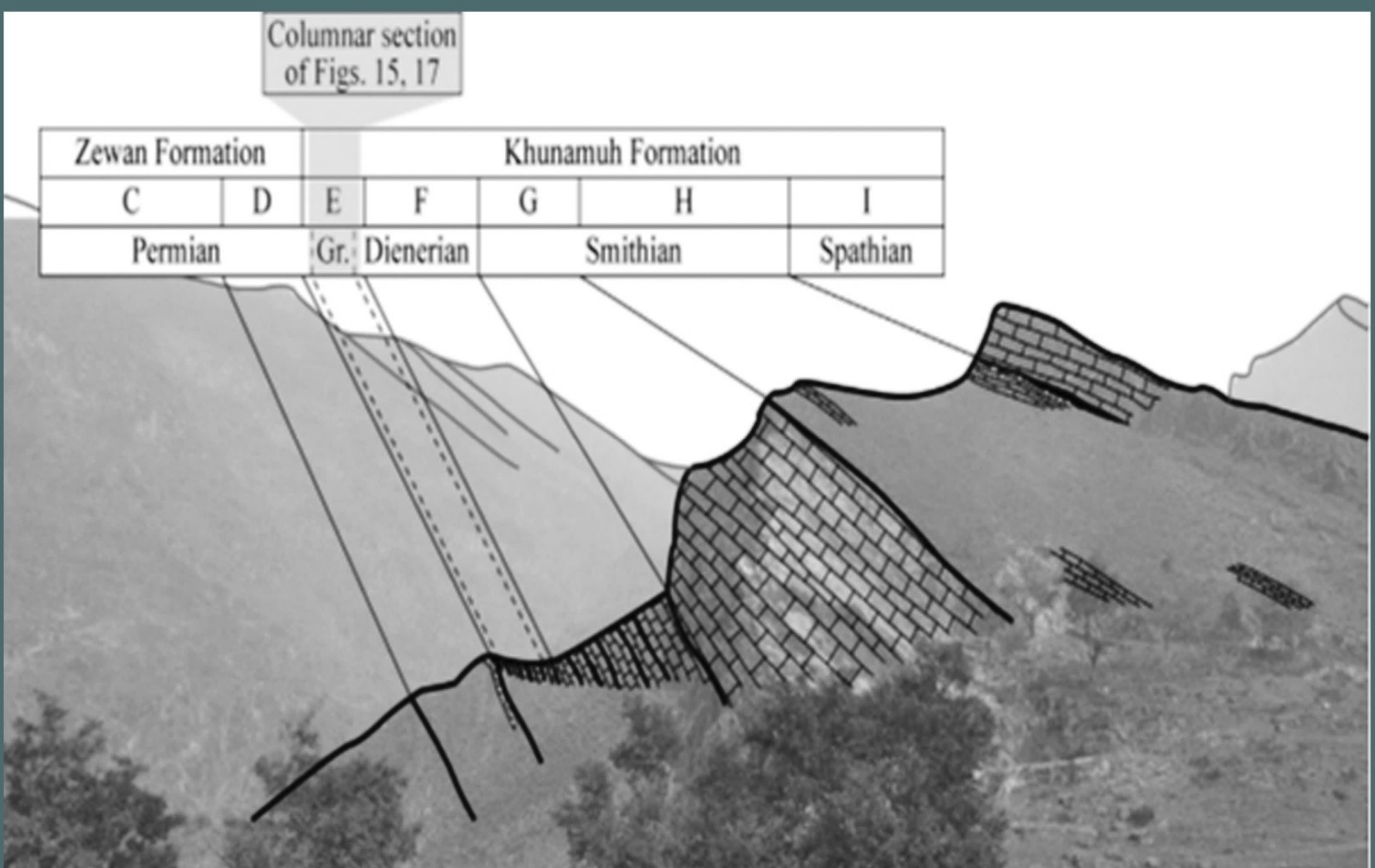

Late Permian-Triassic boundary section at Guryul Ravine

JOURNAL INDIAN ASSOCIATION OF SEDIMENTOLOGISTS ISSN NO 2582 – 2020
Vol. 40, Issue 1, 2023, pp. 1-4
DOI: https://doi.org/10.51710/jias.v40iI.272

Indian Association of Sedimentologists

http://www.indiansedimentologists.com

BACKGROUND

The idea to constitute a forum Indian Association of Sedimentologists (IAS) was floated in the valedictory session of a conference hosted by Delhi University, Delhi in 1975, for providing an opportunity to sedimentologists of the country to meet, discuss and extend ideas of mutual interest. The idea was appreciated and got support from veteran geologists and academicians. Soon after, in 1976, the Indian Association of Sedimentologists was formed and duly registered with its headquarters at the Department of Geology, Aligarh Muslim University, Aligarh in recognition of leading research carried out in the Department in the field of sedimentology.

The Indian Association of Sedimentologists is by now a recognized scientific forum with highly qualified and experienced sedimentologists as its Fellows and Life Members representing Universities, National and state owned geological and geophysical Institutes and organizations from all over the country. Also, on the rolls of IAS are Fellows and Life Members from Bangladesh, Canada, USA, Mexico and England.

Indeed, the Association could not have achieved its present high status without inspiring and selfless support and contributions from its members at large and founding members in particular, especially Prof. M. N. Mehrotra, Prof. V. K. Srivastava, Prof. V. K. Verma, Shri S. M. Mathur, Shri V. Raiverman, Prof. Vinay Jhingran, Prof. S. M. Casshyap, Prof. S. K. Tandon and Prof. B. D. Bhardwaj.

The Association has the honour to have a galaxy of eminent geoscientists as it's Presidents as below -

1. Prof. A. G. Jhingran	1976 - 1979
2. Prof. M. N. Viswanathan	1980 - 1981
3. Prof. M. N. Mahrotra	1982 - 1983
4. Prof. V. K. Srivastava	1984 - 1986
5. Prof. V. K. Verma	1987 - 1990
6. Prof. S. M. Mathur	1991 - 1992
7. Prof. S. M. Casshyap	1993 - 2004
8. Prof. S. K. Tandon	2005 - 2012
9. Prof. G. N. Nayak	2013 - till date

OBJECTIVES

The prime objective of the Association is to promote recent advances in sedimentary petrology, sedimentology, applied sedimentation, basin modelling and related disciplines namely, remote sensing, hydrogeology, society and environment. Also, it provides a forum for the advancement of research and development in sedimentology and related disciplines of Geology. An equally important objective is to encourage interactions among the sedimentologists at the level of Universities, National Institutes and exploration companies of India engaged in the study of sedimentary basins regarding their evolution, origin and resource potential.

CONVENTIONS & SEMINARS

Ever since the first convention of the Indian Association of Sedimentologists held at Aligarh Muslim University, Aligarh in the year 1976, the Association has been organizing National Conventions regularly. Since 1992, the convention is a regular annual activity being organized at different centers of the country in response to the invitations it receives from hosting institutions. It has so far organized 38 Conventions at different centers of sedimentology as listed below –

1. Convention, 1976, Aligarh Muslim University, Aligarh
2. Convention, 1979, University of Mysore, Mysore
3. Convention, 1982, Banaras Hindu University, Varanasi
4. Convention, 1984, Aligarh Muslim University, Aligarh
5. Convention, 1985, Osmania University, Hyderabad
6. Convention, 1986, Wadia Institute of Himalayan Geology, Dehradun

7. & 8 Conventions, 1990, Delhi University, Delhi

9 Convention, 1992, Pune University, Pune

10 Convention, 1993, Karnataka University, Dharwar

11 Convention, 1994 (held in Jan. 1995), University of Roorkee, Roorkee

12 Convention, 1995, Goa University, Panaji

13 Convention, 1996, Banaras Hindu University, Varanasi

14 Convention, 1997, University of Madras, Chennai

15 Convention, 1998, Gauhati University, Gauhati

16 Convention, 1999, University of Jammu, Jammu

17 Convention, 2000, Cochin University of Science and Technology, Kochi

18 Convention, 2001, Aligarh Muslim University, Aligarh

19 Convention, 2002, Andhra University, Visakhapatnam

20 Convention, 2003, H. N. B. Garhwal University, Srinagar, Garhwal

21 Convention, 2004, Annamalai University, Annamalai Nagar, TN

22 Convention, 2005, Wadia Institute of Himalayan Geology, Dehradun

23 Convention, 2006, Anna University, Chennai

24 Convention, 2007, Aligarh Muslim University, Aligarh

25 Convention, 2008, M. S. University, Vadodra

26 Convention, 2009, Andhra University, Visakhapatnam

27 Convention, 2010, Jammu, University, Jammu

28 Convention, 2011, JNU, New Delhi

29 Convention, 2012, Pondicherry University, Puducherry

30 Convention, 2013, Manipur University, Imphal, Manipur

31 Convention, 2014, University of Pune, Pune

32 Convention, 2015, Annamalai University, Annamalai Nagar, TN

33 Convention, 2016, Banaras Hindu University, Varanasi

34. Convention 2017, Amravati University, Amravati

35. Convention 2018, Saugar University, Sagar, MP

36. Convention 2019, AMD Hyderabad (no convention was held in 2020 and 2021 due to Covid-19 pandamic)

37. Convention, 2022, Jammu University, Jammu

38. Convention 2022, Delhi University, Delhi

JOURNAL

To propagate recent advances in sedimentology the Association undertook the publication of the “Journal of the Indian Association of Sedimentologists”. The papers presented at the Annual Convention or submitted directly are selected for publication after proper and critical scrutiny by the Editor and his team of expert reviewers. The journal was revamped and regularized under the expert’s guidance and patronage of Shri. S. M. Mathur as editor (1990-1997). It progressed steadily both in quality and regularity under the command of Prof. Vinay Jhingran, Department of Geology, Delhi University, Delhi and later under the editor, Prof. D. Rajasekhara Reddy, Andhra University, Vishakapatnam. Volume numbers 1-34 were published in print. From volume 35, the publication of the Journal is online and is being handled by Managing editors Prof. G. M. Bhat and Dr. Bashir A. Lone, Jammu University, Jammu, who are responsible for editing and uploading on the IAS website. The papers submitted online after due scrutiny, processing and acceptance by the Editor-in-Chief(s) are published in the online Journal of the Indian Association of Sedimentologists from the year 2018. The JIAS has an editorial board with members among sedimentologists from India and abroad. The review process will involve two blind reviewers. Each volume will have two numbers and are released in June and December.

SHORT-TERM COURSES

The Association organizes other scientific/academic programmes, such as short-term courses, workshops, lectures and field and/or laboratory programmes, for the advancement of sedimentology.

YOUNG SEDIMENTOLOGIST AWARD

The association introduced the 'Young Sedimentologists Award' from the year 1995 to encourage young sedimentologists below the age of 35 years for the best paper presented under the category during the convention. The paper with the candidate as the first author and his/her research supervisor as the second author is permitted. A committee constituted will adjudge the best paper presented by the candidate/s. The award is a Life Membership of the association. Paper presented under this category has to be compulsorily submitted to JIAS for consideration for publication.

GUIDELINES AND INSTRUCTIONS TO HOST INSTITUTION ORGANISING ANNUAL CONVENTION OF IAS

The following instructions and guidelines shall be observed by the host institution organizing the annual convention of the Indian Association of Sedimentologists, as per the constitution and decision taken by the Governing Council and the General Body of IAS.

a. General

1- The inviting institution shall submit a letter of hosting the convention with the date and venue, and for providing infrastructure facilities and suitable accommodation for boarding and lodging of the delegates, duly certified by the Head of the Department and Vice-chancellor or chairman/Director of the institute.

2- The inviting institute shall designate a convener and other functionaries of the convention and do all acts pursuant to the organization and conduct of the convention in consultation with the president of the Association.

3- The convener and his colleagues in the field of sedimentology in the Institution shall enroll as fellow/Life members of IAS on payment of fees of Rs 5000/- lump sum or as decided by the coucil from time to time. They should be a member in good standing (without any pending dues).

4- The circular/invitation for attending the convention shall be mailed to all members of IAS, as per the Membership List supplied by the General Secretary (Head Quarters). They will be entitled to hold office and participate in the meeting of the General Body.

5- The IAS Logo shall be inserted in all correspondence and pre-conference material (letters, envelopes, etc.) including Abstract Volume.

6- The papers presented at the convention may be submitted online on the website for consideration for publication in the Journal of the Association.

7- The papers presented under the "Young Sedimentologists Award" category at the convention shall be compulsorily submitted online on the website for consideration for publication in the Journal of the Association.

8- The Annual convention of IAS can be clubbed / combined with any other National / International/ Seminar / Conference.

b. Finances

9- A non-life member wishing to attend the convention shall enroll himself/herself as a Sessional Member by registering at the convention on payment of prescribed registration fees.

10- The finances for holding the convention shall be generated and managed by the convening organization. The inaugural address by the president or invited speaker; the other addresses, the volume of abstracts and other convention material shall be brought out by the organizer from their own resource.

11- The convener shall remit to the IAS at least Rs. 60,000/- to meet the partial cost of publication of JIAS.

12- Amount collected by the convener of the convention in the form of Registration fees from delegates shall be utilized by the Organizing Committee for the expenditure.

13- Fee, collected at the time of convention from new life members should be necessarily remitted to the IAS.

14- The members of the Governing Council will be exempted from registration fees and if desired, the office bearers of the association will be provided travelling expenses on top priority.

c. Young Sedimentologist Award

The paper preferably shall be of single authored and the age of the presenter should be 35 years or less on July 1st of that year. However, the name of the research supervisor as the second author can be allowed. A certificate and Life Membership of IAS shall be presented to the winner. The prescribed guidelines shall be observed in the evaluation of the Young Sedimentologists Award.

PRESENT GOVERNING COUNCIL

The Governing Council with effect from 01.01.2022 for 4 years

President:
Prof. G. N. Nayak, Goa University, Goa

Past Presidents:
1. Prof. S. M. Cassyap, Delhi
2. Prof. S. K. Tandon, Bhopal, MP

Vice Presidents:
1. Prof. G. M. Bhat, Jammu University, Jammu, J&K
2. Prof. S. Banerjee, IIT Bombay, Mumbai, Maharashtra

General Secretary:
1. Prof. M.E.A. Mondal, AMU, Aligarh, UP
2. Prof. A. V. Joshi, M.S. University of Baroda, Vadodara, Gujrat

Joint Secretary:
1. Prof. Subir Sarkar, Jadavpur University, Kolkata, WB
2. Prof. B. P. Singh, BHU, Varanasi, UP

Treasurer:
Dr. Abdullah Khan, AMU, Aligarh, UP

Joint Treasurer:
Dr. S. H. Alvi, AMU, Aligarh, UP

Editor / Joint Editor:
1. Prof. R. Nagendra, Bangalore, Karnataka
2. Dr. Bashir A. Lone, Jammu, J&K

Foreign Secretary:
Prof. John S. Armstrong-Altrin, Mexico

Members with effect from 01.01.2022 for 2 years

1. Prof. M. G. Kale, S.P. Pune University, Pune, Maharashtra
2. Prof. S. K. Pandita, Jammu University, Jammu, Jammu & Kashmir
3. Prof. T. Ramkumar Annamalai University, Annamalainagar, Tamil Nadu
4. Dr. S. K. Srivastava, Nagaland University, Kohima Campus, Nagaland
5. Dr. Pramod Kumar, University of Delhi, Delhi
6. Dr. Biplab Bhattacharya, IIT Roorkee, Uttarakhand
7. Dr. Rajeev Guhey, Pt R. S. University of Raipur, Raipur, Chhattisgarh
8. Dr. Nivedita Chakravorty, Govt. College, Bankura, West Bengal
9. Dr. Pramod T. Hanamgond, GSS College, Belgaum, Karnataka.
10. Dr. Iftikhar Ahmad, AMU, Aligarh, Uttar Pradesh.

G N. Nayak
President, IAS,
Former CSIR Emeritus Scientist & Senior Professor, School of Earth, Ocean and Atmosphere Science, Goa University, Goa
gnnayak57@gmail.com

JOURNAL INDIAN ASSOCIATION OF SEDIMENTOLOGISTS ISSN NO 2582 – 2020
Vol. 40, Issue 1, 2023, pp.5-19
DOI: https://doi.org/10.51710/jias.v40iI.276

Effects of transgression on sedimentation system vis-à-vis coastal erosion on the Chandipur coast, Odisha, India

Bikas Saha[1], Pradip Samanta[2], Soumik Mukhopadhyay[3] and Patrick G. Eriksson[4]

[1]Department of Geology, Durgapur Government College, Durgapur – 713 214
[2]Department of Geology, University of North Bengal, Darjeeling, Siliguri – 734 013
[3]Department of Geological Sciences, Jadavpur University, Kolkata – 700 032
[4]Department of Geology, Pretoria University, South Africa
E-mail: sahabikas@gmail.com
ORCID: 0000-0002-1288-585X (BIKAS SAHA)

ABSTRACT

There has been a decade-long debate about global warming and its far-reaching effect on sea level rise. However, little attention has so far been given to the effects of transgression in sedimentation systems. The present paper deals with the effects of transgression on sedimentation dynamics of a meso - to micro - tidal coastal environment. The sediment characteristics, flow dynamics, current flow patterns giving rise to facies of the individual environments have been analysed in detail. Shallow vertical trenches excavated in different parts of the coastal area elucidated facies characteristics and shifting of facies in response to transgression. The temporal variation in facies gave rise to a facies model that can be used as an authenticated tool for interpreting similar ancient environments. The coastal erosion resulting from on-going transgression and other short-term causes has also been evaluated with the help of facies mapping for last ~15 years and modifications in geomorphic features along and across the coastline. The coastal erosion concomitant with anthropogenic interventions cause serious stress on biological inhabitants of coastal areas. Coastal conservation and management studies will help in protecting further degradation of coastal areas and also help to maintain the biodiversity and ecosystem.

KEY WORDS: Transgression, sedimentary facies, facies model, coastal erosion, biological crisis, coastal management

INTRODUCTION

Water covers around 71 % of the Earth's surface and total length of global coastlines is about 356,000 km. India is also surrounded by the Arabian Sea in the West, the Indian Ocean in the South and the Bay of Bengal in the East and the total coastline of India is about 7,517 km. The landward retreat of the shoreline caused by the forces of wave action, tidal currents along with human activities is termed 'coastal erosion'. Effects of coastal erosion can be witnessed from cliff areas, tidal flats, marshes and beaches. Seventy percent of global shorelines are retreating landward because of coastal erosion and as a result, it has become a global concern (Bird, 1985). Shifting of the shoreline is one of the most dynamic processes in the coastal zone that also has large environmental significance (Chen et. al., 2005). These shoreline changes, which occur over both long and short periods of time, involve hydrodynamic, geomorphic, tectonic and different climatic forces (Scott, 2005; Thom and Cowell, 2005). The combination of different factors of different intensities result in coastal erosion, among which sea level rise, frequency and intensity of coastal-area storms, and anthropogenic interventions are the major contributing factors. The shifting of shoreline towards the land, causing coastal erosion, is recognized as a very real threat because of global climate change and other anthropogenic activities that change the natural processes of beaches and coasts. Human populations are concentrated along coasts, and consequently coastal ecosystems are some of the most impacted and altered worldwide. Topography and morphology of the coastal area, the geological character of the coastal zones, climate, frequency and intensity of the waves and sediment supply in the coastal area also affect coastal erosion. For the last decade, sea level rise has become a well-discussed subject among the scientific community and also among government agencies because of coastal erosion. In addition, continuous and arbitrary coastal development, tourism development and destruction of coastal landforms also create different hazards along the coastal areas along with erosion.

Indian coasts are no exception in experiencing transgression, and several works point out the vulnerability of the Indian coastline. The southern coastal area of Tamil Nadu faces a severe threat due to rapid changes in geology and geomorphology along the coast, sea-level change, tropical cyclones and associated storm surges (Sheik Mujabar and Chandrasekhar, 2013). Coastal erosion at Sagar

Fig. 1: Location Map: Geographic details of the study area. Note that the River Buribalam confluences with the Bay of Bengal forming an estuary, the large barrier bar near the mouth of the river and a swamp developed behind the barrier bar.

Island of the Sundarban delta is a matter of concern, and has been subjected to erosion by natural processes and to a lesser extent by anthropogenic activities over a long period (Gopinath and Seralathan, 2005). The effects of sea level change and anthropogenic interventions resulted in serious threats to the survival of biological communities and their life modes throughout the eastern Indian coast (Sur et. al., 2006; Das et. al., 2014). The coastal zone of India is under increasing pressure due to rapid urbanization, tourism development, discharge of waste effluents, municipal sewage, over-exploitation of coastal resources and continued development in hazard prone areas (Barman et. al., 2015 b).

Despite critical concern about the detrimental effects of transgression none of the published work deals with the sedimentological aspect. The present work takes a holistic approach to determine the effects of sea level changes in sedimentation and concomitant erosion of coastline in response to sea level rise. The present study area gives an opportunity to investigate the sediment transport mechanism, grain size, sediment dispersal and (palaeo-) current pattern in different environments associated with meso- to microtidal sea coasts. The facies maps of the last 15 years have been utilized to compare the changes in geomorphic relief features and shifting of coast lines through erosion. Shallow trenches, not exceeding 2 m, have been excavated to record the temporal shift of (palaeo-) environments in response to sea level rise giving an opportunity to understand the facies model of a meso- to microtidal coastline (cf. Walker, 1984). The on-going transgression in combination with others factors resulting in coastal erosion can be determined from geomorphic alterations along and across the coastline. The resulting coastal erosion causes a severe crisis for many organisms to thrive in altered ecological niches.

STUDY AREA

The present study area is situated near the confluence of the River Buribalam with the Bay of Bengal in the eastern coast of Chandipur, Balasore district of Odissa, India representing a stretch of coastal plain of around 4 km length (Latitude: 21.4399°N, Longitude:87.0149° E) (Fig. 1). The Chandipur coast is characterized by a very low-energy environment with semi-diurnal tidal cycle of mean tidal range varying between 4.89 m (equinoctial, spring) and 1.87 m (equinoctial, neap) (Sarkar et. al., 1991), and with seasonal storm surges never exceeding 1 m (Mukherjee et. al., 1987). The micro- to mesotidal coast trends in a northeast – southwest direction and documents a wide variety of sedimentary environments within the studied stretch. The study area holds a vast, gently dipping (<2° dip) tidal flat (almost 3.8 km wide) with a narrow beach on the landward side (40 – 140 m in width) (Sarkar et al, 1991; Chakrabarti, 2005). Towards the north-eastern margin, the River Buribalam formed an estuary at the confluence with the sea (Fig. 1). The boundary between the estuary and the tidal flat is demarcated by development of a huge spit-transformed barrier bar, resulting in the formation of a calm and quiet swampy environment on the landward side (Fig. 1). The sediments are mainly supplied by the River Buribalam and get dispersed by the marine processes forming a concentration of barrier bars near the confluence; however, several minor shore-parallel bars are also dispersed along the vast tidal flat. These barrier bars eventually get merged with the aeolian dune field along the coastline, which is migrating over the tidal flat. The minor barrier bars on the tidal flat produce local swamps on the landward side which promote a patchy calm and quiet environment where mud can settle. The few tidal channels traversing the tidal flat are the conduits for river water to enter into the tidal flat and to drain from it.

METHODS AND MATERIALS

In the present work, field study received the most attention. Equipment used was mostly inexpensive including chisels, measuring tape, shovels, clinometers, Brunton compass, Abni level, camera, GPS etc. Measurement and documentation of sedimentary features have been performed, encompassing bed thickness, mudball diameter and orientation, burrow size, depth and inclination, ripples amplitude and wave length, as well as (palaeo-) current direction. Recording also focused on patterns of sedimentary structures in detail and their mutual relationships. Shallow trenches have been excavated to determine the sedimentary structures that characterized each facies, in cross section. These trenches at different parts of the coastal area allowed the construction of vertical logs for documenting the facies characteristics and temporal facies transitions. Field data were, however, analysed and interpreted mostly in the laboratory.

FACIES ANALYSIS

The facies classification of the study area is done on the basis of lithology and sedimentary structures, both on bed surfaces as well as in transverse section, with the aim to characterize each environment.

Beach Facies

The beach (Fig. 2 A) at the Chandipur study site is confined between the tidal flat and coast line with sharp contact on the seaward side and erosional contact with the aeolian dune field on the landward side, respectively. The beach in Chandipur is not a true beach, but formed at the top of large barrier bars due to erosion. The beach, which widens towards the mouth of the river Buribalam, is divisible into two sub-facies namely back-shore and fore-shore.

Fore-Shore Subfacies

This subfacies occurs on the seaward side of the beach bordering the tidal flat (Fig. 2 A). The

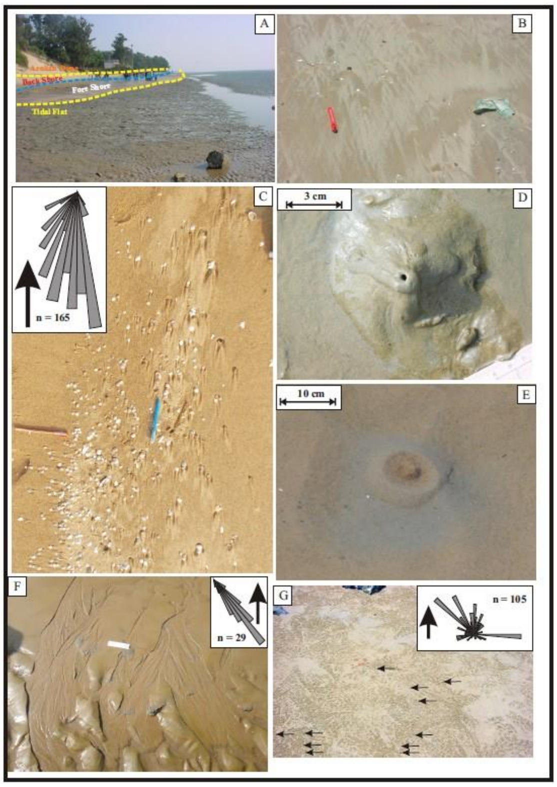

Fig. 2: Occurrence of different environmental zones (marked by dotted lines): Tidal flat on the seaward side followed by beach that is divided into Foreshore and backshore from seaward to landward side respectively and aeolian dune field further landward (A). Bed surface features within foreshore facies: rhombic ripples (B) Current crescent forming around coarser particles. Note the current directions are towards sea (C) Mud volcano (D), Sand volcano (E), Rill Marks. Note seaward current direction shown by palaeocurrent roses (F), numerous Crab Burrows. Note seaward inclination of the burrows shown by palaeocurrent roses (G).

surface morphology is generally planar, sediment is fine grained, sand sized with the occurrence of shells and shell fragments gradually increasing upslope. The sediment is highly compact and firm. The shale content is high and it is highest along the high water marks. The more or less planar surface is interrupted with minute and closely spaced ridges, recognised as current lineation and showing two divergent sets forming rhombic ripples (Fig. 2 B). There are also current crescents (Fig. 2 C) around coarser particles, oriented at high angles to the shore line and the crescents generally open in the seaward direction. The bed surface in the foreshore facies additionally contains sand and mud volcanos, rill marks and hermit crab burrows (Figs. 2 D, E, F and G). The burrows on the fore-shore are very small in diameter (1 – 2 mm) and of relatively shallow depth (4 – 5 mm) (Fig. 3 A). The burrow diameter generally increases away from the shore and the inclinations

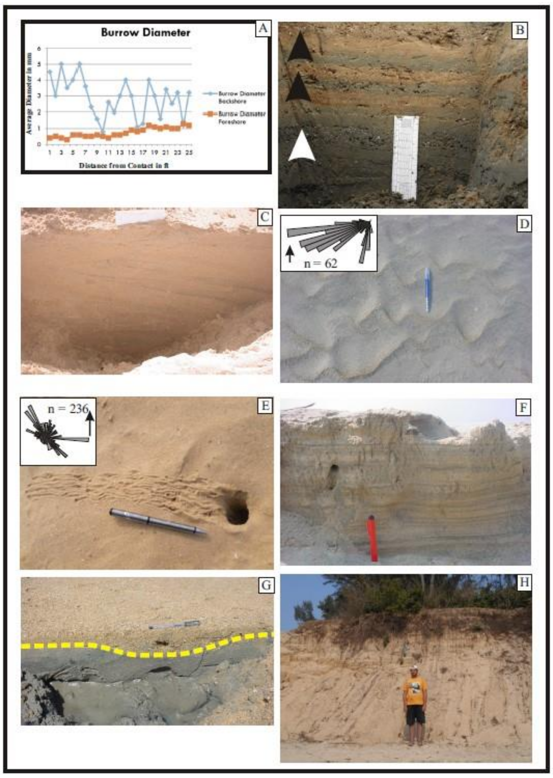

Fig. 3: Bi-variant plot showing differences in average burrow diameter against landward distance from the contact of foreshore and backshore facies. Average burrow diameter measured by constructing grids (1m × 1m), average of 4 to 5 grids for each reference point. Note that the average diameter is higher for backshore compared to foreshore. Also note that the average diameter gradually increases and decreases with distance for foreshore and backshore respectively (A) Shallow trench within foreshore showing vertical lithological constituents: alternations of planar laminated silt-mud and fine sand layer with frequent shell-hash layers (marked by arrows) (B) Low angle cross sets where set boundaries are defined by heavy minerals dipping seaward (C) Bed surface feature within backshore facies: Aeolian ripples. Note the current direction, shown by palaeocurrent roses, and coarse grain concentration along the crests of the ripples. Pen length 14 cm (D) Large crab burrow with trails. Note the variable inclination angle of the borrows but mostly directed landward (E). Shallow trenches within backshore showing vertical lithological constituents: Coarse grained, massive sand alternating with heavy mineral layers (F) Backshore coarse massive sand underlain by thick mud layers of palaeoswamp (G) Aeolian dune field. Note the sharp seaward cliff due to erosion (H).

are generally seawards (Figs. 2 G and 3 A). Besides the burrows there are numerous trails of gastropods, however despite their abundance, the preservation potential of these surface traces is thought to be minimal. In the upper part of the fore-shore there are shore parallel swash ripples, characterized by very low amplitude but very wide wave length.

In cross-section, the sediment is characterized by alternations of mm-thick planar laminae or low angle cross strata of light coloured fine sand and dark coloured heavy minerals with frequent occurrence of shell-hash layers (Fig. 3 B and 3 C). The low angle sets of cross strata are separated by low angle erosional surfaces giving rise to multiple sets dipping seawards. The laminations are often interrupted by the minute near-vertical burrows. This facies is underlain either by coarse sandstone of barrier bar or beach affinity, or by mud of palaeoswamp deposits (Fig. 3 B).

Backshore Subfacies

The backshore subfacies occurs on the landward side of the foreshore facies (Fig. 2 A). Backshore sand is coarser with respect to the foreshore sand, coarsens further towards the berm. The sand is fluffy in nature due to being dry and frequently reactivated by wind. Aeolian ripples (Fig. 3 D) especially aerodynamic ripples are present abundantly in its upper part, characterized by strong asymmetry, high wave length (4 – 5 cm) and low amplitude (0.5 – 1. 5 mm). The migration direction is landward, despite wide variability (Fig. 3 D). Shells are scarce and their sizes are larger than their foreshore counterparts. The burrows are relatively fewer in concentration and larger in size relative to foreshore equivalents (Fig. 3 E). The burrow concentration generally decreases away from the shore and the burrows show a preferred landward inclination (Figs. 3 A and E); the degree of inclination is about 60^0 – 75^{0}. Animal trails are infrequent except for a few crab trails.

In profile the backshore coarse grained sand particles are structurally massive, occasionally planar laminated and then dipping landward, with rare occurrence of shell-hash layers and/or heavy mineral layers (Fig. 3 F and G). The backshore sediments in cross section are underlain by thick mud layers of palaeoswamp deposits (Fig. 3 G).

Aeolian facies

This facies occurs on the landward side of the backshore (Fig. 3 H). This facies is characterized by fine grained, well sorted, well rounded sand. Abundant primary sedimentary structures observed on bed surfaces include adhesion ripples (Fig. 4 A), setulfs (Fig. 4 B) and aerodynamic ripples (Fig. 3 D), as well as dunes with ripple index generally > 20.

The setulfs are positive relief structures, diametrically opposite to flutes, spatulate in form with one end pointed and steep and flaring on the other end (Fig. 4 B; Sarkar et al., 2011). The flaring end represents the current direction and closely matches with the inferred airflow direction as they formed by aeolian processes (Fig. 4 B).

In cross section this facies is characterized by translatent strata and grain-flow and grain-fall cross strata (Fig. 4 C).

very low amplitude bar and inter–bar areas. Some active swamps are developed locally on the landward side of the bars providing low energy areas for deposition of mud. The ubiquitous occurrence of ripples of different forms, dimensions and orientations on the bed surfaces characterizes the facies (Fig. 4 D). Different varieties of ripples, like interference ripples, superimposed and ladder ripples are common (Figs. 4 H and I). Both straight and curved crested ripples are present, some are double crested. Both current and wave ripples, with bifurcation of crests, are observed.

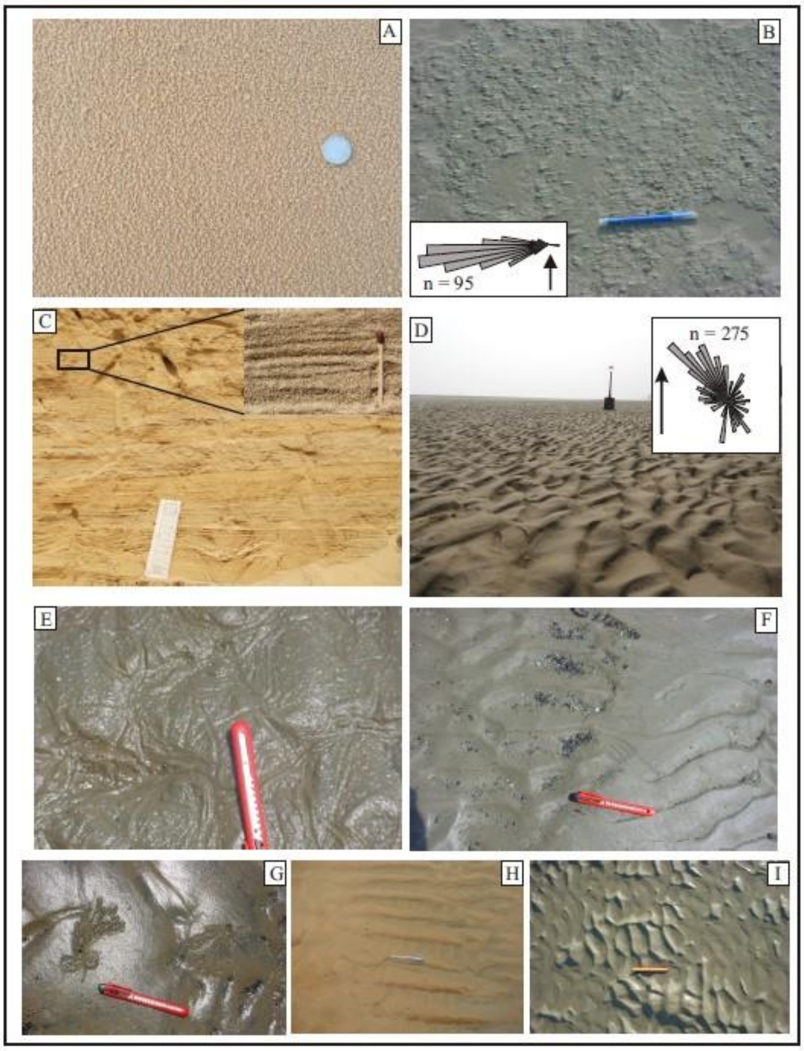

Fig. 4: Bed surface features within backshore facies: Adhesion ripples on wet surface (A) Setulfs. Note the current direction matches with the airflow direction (B) Vertical section of an aeolian dune: Translatent strata and grain- flow - fall cross strata. Note the reverse grading within the grain flow –fall strata showing within inset. Match-stick length 2.5 cm (C) Bed surface features within tidal flat: Occurrence of profuse ripples. Note the diverse current direction represented by palaeocurrent roses (D) Numerous trails of gastropods. Knife length 12 cm (E) Polychaete burrows (F) Crab burrows (G) Ladder ripples (H) interference ripples (I).

Tidal Flat Facies

The tidal flat facies occurs on the seaward side of the beach and away from the river mouth, and covers most of the study area (Fig. 2 A). The tidal flat sediments are marked by ripples on the bed surfaces and get nearly completely exposed twice daily; however, a thin film of water remains on the bed surfaces, even during the ebb. This flat has a gradient lower than that of the foreshore and as a result a distinct slope break occurs at the boundary with the beach (Fig. 2 A). This flat surface however bears very broad undulations, representing a set of

Numerous trails of gastropods, bi-valves and a large variety of worms occur in crisscross pattern on the sediment surface (Fig. 4 E). Burrows of relatively small diameter are also present in medium frequency. The burrows include polychaetas (Fig. 4 F), which preferably occur towards the outer part of the flat and concentrate near the tidal channels traversing the tidal flat. The crab burrows are relatively common on the landward side (Fig. 4 G).

In cross section the tidal flat sediment is characterized by alternations of silt and mud laminae with lenses of sand and shell-hash (Fig. 5 A). Most of these layers with different lithologies are massive with rare occurrence of planar laminae within the sand lenses (Fig. 5 A). The facies is underlain by coarse sand of barrier bar or backshore affinity, fine sand and silt layers of foreshore genesis, or mud deposits of palaeoswamp deposits (Fig. 5 A).

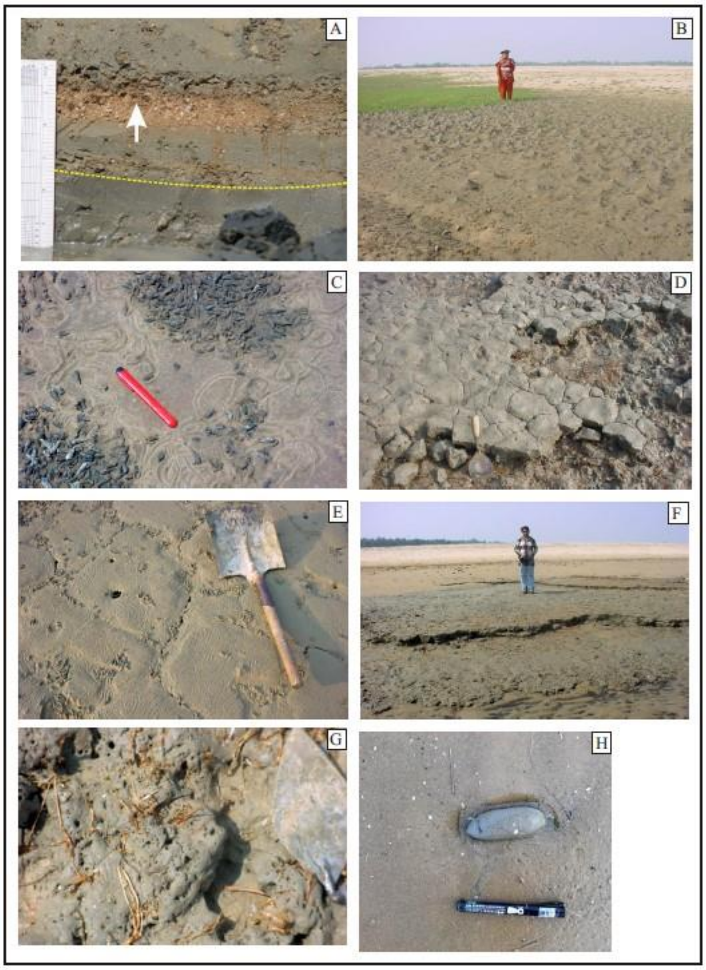

Fig. 5: Shallow trench showing vertical lithological constituents within tidal flat: alternations of find sand-silt with mud layers with infrequent occurrence of sand lenses (arrow). Note that the tidal flat sediments underlain by palaeoswamp mud (demarcated by dotted line) (A) Active swamp deposits: numerous *Ophiomorpha* burrows with vegetable (B) Occurrence of *Cerithium* sp and *Telescopium sp.* with their trails (C) Desiccation cracks (D) Desiccation cracks draped by sandy layers thereby filling the cracks (E) Exhumation of palaeoswamp in front of barrier bar due to erosion (F) Occurrence of numerous rootlets within the palaeoswamp (G) Elongated mudballs, transported and mostly concentrated near the contact of beach and barrier bar. Note that their long axis oriented parallel to the shoreline (marked by the marker pen) (H).

Barrier Bar facies

The barrier bars occur on the landward side of the tidal flat, the largest one situated on the northeastern side of the study area near the river mouth encircling the swamp area (Fig. 2 A). However, some smaller bars are also present within the tidal flat itself, with low relief. The largest bar in the study area, representing the maximum recorded height up to ~ 2 m, above the tidal flat surface, has a length of one and half kilometres. The bars have more or less straight or broadly sinuous crests with their lee sides oriented in the landward direction. The largest bar has already merged with the shoreline, passing laterally into the beach and aeolian dune field. Most of the smaller bars in the tidal flat region have either been eroded away or have the tendency to migrate landward. The top of the bars with higher elevations often interact with aeolian activity and numerous aeolian features, such as aeolian ripples, setulfs and adhesion ripples are frequently present on them (Figs. 3 D, 4 A and 4 B).

Swamp facies

The swamp facies comprises both active swamps, occurring on the landward side of the barrier bar or beach facies, and palaeoswamps. The former swamp facies is dominated by thick mud deposits with black to grey colour with vegetation and abundant *Ophiomorpha* burrows (Fig. 5 B). Numerous *Cerithium* sp. and *Telescopium sp.* and their trails are present on the bed surfaces (Fig. 5 C). Desiccation cracks (Fig. 5 D) are often found, sometimes filled by coarser sand (Fig. 5 E). The palaeoswamps are found as patches within the tidal flat or even on the beach (Fig. 5 F). These older deposits represent pre-existing swamps which were buried due to facies shifting landward, and then became re-exposed during later erosion by waves and tides (Fig. 5 F). The characteristics of the sediments are similar to those of the active swamps where the occurrence of earlier vegetation is represented by rootlets (Fig. 5 G). The palaeoswamp muds are more thixotropic because of dewatering during burial and frequently produce mudballs that are abundantly present immediately adjacent to the palaeoswamp deposits. These mudballs were later transported to other parts of the study area, being concentrated mostly near the beach and barrier bars (Fig. 5 H).

EVIDENCE OF COASTAL EROSION

Comparison of facies maps

Facies maps of the coastal area of Chandipur have been prepared each year for the last

15 years to document the temporal variations within this short time interval. Three maps, from 2003, 2005 and 2018 are presented here to manifest the differences in physiographic features and coast line shifting. The maps clearly show that the coast line has gradually moved landwards (Figs. 6 A, 6 B and 6 C). The facies belts move in the landward direction, eroding the beach area and reducing the width with concomitant increase in the tidal flat area (Figs. 6 A, B and C). The bars within the tidal flat have either been eroded away or migrated landward to merge with the present coastline (Fig. 6 B). The largest bar of the study area has been gradually moving landward, even migrating over the present active swamp and exposing palaeoswamp deposits on the seaward side (Fig. 6 C). The erosional effects of transgression are clearly visible from the patchy exhumation of palaeoswamps in different parts of the present beach and tidal flat facies belts (Fig. 5 F).

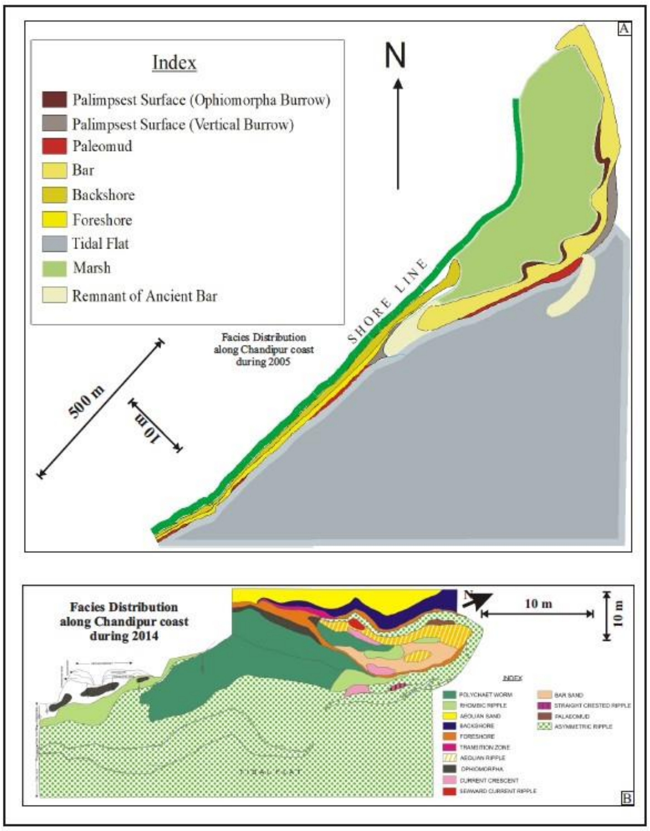

Fig. 6: Facies maps of the study area: 2005 (A), 2014 (B) and 2018 (C). Note the differences of geomorphic features through time: Destruction and re-appearance of smaller bars within the tidal flat, migration of smaller bars landward over the tidal flat thereby exhumation of palaeoswamp as patches within the tidal flat. Gradual increase in width of tidal flat. Gradual shifting of large barrier bar landward thereby exhumation of palaeoswamp in front of the large barrier bar. Gradual decrease in width of beach and shifting landwards (A) Relict bar at the study area depicting coastal erosion.

Physiographic Evidence

Relict Bar

The top of this bar eroded away due to ongoing transgression and a beach developed on this wave-cut bar top (Figs. 6 A, 6 B, 6 C and 6 C). The litho-succession shows large scale tabular cross strata in which alternate sand-mud laminae represent tidal bundles. Uncommon shell-hash and heavy mineral layers are also present within the transverse section. The tabular cross strata are overlain by fine sand/silt and shell-hash alternations repressing deposition within the foreshore environment, suggesting the shifting of the beach and thus of the shoreline.

Drowned River Channel

The old channel of the Buribalam River still exists within the intertidal flat and provides the main sea way for fishermen who use the flood–tide to get out to sea (Fig. 7 A). From the river–mouth the channel sweeps southwestward and runs obliquely across the intertidal flat and eventually becomes drowned below the eroding coastal deposits. This drowned river channel provides most conspicuous evidence of transgression.

Exhumation of Palaeoswamp

As already mentioned, due to ongoing transgression, the present swamp on the landward part of the aeolian dune-field may not be in equilibrium with the present marine system at Chandipur. The more interesting feature in the study area is the patchy exhumation of older swamp (Fig. 5 F) across the boundary between the present beach and tidal flat, and in all other areas of the tidal flat. Abundant *Ophiomorpha* burrows (Fig. 5 B) are concentrated on the surface of the palaeoswamp. In vertical section numerous plant roots and burrows characterize the litho-units of the palaeoswamp. The sticky mud gets desiccated, thereby losing its cohesion, and is then eroded during strong tidal and wave surges generating mud-clasts. These clasts are mostly elliptical and have various dimensions. The orientations of these mud-clasts are found to be diverse but long axes are oriented preferably parallel to the shore-line (Fig. 5 H). The mud-clasts are mostly armoured with shell fragments, indicating their transportation by rolling as bed-load sediments.

Wave Cut Dunes

The berm at the landward extremity of the beach at Chandipur is erosional and is represented by the steep wave cut face on the seaward side (Fig. 3 H). It is apparent that the existing dune field is in no way in equilibrium with the contemporary marine system. Ongoing transgression has washed off the sandy soil concomitant with uprooting of big trees (Fig. 7 B).

All this evidence clearly suggests that the coast line is retreating landward due to transgression. However, extreme waves formed during high-tide conditions, may also have caused wave cut dunes.

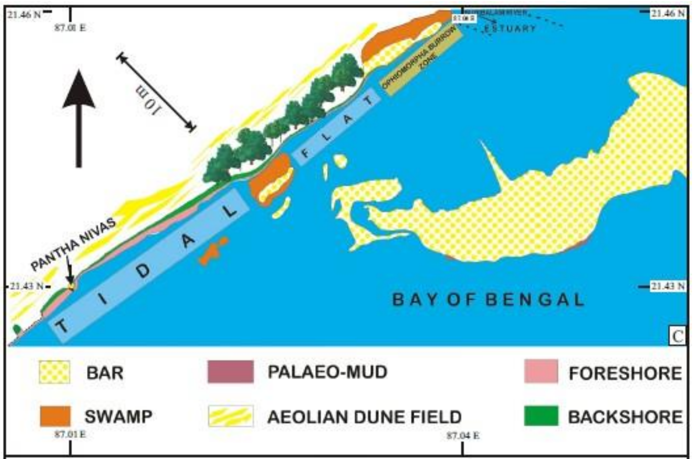

Fig. 6

Fig. 7: Note the occurrence of numerous ripples on top of the bar indicating reworking of the bar top by waves and currents (A) Relict occurrence of earlier river channel within the intertidal flat now drowned under the sea (B) Washed off the sandy soil causing uprooting of big trees (C).

CAUSES OF COASTAL EROSION AT CHANDIPUR

Although coastal erosion is a natural phenomenon, resulting from the interactions between different types of natural processes and different geomorphological systems, anthropogenic interventions sometimes inhibit these processes and change the patterns of erosion and accretion. Coastal erosion caused by natural and / or anthropogenic processes alter the sediment itself, both sources and sinks of the beach sediment budget or the processes that influence the sediment budget. Notwithstanding that transgression is the key factor causing coastal erosion at Chandipur. However, there are other factors that probably influenced the process of coastal erosion including *waves, winds, tides, tsunami of 2004* and *Nisha cyclone of 2008* and because of these natural phenomena, the sediments are deposited on the seabed, aeolian erosion, cliff undercutting and the extensive damage of the coastal region took place, respectively.

Storms:

The entire coastline of Odisha is highly vulnerable to periodic and frequent cyclones and storms especially during monsoon time (Chittibabu et. al., 2004; Mohanty et. al., 2004; Sundar et. al, 2007). These tropical monsoons and cyclonic depressions, invariably after origination in the Bay of Bengal, are associated with heavy precipitation and frequent flooding. Normally the storm surges of around 6 to 7 m height may go up to 10 – 12 m depending on the severity of cyclones the (Mohanty et. al., 2004) and storms can be simple storms, severe storms, cyclones or severe cyclones depending on speed of wind. In the October, 1999, a super cyclone, accompanied by heavy rainfall and flooding hit the coast of Odisha that lasted for a week and caused extensive damage to the coastal infrastructures, beaches and dune field of Chandipur.

Anthropogenic Causes:

Chandipur coast is also affected by human influence, particularly through urbanisation and economic activities in the coastal zone. Along with different natural phenomena as mentioned above, the activities of mankind have increased the risk of coastal erosion on the Chandipur coast. Coastal tourisms and coastal resources have changed the socio-economic conditions of the local communities of Chandipur and adjoining areas throughout the Odisha Coast. But this mass tourism on the Chandipur coast is producing sewage and solid waste pollution, and causing deforestation, coastal erosion and sedimentation from construction activities (Biswas, 2014). Moreover, the conditions of the beach area along the Chandipur coast are degrading at a faster rate because of the tourism industry, depending upon the increasing number of tourists, the increased rate of growth of the tourism industry, improper planning and lack of controls (Gossling, 2003; McLaren, 2003; Neto, 2003). Physical changes like tourism-related hotels, resorts, shops, roads and other infrastructures like dredging of tidal entrances, construction of fisheries, construction of jetties, hardening of shorelines with seawalls or revetments, destruction of mangroves and other natural buffers, poor coastal zone management, over-exploitation of marine resources & biota are also widespread. Thus, factors such as human activities, increased storminess, the change in angle of wave approach, reduction in sediment supply to the beach systems together play a significant role in inducing coastal erosion (Nair et. al., 2018).

Only 8 % of Earth's habitable terrestrial surface is occupied by the coastal zone of the world and, as of 1994, this coastal zone accommodates about 37 % of the World's population within 100 km and 44 % within 150 km of a coastline (Cohen et al., 1997). As these coastal zones contribute one-fifth of total global primary production and enjoy rich natural resources, they are becoming highly populated (Mohanty et. al., 2008). Therefore, the ecosystems of these coastal zones are experiencing tremendous pressure.

The environment first began to change from anthropogenic activities when human societies changed their role from hunter-gatherer communities for sustaining life, and started to settle in one place as agriculture developed. Due to a rich abundance of food and water, particularly in the shallow estuaries and seas, mankind commonly started settlements near coastal zones. At the very beginning of human settlements in these coastal zones, they had little impact on the natural development of those coastal areas. Moreover, they had to accept sea level changes, tidal movement and storms as the cost of living there in coastal zones (Doddy, 2001). Now due to rapid urbanization, coastal tourism, discharge of waste materials into sea or ocean, sewage discharge through rivers, over-exploitation of marine resources and infrastructural development within these hazard prone areas, the coastal areas of India are under increasing environmental pressure, like rest of the World too. The coastal zones of India also suffer from over-population. Different types of natural hazards such as cyclones, floods, tidal waves etc. along with on-going transgression are responsible for coastal as well as environmental changes along the Chandipur coastal area. The Chandipur coastal zone is very vulnerable to cyclones, storms and floods; these events cause considerable damage to life and property as well. There were 72 and 56 flood associated cyclones in the nineteenth century and in the twentieth century, respectively, along the Odisha coast (Dube et al., 2002). As a result, there were rapid changes of the marine environment along the Chandipur coast.

The Chandipur area is over populated by poor people, mainly fishermen. For this growing population, housing construction, both legal and illegal, is increasing day by day. Some of this construction is well within the coastal zone, violating coastal zone management (CZM). As a result, the interplay of natural factors is facing an additional problem which is changing the geomorphology of the coastal zone. Moreover, excess land use and increased pressure of population on limited energy and freshwater resources of Chandipur are damaging the coastal ecosystems due to deforestation, erosion, disruption of ecology & biological diversity, pollution and waste generation (UNWTO-1994). Due to the increasing number of fishermen, over exploitation of natural resources is taking place which directly affects the biodiversity of the region and thus damages the ecological balance. Due to this rampant fishing, there is a fish market along with another, accessory materials market at Balaramgadi, near the mouth of Buribalam estuary (Fig. 1). To accommodate the huge number of fishermen, there is also a boat industry at Balaramgadi near the estuary of Buribalam river. Both these industries are degrading the ecological balance of the Chandipur coastal area. This is also accelerating the landscape change of the area. Another alarming fact due to excess fishing, is that sometimes the Olive Ridley sea turtle (*Lepidochelys olivacea*), an endangered species which is especially known for its mass nesting, come to the beach and then fishing nets, the local people as well as fishermen do not allow them to go back to sea again. As a result, the population of this beautiful species is decreasing day by day.

There is no doubt that the "Tourism Sector" builds up much more job opportunities in comparison to any other sector in respect of investment (Barman et al., 2015 a). Chandipur is also not an exception. The Chandipur beach is wide, golden and calm. The sea water advances towards the shore as much as 5 km at the time of high tide and retreats by the same during the low tidal ebb. There is huge scope for tourism and its expansion because of the location of Chandipur along the eastern coastal area of India and the significant cultural heritage of Odisha. Because of vast diversity in both fauna and flora, the history of the area, its location and local culture, tourists from both India and foreign countries are increasing in Chandipur and adjoining areas of Odisha.

Due to the overpopulation along the coastal area and overcrowded tourists along the coastal zone of Chandipur, coastal landscapes are changing rapidly. Because of lack of knowledge, most of the time, these tourists are degrading the sand dunes, biking over the beach areas. As a result, these zones are becoming vulnerable during high tides or storms and thus rapid shifting is taking place among the different facies / zones of the coastal area (Fig. 6). Moreover, due to the increase in the tourism industry of Chandipur, number of hotels and associated business increased significantly over the time. As a result, hoteliers are building constructions which violate Coastal Zone Management Laws and Policies of the Government. Apart from this, these hotels are disposing off their waste materials along with sewage materials directly into the sea, polluting the regions. Also, they are building illegal retaining walls to protect their premises causing the tidal flat area to overlap the beach area, reducing the width of the beach day by day in Chandipur (Fig. 6).

According to Erwin (1982), there are over 30 million living species in the universe but taxonomically we know only less than 2 million species among them. We are forcing the Earth's faunas and floras into another neo-mass extinction by fishing, indiscriminate killing, destruction of habitat, food harvesting etc. (Simberloff, 1986). As a result, by doing so, human beings will be the one and only architect of their own demise (Ehrlich, 1986). This situation demands much concern since a vast majority of living species will go extinct silently before being identified, classified and studied.

There was an abundance of Horseshoe crabs (*Tachypleus gigas*), the blood of which has commercial and medical applications, at Balaramgadi, a small fishing village near the sea at Chandipur. But now dead crabs are commonly found along the beach. This is due to overcrowded, unaware tourists and their leisure activities along the beach. There was also an abundance of red crabs all along the wide, long beach of Chandipur during 2004-2005, now they are scant in occurrence, and are now restricted within the shore zone only.

Molluscs all over the world, like-wise most of the intertidal taxa, are threatened due to alteration of habitat and over-exploitation by man (Branch & Moreno, 1994; Lindberg, 1998; Roy et al., 2003). Molluscs contribute about 4-5% of the total annual Indian fishery production (Appukuttan, 1996). The Indian coastline is very rich in living resources. But, due to anthropogenic impact, the living resources are deteriorating at an alarming rate. Shells of molluscs are used for food, shell-craft and for other industrial purposes. Due to fishering boat construction, tourism, coastal population growth, shrinkage of wetland is causing drastic reduction of the population sizes of molluscs and sometimes even excluding them from their type localities (Subba Rao, 1998 and Bhattacharya and Sarkar, 2003). Trampling and removing of dead shells which act as microhabitats of other organisms also affects the biodiversity of coastal areas (Roy et al., 2003). In India, shells of bivalves are collected by netting and by handpicking from tidal flat areas (Bhattacharya and Sarkar, 2003). These shells are used for preparation of edible lime, poultry feed and shell crafts (Bhattacharya and Sarkar, 2003). Due to over-exploitation of shells in and around the coastal areas, immediate action must be taken as bivalves act as "ecosystem engineers" (Jones et al., 1994). Because they "modify" and "create" habitats and as they are highly sensitive to environmental change, they are good indicators of environmental degradation (Bhattacharya and Sarkar, 2003).

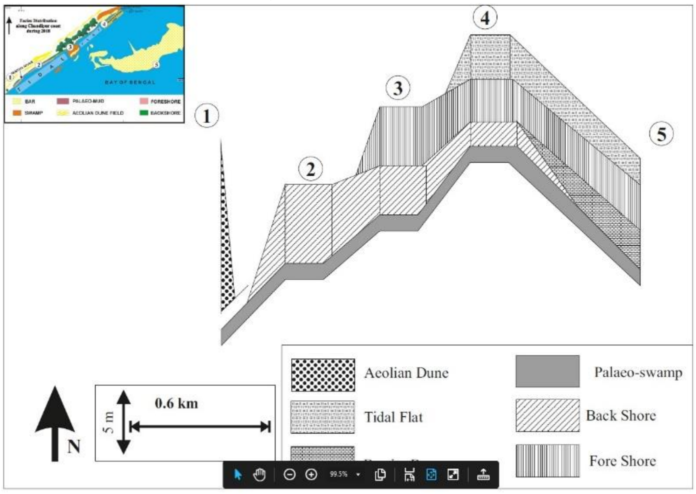

Fig. 8: The fence diagram is reconstructed from litho-successions of different locations within the study area, correlating the litho-successions, using palaeoswamp as reference surface. The log locations are shown (within inset) in facies map of 2018. Note the shifting of facies belts through time.

In response to these crises and to overcome these coastal problems, India, like other developed and developing countries of the world, implemented some rules, regulations and management laws. For this purpose, these countries, along with India, have developed Integrated Coastal Zone Management (ICZM) or Integrated Coastal Management (ICM) (Clark, 1991; Mohanty et. al., 2008) policies and practices to address these growing problems.

DISCUSSION

The coastal environment, generally, is a complex and dynamic system as it represents the interfaces of land, sea and air. It is continuously undergoing both gradual and sudden changes with many physical processes being active, such as tidal flooding, sea level rise, land subsidence, volcanic activity and erosion – sedimentation (Maiti and Bhattacharya, 2009). The coastal area of Chandipur represents an active, transgressing meso- to micro-tidal coast. The present study gives an opportunity to investigate the sediment grain size, sediment dispersion, flow dynamics and resulting primary sedimentary structures and facies composition in different environments of a meso- to micro-tidal coast. The vertical transition of facies clearly suggests shifting of facies belts landward concomitant with coastal erosion. The ongoing transgression results in shifting of facies landward, giving rise to a facies model that can be considered as a verified model for the said environment (Fig. 8). The sediment characters have a key role during shifting of facies. The sandy facies move landward more frequently in response to tidal current while the muddy facies do not because of their inherent cohesion. The sandy bars are migrating over the swamp, formed immediately behind (i.e. landward of) the bars, which makes the swampy mud more cohesive and more thixotropic. These swampy muds are later exhumed during subsequent strong current events and storms giving rise to patchy occurrence of palaeoswamp in different parts of the facies belts, particularly near the beach and barrier bar. It is found that at Sagar Island, which is laterally adjacent to the study area, the western part of the beach is sandy whereas the eastern part is silty to clayey, as a result of accretion in the western part and erosion along the eastern part (Purkait, 2009). However, in Chandipur, the beach is grossly sandy and erosion is taking place all through the beach and the sands are mostly dumped near the confluence of the River Buribalam. The aeolian dune fields are gradually being eroded and retreating giving rise to shrinking of the beach area and expansion of the tidal flat. In the adjacent Sagar Island, the coastal dune fields have retreated 20 m since 1985 (Purkait, 2009). Field measurements also suggest that the island's beach on the eastern part has been lowered by about 2 m since 1985 and that the beach area of the western part has been raised about 2 m since 1995 (Purkait, 2009). Like the present study area, Sagar Island is also suffering from frequent bank-failures, flooding, erosion of beach, siltation at jetties and navigational channels, and cyclones, together resulting in Sagar Island becoming increasingly vulnerable (Purkait, 2009). On the Udupi coast, a sandy beach in Karnataka along the west coast of India, the beach is affected by the accelerated sea level rise due to its low topography, and also as a result of the high ecological and tourist value. The Udupi beach eroded about 0.60 square km per year during 2005 – 2006 (Dwarakish et. al., 2009). The coastal zones of the Cuddalore, Pondicherry and Villupuram districts of Tamil Nadu along the southeast coast of India are experiencing threats from many disasters, such as storms, cyclones, floods, tsunamis and coastal erosion (Mahendra et. al., 2011). The 56 km long coastal line of Chennai, Tamil Nadu on the southeast coast of India includes tourist resorts, ports, hotels, fishing villages and towns. This coastline also experienced threats from storms, cyclones, floods, tsunamis, sea level rise and erosion (Kumar and Kunte, 2012). The Kalpakkam beach of Tamil Nadu, south-east coast of India, records a sand sheet deposit of the 2004-tsunami that begins at 25 m from the shore and extends up to 420 m in a landward direction (Srinivasalu et. al., 2007). The coastal areas are also sensitive to many hazards and risks, from floods to disease epidemics (Adger et. al., 2005). The coastal region along the east coast of India is a thickly populated belt and exposed to high risk and vulnerability from natural hazards such as tropical cyclones (Sahoo and Bhaskaran, 2018). The frequent tropical cyclones, developed over the Bay of Bengal are much more common than those of the Arabian Sea region. As a result, risk factors associated with storm surge, inland inundation, wind gusts, intense rainfall are always high on the east coast of India. The effects of anthropogenic intervention severely affect the invertebrate coastal inhabitants particularly the Mollusca. The shallow infaunal habitat of *Meretrix meretrix* makes them vulnerable to human exploitation (Sur et. al., 2006). The confamilial predation rates in the Chandipur area are very high and the predators are very efficient as is evident from high drilling frequencies (Das et. al., 2014). High drilling frequency on the species *Natica gualteriana* are attributed to its new arrival in the present study area where it is facing competitive elimination by sympatric naticid predators (Das et. al., 2014). The transgression results in changes in physicochemical environment that trigger severe stress on invertebrate populations pose a serious threat to their existence even with the potential to lead to extinction.

Over the last 100 years the average global sea level has been rising due to an increasing rate of global warming, resulting in shifting of coastlines landward, causing transgression. The rate of annual sea level rise is expected to be two to five times more than that of the present rate within the next 100 years (Cai et. al., 2009). Two-thirds of the world's major cities, containing about 60% of the total population with higher levels of economic development, are located in coastal zones (Chen and Chen, 2002). For example, more than 85 % of Australians live within 50 km of the coastline. According to Miller and Dauglas (2004) sea level is rising globally by 1.5 to 2 mm per year; since 1993, however, Church and White (2006) opined that it is increasing at the rate of 3 mm per year, that may lead to the global sea level rise of about 60 cm by 2100 (Solomon et. al., 2007). For socio-economic developments in coastal cities of China, erosion has become a major concern. The shoreline of the different low-lying areas of the Shandong Peninsula is retreating day by day (Zhuang, 1989). However, if global warming continues to increase and ice melts then it could rise up to 1 m by the end of the twenty first century (Pfeffer et. al., 2008). The sea level rise in association with the storms and flooding of coastal-areas results in coastal areas becoming more vulnerable to erosion. The coastal area is retreating 300 m per year at the Luanhe River mouth (Qian, 1994). Transgression and coastal erosion seem to be global phenomena, shorelines of about 70% of the sandy beaches around the world are retreating towards land (Bird, 1985). About 86 % of the barrier beaches of the east coast of the USA are witnessing coastal erosion for the last 100 years (Zhang et. al., 2004). Erosion is also seen in California (Moore et. al., 1999) as well as in the Gulf of Mexico (Morton and McKenna, 1999). In Southern California diminished river flow during droughts resulted in beach erosion, but the beaches were restored during intervening wet years when the fluvial sediment supply revived (Orme, 1985). Since the 1960s, intense urbanization encompassing the building of a sea wall, road and several high-rise buildings has been started on Balneario Camboriu Beach in southern Brazil. This urbanization reduced the amount of sediment exchange between beach and aeolian dune fields, resulting in coastal erosion during storms and the beach has become reduced in width (Temme et. al., 1997). Coastal management studies, involving planning and development of the coastal zone, zonation of hazardous areas, determination of coastal erosion, regional sediment budget estimations, and the study of shoreline position, is essential in order to mitigate coastal erosion and resulting distresses (cf. Sherman and Bauer, 1993; Zuzek et. al., 2003).

CZM programmes have been developed in different countries in response to their crises (Clark, 1991). Along the coastal area of Odisha, tropical cyclones are the most dangerous natural hazard and responsible for loss of life and property. So the Odisha State Disaster Mitigation Authority has been constituted by the Odisha government, which is dedicated to construction of shelters during cyclones, and in ensuring roads and communication facilities can be used during natural disasters along the coastal belt of Odisha in cooperation with other government and nongovernment bodies at national and international levels. Moreover, existing conservation rules and management practices are not sufficient to protect the vast coastline and coastal resources of Odisha (Dash & Kar, 1990; Pandav et al., 1998; Untawale, 1993).

A lack of cooperation in the sum of activities among the different departments may create problems regarding the effective conservation of coastal resources. Therefore, it is necessary to construct a coastal zone management authority with well-defined coastal zone management programmes. Moreover, any comprehensive, integrated and sustainable CZM programme should embrace components like conservation and restoration of mangroves, beach replenishment, protection and development of sand dunes, afforestation, catchment area management plans, and effective communications (Mohanty et. al., 2008).

CONCLUSIONS

The present study area offers an opportunity to determine the sedimentation dynamics, sediment dispersal pattern and facies compositions of a meso- to micro-tidal modern coastal environment. The on-going dynamics result in facies transitions and shifting of facies belts, giving rise to a facies model that can be used as a reference for future investigation of similar ancient environments. Transgression along with other factors leading to coastal erosion have been studied with the help of facies mapping carried out for the last 15 years and documentation of changes in geomorphic features along and across the coastline. The combined effects of transgression and other natural phenomena, anthropogenic interventions also contribute to coastal erosion and resulting environmental stresses which cause a severe threat for many thriving coastal communities including those of human beings. Coastal management and conservation rules need to be reinforced and implemented properly in order to save the ecosystem and life.

ACKNOWLEDGEMENTS

PS acknowledges NBU Assistance for Research funding (2022 - 23), University of North Bengal for funding related research project. All the authors express gratitude to their respective institutions for infrastructural facilities. The authors were highly benefitted by the advice, suggestions and comments received from the reviewers Dr. John S. Armstrong-Altrin and Dr. Mayla A. Ramos-Vázqueza.

CONFLICT OF INTERESTS:

The authors declare no conflict of interest.

REFERENCE:

Adger, W.N., Hughes, T.P., Folke, C., Carpenter, S.R., Rockstrom, J. (2005), Social-Ecological Resilience to Coastal Disasters. Science 309 (5737): 1036-1039.

Appukuttan, K.K. (1996), Marine molluscs and their conservation. In Menon, N.G. and Pillai, C.S.G. (ed) Marine Biodiversity conservation and management. Central Marine Fisheries Research Institute, Cochin, India. Pp 66-79.

Barman, N.K, Bera, G, and Pradhan, M.K. (2015 a), Assessing sustainability in coastal tourism sectors of Odisha coast, India. European Journal of Geography 6 (4): 35-50.

Barman, N.K., Paul, A.K., and Chatterjee, S. (2015 b), Tourism Interfaces in Balasore Coastal Tract, Odisha: A Geo-Perspective View to Develop the Sustainability of Tourism Sectors. International Research Journal of Social Sciences 4(12): 28-37.

Bhattacharya, A., and Sarkar, S.K. (2003), Impact of Overexploitation of Shellfish: Northeastern Coast of India. Ambio. 32(1): 70-77. doi: 10.1579/0044-7447-32.1.70.

Bird, E.C.F. (1985), Coastline changes: A Global Review. Wiley Interscience, Chichester, UK.

Biswas, S.N. (2014), Coastal Tourism in Odisha and Its Impact on Beach Degradation. International Journal of Tourism and Travel 7(1/2): 48-58.

Branch, G.M., and Moreno, C.A. (1994), Intertidal and sub tidal grazers. In Siegfried WRE (ed) Rocky Shores: exploitation in Chile and South Africa. Springer-Verlag, New York. pp 75-100.

Cai, F., Su, X., Liu, J., Li, B., Lei, G. (2009), Coastal erosion in China under the condition of global climate change and measures for its prevention. Progress in Natural Science. 19: 415-426. doi:10.1016/j.pnsc.2008.05.034

Chakrabarti, A. (2005), Sedimentary structures of tidal flats: A journey from coast to inner estuarine region of eastern India. J. Earth Syst. Sci. 114 (3): 353 – 368.

Chen, J.Y., and Chen, S.L. (2002), Estuarine and coastal challenges in China. Chinese Journal of Oceanology and Limnology. 20(2): 174-181. https://doi.org/10.1007/BF02849656

Chen, S., Chen, L., Liu, Q., Li, X., Tan, Q. (2005), Remote sensing and GIS based integrated analysis of coastal changes and their environmental impacts in Lingding Bay, Pearl River Estuary, South China. Ocean & Coastal Management. 48: 65-83. doi: 10.1016/j.ocecoaman.2004.11.004.

Chittibabu, P, Dube, S.K., Macnabb, J.B., Murty, T.S., Rao, A.D., Mohanty, U.C., Sinha, P.C. (2004), Mitigation of Flooding and Cyclone Hazard in Orissa, India. Natural Hazards 31: 455-485.

Church, J.A., and White, N.J. (2006), A 20th century acceleration in global sea level rise. Geophysical Research Letters 33: L01602. doi:10.1029/2005GL024826.

Clark, J.R. (1991), The status of integrated coastal management: a global assessment, FFl: CAMPNET, Rosenstiel School of Marine and Atmospheric Sciences. Miami: University of Miami.

Cohen, J.E., Small, C., Mellinger, A., Gallup, J., Sachs, J., Vitousek, P.M., Mooney, H.B. (1997), Estimates of coastal populations. Science 278: 1209-1213.

Das, A., Mondal, S., and Bardhan, S. (2014), A note on exceptionally high confamilial naticid drilling frequency on Natica gualteriana from the Indian subcontinent. Historical Biology 26(6): 758-764. doi: 10.1080/08912963.2013.841684

Dash, M.N. and Kar, C.S. (1990), The Turtle Paradise Gahirmatha (An Ecological Analysis and Conservation Strategy). New Delhi: Interprint Publisher. pp. 1-272.

Doddy, J.P. (2001), Coastal Conservation and Management – An Ecological Perspective. Springer, NY.

Dube, S.K., Sinha, P.C., Rao, A.D., Murty, T. (2002), Storm Surge Prediction and Mitigation with Particular Reference to Orissa. In: Proceedings of the Workshop on Forecasting and Mitigation of Meteorological Disasters: Tropical Cyclones, Floods, and Droughts. Bhubaneswar. Tropmet 62-87.

Dwarakish, G.S., Vinay, S.A., Natesan, U., Asano, T., Kakinuma, T., Venkataramana, K., Pai, B.J., Babita, M.K. (2009), Coastal vulnerability assessment of the future sea level rise in Udupi coastal zone of Karnataka state, west coast of India, Ocean & Coastal Management. 52 (9): 467-478. doi: 10.1016/j.ocecoaman.2009.07.007

Ehrlich, P.R. (1986), Extinction: what is happening now and what needs to be done. In: Elliot DK (ed) Dynamics of extinction. John Wiley and Sons, New York. pp 157-164.

Erwin, T.L. (1982), Tropical forests their richness in Coleoptera and other arthropod species. Coleopter. Bull. 36: 74-75.

Gopinath, G., and Seralathan, P., (2005), Rapid erosion of the coast of Sagar island, West Bengal – India. Environmental Geology 48(8): 1058-1067.

Gossling, S. (2003), Market integration and ecosystem degradation: Is sustainable tourism development in rural communities a contradiction in terms? Environment, Development and Sustainability. 5: 383-400.

Jones, C.G., Lawton, J.H., and Shachack, M. (1994), Organisms as ecosystem engineers. Oikos. 69: 373-386.

Kumar, A.A., and Kunte, P.D. (2012), Coastal vulnerability assessment for Chennai, east coast of India using geospatial techniques. Natural Hazards 64(1): 853-872. DOI: 10.1007/s11069-012-0276-4.

Lindberg, D.R. (1998), Human influences on trophic cascades along rocky shores. Ecological Applications 8(3), 880-890.

Mahendra, R.S., Mohanty, P.C., Bisoy, H., Srinivasa Kumar, T., Nayak, S. (2011), Assessment and management of coastal multi-hazard vulnerability along the Cuddalore-Villupuram, east coast of India using geospatial techniques. Ocean & Coastal Management 54(4): 302-311. http://doi.org/10.1016/j.ocecoaman.2010.12.008.

Maiti, S., and Bhattacharya, A. (2009), Shoreline change analysis and its application to prediction: a remote sensing and statistics based approach. Marine Geology 257: 11-23. doi: 10.1016/j.margeo.2008.10.006

McLaren, D. (2003), Rethinking tourism and ecotravel (Second Edition). Kumarian Press.

Miller, L., and Douglas, B.C. (2004), Mass and volume contributions to twentieth-century global sea level rise. Nature 428: 406-409. doi: 10.1038/nature02309.

Mohanty, P.K., Panda, U.S., Pal, S.R., Mishra, P. (2008), Monitoring and Management of Environmental Changes along the Orissa Coast. Journal of Coastal Research 24(2B): 13-27.

Mohanty, U.C., Mandal, M., Raman, S. (2004), Simulation of Orissa Super Cyclone (1999) using PSU/NCAR Mesoscale Model. Natural Hazards 31: 373–390.doi: 10.1023/B:NHAZ.0000023358.38536.5d

Moore, L.J., Benumof, T., Griggs, G.B. (1999), Coastal erosion hazards in Santa Cruz and San Diego counties, California. Journal of Coastal Research 28: 121-39.

Morton, R.A., and McKenna, K.K. (1999), Analysis and projection of erosion hazard areas in Brazoria and Galveston counties, Texas. Journal of Coastal Research 28: 8:106-120.

Mukherjee, K.K., Das, S., and Chakraborti, A. (1987), Common physical sedimentary structures in a beach-related open-sea siliciclastic tropical tidal flat at Chandipur, Orissa, India, and evaluation of the weather conditions through discriminant analysis. Senckenbergiana Marit 19: 261-293.

Nair, L.S., Prasad, R., Rafeeque, M.K., Prakash, T.N. (2018), Coastal Morphology and Long-term Shoreline Changes along the Southwest Coast of India. Journal Geological Society of India 92: 588-595. doi: 10.1007/s12594-018-1072-x

Neto, F. (2003), A new approach to sustainable tourism development: Moving beyond environmental protection. Natural Resources Forum. 27 (3): 212-222.

Orme, A.R. (1985), California. In: Bird, E.C.F., and Schwartz, M.L. (ed) The World's Coastline. Van Nostrand Reinhold, New York, pp. 27-36.

Pandav, B., Choudhury, B.C., and Shankar, K. (1998), The Olive Ridley sea turtle (*Lepidochelys olivacea*) in Orissa: an urgent call for an intensive and integrated conservation programme. Current Science. 75(12): 1323–1328.

Pfeffer, W.T., Harper, J.T., and O'Neel, S. (2008), Kinematic constraints on glacier contributions to 21st century sea-level rise. Science 321: 1340-1343. doi: 10.1126/science.1159099

Purkait, B. (2009), Coastal erosion in response to wave dynamics operative in Sagar Island, Sundarban delta, India. Frontiers of Earth Science in China 3(1): 21-33. doi: 10.1007/s11707-009-0001-0

Qian, C.L. (1994), Effects of the water conservancy projects in the Luanhe River basin on the Luanhe River delta. Acta Oceanologica Sinica 49(2): 158-166.

Roy, K., Collins, A.G., Becker, B.J., Begovic, E., Engle, J.M. (2003), Anthropogenic impacts and historical decline in body size of rocky intertidal gastropods in southern California. Ecology Letters. 6: 205-211.

Sahoo, B., and Bhaskaran, P.K. (2018), Multi-hazard risk assessment of coastal vulnerability from tropical cyclones – A GIS based approach for the Odisha coast. J. Environ. Manage 206: 1166-1178. doi: 10.1016/j.jenvman.2017.10.075

Sarkar, S., Bose, P.K., and Bandhyopadhayay, S. (1991), Intertidal occurrence of mesoscale scours in the Bay of Bengal, India, and their implications. Sedimentary Geology 75(1): 29-37.

Sarkar, S., Samanta, P., and Altermann, W. (2011), Setulfs, modern and ancient: Formative mechanism, preservation bias and paleoenvironmental implications. Sedimentary Geology 238(1-2): 71-78.

Scott, D.B. (2005), Coastal changes, rapid. In: Schwartz, M.L. (ed.), Encyclopedia of coastal sciences. Springer, Dordrecht, pp. 253-255.

Sheik Mujabar, P. and Chandrasekhar, N. (2013), Coastal erosion hazard and vulnerability assessment for southern coastal Tamil Nadu of India by using remote sensing and GIS. Natural Hazards 69(3): 1295-1314. DOI: 10.1007/s11069-011-9962-x

Sherman, D.J. and Bauer, B.O. (1993), Coastal geomorphology through the looking glass. Geomorphology 7: 225-249. https://doi.org/10.1016/0169-555X(93)90018-W

Simberloff, D. (1986), Are we on the verge of a mass extinction in the tropical rain forest? In: Elliot, D.K. (ed) Dynamics of extinction. John Wiley and Sons, New York. pp 165-180.

Solomon, S., Qin, D., Manning, M., Chen, Z., Marquis, M., Averyt, K.B., Tignore, M., Miller, H.L. (2007), Climate change 2007: the physical science basis. Contribution of the Working Group I to the Fourth Assessment Report of the Intergovernmental Panel on Climate Change. Cambridge University Press, Cambridge.

Srinivasalu, S., Thangadurai, N., Switzer, A.D., Ram Mohan, V., Ayyamperumal, T. (2007),

Erosion and sedimentation in Kalpakkam (N Tamil Nadu, India) from the 26th December 2004 tsunami. Marine Geology 240 (1-4): 65-75. https://doi.org/10.1016/j.margeo.2007.02.003

Subba Rao, N.V. (1998), Faunal Diversity in India: Mollusca. In Alfred JRB, Das AK and Sanyal AK (ed) Faunal Diversity in India. Envis Centre, Zoological Survey of India, Kolkata, pp 103-117.

Sundar, V., Sannasiraj, S.A., Murali, K., Sundaravadivelu, R. (2007). Run-up an inundation along the Indian Penninsula including Andaman Islands due to great Indian ocean tsunami. Journal of waterway, port, coastal, and ocean engineering, ASCE 133(6): 401-413.

Sur, S., Konar, R., Das, P., Roy, P., Paul, S., Bardhan, S. (2006), Ecology of an endangered bivalve species *meretrix meretrix* (linnaeus): a case study from Chandipur – on – sea, Orissa, India. Indian Journal of Earth Sciences 33(1-4): 1-14.

Temme, B., Klein, A.H.F., Carvalho, J.L.B., Diehl, F.L. (1997),lllllllllll Morphological behavior of beach of Balneario Camboriu: preliminary results. Notas Technicas da FACIMAR 1: 49-65.

Thom, B.G., and Cowell, P.J. (2005), Coastal changes, gradual. In: Schwartz, M.L., (ed) Encyclopedia of coastal sciences. Springer, Dordrecht. pp. 251-253.

Untawale, A.G. (1993), Development of an intertidal mangrove nursery and afforestation techniques along the Indian coast. In: Proceedings of Curriculum Workshop on Management of Mangrove Ecosystem and Coastal Protection, UNESCO-ROSTSCA. Waltair: Andhra University. pp. 1-15.

UNWTO, (1994), National & Regional Tourism Planning: Methodologies & Case Studies. WTO, Madrid.

Walker, R.G. (1984), Facies models. Geol. Assoc. Can., Newfoundland, Canada.

Zhang, K., Douglas, B.C., and Leatherman, S.P. (2004), Global warming and coast erosion. Climate Change 64 (1/2): 41-58.

Zhuang, Z.Y. (1989) Severe shoreline retreat of some straight sandy coasts in Shandong peninsula. Journal of Ocean University of China, Qingdao 19 (1): 90-107.

Zuzek, P.J., Nairn, R.B., and Thieme, S.J. (2003), Spatial and temporal consideration for calculating shoreline change rates in the Great Lakes Basin. Journal of Coastal Research 38: 125-146.

Received on : *02nd Feb 2023*
Revised accepted on : *19th March00 2023*

JOURNAL INDIAN ASSOCIATION OF SEDIMENTOLOGISTS ISSN NO 2582 – 2020
Vol. 40, Issue 1, 2023, pp. 20-28
DOI: https://doi.org/10.51710/jias.v40iI.277

Geochemistry of Neoproterozoic Nagod Limestones from the Girgita Mine, Bhander Group, Madhya Pradesh, India

Ravendra Singh, Gyanendra Pratap Singh, and H.U. Usmani

Department of Geology, Government Motilal Vigyan Mahavidyalaya, Bhopal Madhya Pradesh India – 462008
E-mail: thakur.ravendrasingh@gmail.com

ABSTRACT

Vindhyan limestone of the Bander Group (Late Neoproterozoic) in the Maihar area, Satna district, is a part of an anticlinal fold and it forms an outlier in the study area. Geochemical analysis reveals that the proportion of Rare Earth Elements (REEs; La-Lu) in limestones varies between 14.8 ppm and 49.5 ppm. The Eu and Ce anomalies (normalized against Post Archean Australian Shale; PAAS) range from ~ 0.53 to 0.69 and ~ 0.57 to 1.07, respectively. The results of this study revealed that the limestones were principally controlled by the admixture of detrital materials, i.e., (i) The low values of REEs (ii) high values of Y/Ho (iii) positive correlation between REEs and Si, Al, Ti, V, Co, Ni, and Nb, and (iv) slightly negative correlation between CaO and REEs. Further, the variations in Ce anomaly may be due to the influx of detrital materials and positive Ce anomaly was attributable to the shallow marine depositional condition. The distribution of REEs (Chondrite normalized values) illustrates different patterns in the Nagod limestone due to the degree of differentiation in terms of LREEs and HREEs and Eu anomaly. The variations in elemental concentrations and the REE patterns revealed the mixing of detrital materials in the Nagod limestones.

KEY WORDS: Rare Earth Elements, Geochemistry, Nagod limestone, Bhander Group, Vindhyan limestone.

INTRODUCTION

The behavior and mode of distribution of REEs in carbonate rocks have extensively been investigated earlier by many researchers. The studies showed that the important factors influencing enrichment and depletion of REEs in carbonate rocks are: (1) the lithology and diagenesis (Madhavaraju and Ramasamy, 1999), (2) biogenic deposition from seawater (Murphy and Dymond, 1984), (3) scavenging processes related to depth, salinity, and oxygen level of seawater (Greaves et al., 1999), (4) the variation in oxygen level of seawater (Liu et al., 1988), (5) the amount of detrital material of terrigenous origin (Piper, 1974; McLennan,1989; Nagarajan et al., 2011), and (6) the variation in surface productivity. The results of recent investigations revealed that geochemical studies on REEs in carbonate rocks, furnish a suitable basis for reconstruction of paleogeographic conditions, environment of deposition and source of sediments.

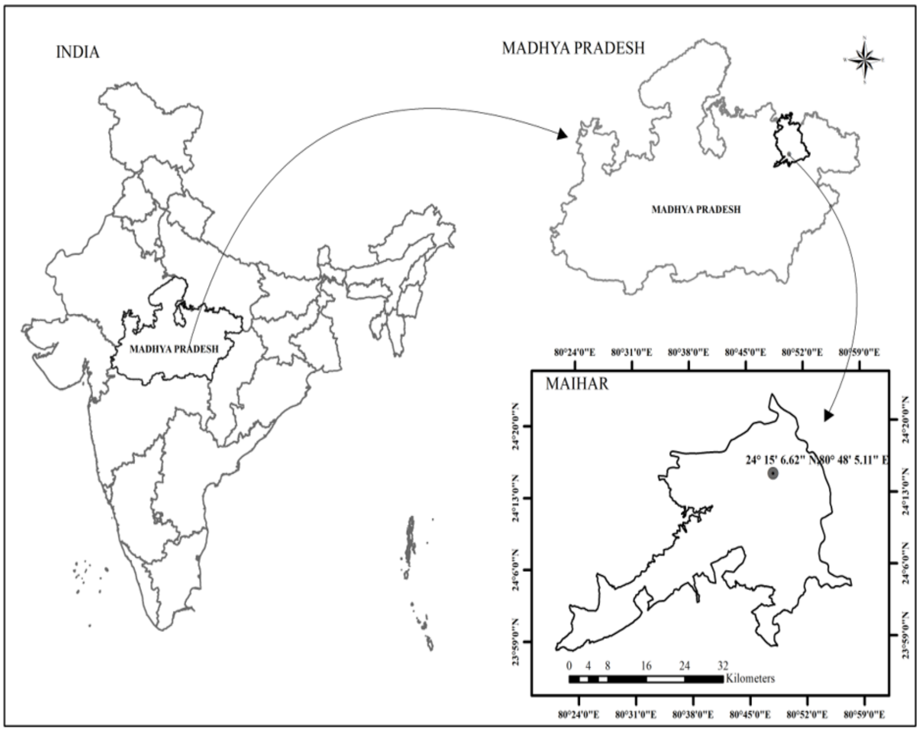

Fig. 1. Location map of the study area.

The Bhander group is widespread to the North of Satna district. The Bihad River flows amidst this limestone belt of Maihar and forms the Chachai Fall down stream. The limestone Fold Belt turns westward from Rewa city and goes westward North of Satna city. In this area, limestone mining is being done by many companies for cement, viz. JP cement, Birla cement, Revati cement, KJS cement plant etc.

The geological map of the study area is shown in Figs. 1 and 2. There are many limestone mines in the Maihar area. The limestone being exploited from Girgita mine is rich in cement grade. A generalized stratigraphic succession of the Vindhyan Supergroup exposed in Maihar area has been given in Fig. 3. Geochemical study of carbonate rocks of the Nagod Formation has been undertaken to investigate the source of REEs and the variations in Eu and Ce anomalies.

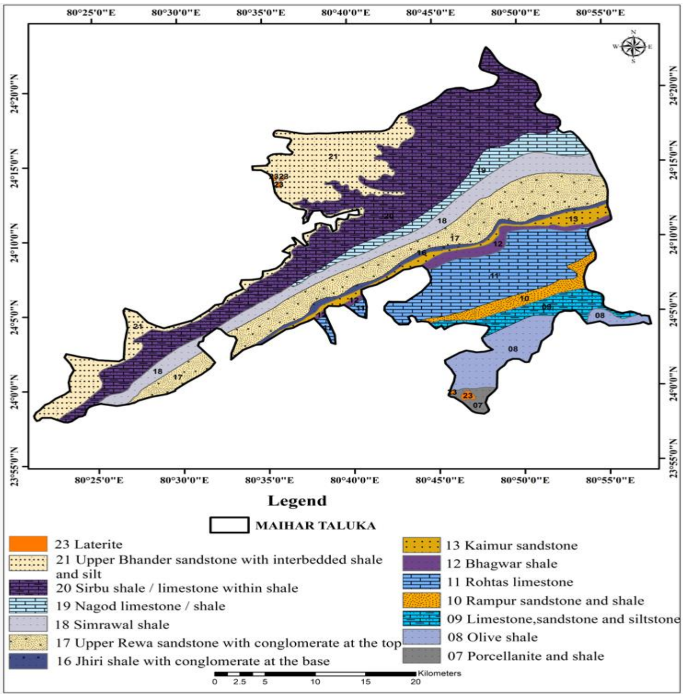

Fig. 2. Geological map of the study area.

GEOLOGICAL SETTING

The study area lies on the Survey of India Toposheet Numbers 63D/15, 63D/16. It is limited by Longitude 80º21′15″ E – 80º57′33″ E and Latitude 24º22′45″ N - 23º58′10″ N (Fig. 1). The Girgita mine is Located 12 km east of Maihar city of Satna district.

The Vindhyan basin is a sickle-shaped basin in the Bundelkhand-Aravalli Province which got stabilized prior to 2.5 Ga. The Vindhyan Supergroup overlies a variety of Precambrian basement rocks comprising Bundelkhand Granite, Mahakoshal Group, Bijawar Group, Gwalior Group, Banded Gneissic Complex (BGC) and Chhota Nagpur Gneissic Complex (CGC). The BGC separates the Vindhyan exposures of the Son Valley area from that of the Chambal Valley. The BGC is dominated by K-rich granite emplaced within the Tonalite-Trondjhemite-Granodiorite (TTG) complex. The BGC and Gwalior Group form the basement of Vindhyan Supergroup in the Rajasthan sector. The CGC, consisting of gneisses, granites and granodiorites with enclaves of tonalitic gneisses and ultramafic rocks, forms the basement of the Vindhyan basin in most parts of the eastern Son Valley area.

Sedimentary litho-units in the Vindhyan Basin represent shallow marine facies along with distal shelf to deep-water sediments. The maximum thickness of the entire Vindhyan Supergroup; consisting of sandstone, shale and limestone, is estimated to be around 5 km. and is divisible as shown in Fig. 3.

The surface expression of this limestone displays Karstic erosion which is recognizable by the presence of various karst features. The oldest lithologic units in the area are porcellanite shale overlain by olive shale of the Semri Group (Lower Vindhyan). The porcellanite shale contains light gray, greenish yellow, compact and jointed porcellanite with gray to khaki gray splintery shale. Olive shale is olive green in color, fine-grained, hard compact and thinly laminated. Semri Group limestone is dark greyish blue, thickly to thinly bedded. Sandstone of Semri Group is ferruginous, purple, flaggy, and fine to medium-grained. Rampur sandstone is light green, fine-grained, thinly bedded, compact sandstone with tiny grains of bluish green glauconite and gray to khaki gray splintery shale.

Rohtas limestone is light to dark gray, fine-grained, compact and bedded blended with sandy and shaly interbeds. Bhagwar shale is yellowish, carbonaceous, micaceous and pyritiferous. Kaimur Sandstone is fine-grained, massive, hard and thickly bedded. Jhiri shale of Rewa Group (Early Neo-Proterozoic age), is soft, reddish, splintery with interbedded siltstone and thin band of conglomerate at the base. Upper Rewa sandstone with conglomerate at the top, found in the upper part of Jhiri Shale, is reddish brown, hard and massive, coarse grained and thickly bedded. Simrawal shale is soft, purple and reddish brown, thinly laminated to flaggy, calcareous with thin bands of calcite, gypsum interbedded with purplish grey limestone. Nagod limestone is fine grained, hard compact, thinly bedded to massive with few stromatolitic bands and interbedded with khaki green shale. Sirbhu shale is purple and olive green, thinly laminated silty shale interbedded with bluish grey limestone within shale.

Upper Bhander sandstone is purple to reddish brown, fine to medium-grained and flaggy to massive. Laterite is reddish brown, hard and massive rock which is preserved in the upper most part of Maihar area (Fig. 2).

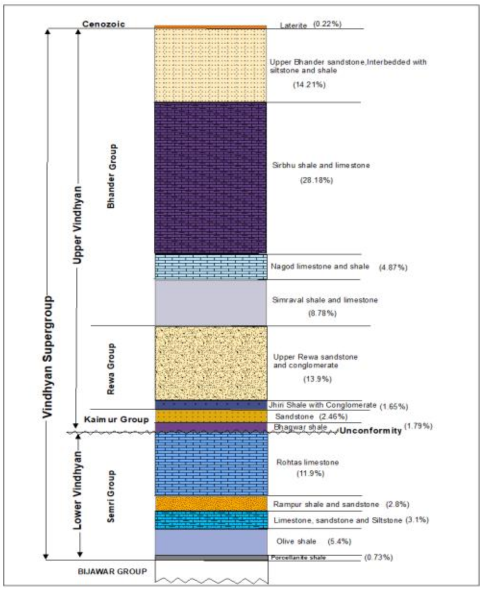

Fig. 3. Stratigraphic succession of the Bijawar Group.

METHODOLOGY

Sampling of Nagod limestone has been carried out at regular vertical interval from the Girgita Mine (Lat. 24°15′7″ N; Long. 80°48′5.11″ E) shown in (Fig. 4). Totally, twelve representative samples have been chosen for chemical analyses. The selected samples were first washed by distilled water to remove contamination and then were air-dried and ground to <2.60 mesh in a tungsten carbide mortar. The powdered samples were analyzed at IIT, Kanpur using ICPMS for REEs, with high quality of analytical precision. The X-Ray Fluorescence Spectroscopy (XRF) analyses of powdered sample were done at the Savitribai Phule University, Pune for trace and major oxide concentrations. Loss on Ignition (LOI) was measured by the loss in dry weight. The results of the values of REEs were normalized to PASS values using the following relation: $Eu/Eu^* = Eu_N/[(Sm_N \times Gd_N)]^{1/2}$ and $Ce/Ce^* = 2Ce_N/(La_N+Pr_N)$, (Where $_N$ stands for the normalization of REEs to PAAS; (Taylor and McLennan, 1985).

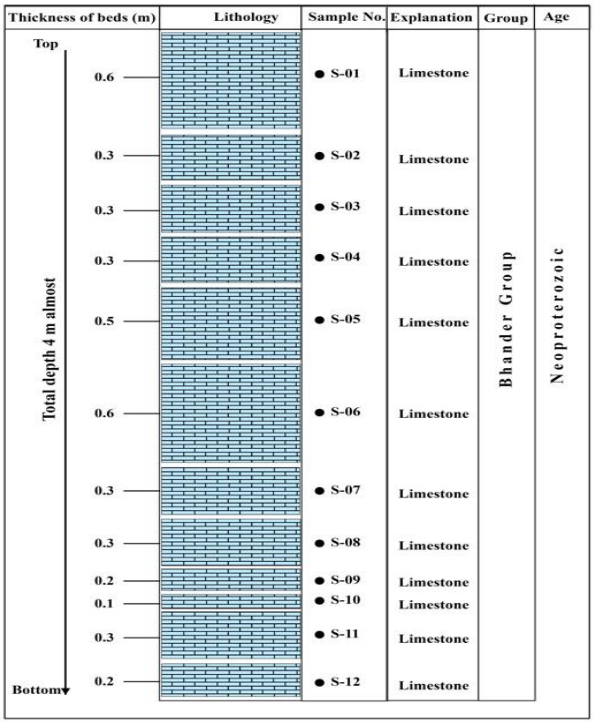

Fig. 4. Lithology map showing sample locations.

RESULTS

The major, trace and REE concentrations in limestones are listed in Table 1: The bivariate plots between the pairs of major oxides show strong and positive correlations between Al_2O_3 and SiO_2 (r = 0.70), Fe_2O_3 and SiO_2 (r = 0.73), Al_2O_3 and TiO_2 (r = 0.93), Fe_2O_3 and TiO_2 (r = 0.60), and SiO_2 and TiO_2 (r = 0.66). The bivariate plots of major oxide show weak and negative correlations, i.e., Al_2O_3 – CaO (r = -0.70), Fe_2O_3 – CaO (r = -0.58), and CaO–SiO_2 (r = -0.88). The samples show strong depletion in elements such as V, Cr, Co, Ni, Cu, Rb, Y, Nb, and Hf. Strong enrichment for elements like Sr and rather notable enrichment for Ba and Zr is observed (Fig. 5). The REE values for all the analyzed REEs have a range of 14.77 to 49.55 ppm. The chondrite normalized REE patterns are shown in Fig. 6, which reveals enrichment in Ce and Nd contents. The Eu/Eu^* and Ce/Ce^* ratio values vary between 0.53–0.69 and 0.57–1.07, respectively. The values of Er/Nd and Y/Ho are also within the range of 0.08–0.12 and 27.62–197.46, respectively. The REEs, in general, have positive correlations with certain major and trace elements such asSiO_2, TiO_2, V, Co, Ni, Rb, and Nb.

Bottom						Sample number						Top
Major elements wt. %												
SiO_2	2.92	12.82	15.30	14.75	9.12	12.55	21.95	4.59	18.89	5.58	20.09	10.48
Al_2O_3	0.68	2.41	3.25	2.74	1.31	2.27	2.07	1.00	1.92	0.89	2.17	1.87
K_2O	0.07	0.48	0.66	0.50	0.17	0.49	0.40	0.15	0.37	0.11	0.41	0.30
CaO	55.01	39.21	38.19	42.81	47.09	46.34	34.63	50.62	32.23	53.44	43.78	47.38
TiO_2	0.05	0.19	0.24	0.14	0.10	0.17	0.16	0.06	0.12	0.05	0.13	0.12
Na_2O	BDL	BDL	BDL	BDL	BDL	BDL	BDL	BDL	BDL	BDL	BDL	BDL
MgO	2.13	5.89	8.45	12.65	6.87	1.85	8.41	4.51	11.85	1.54	4.34	2.97
P_2O_5	BDL	0.03	0.04	0.03	0.02	0.03	0.04	BDL	0.02	BDL	0.03	BDL
MnO	0.02	0.03	0.03	0.03	0.06	0.04	0.03	0.02	0.04	0.03	0.04	0.07
Fe_2O_3	0.36	0.87	1.31	1.09	1.33	1.25	1.26	0.60	1.18	0.80	1.35	1.29
LOI	37.15	39.82	36.78	28.87	35.99	37.21	35.33	37.73	38.57	37.04	30.08	37.10
sum	98.39	101.74	104.00	103.61	102.06	102.19	104.29	99.27	105.20	99.48	102.40	102.58
Trace elements (ppm)												
Li	9.82	36.08	46.49	35.27	22.43	26.38	37.85	16.53	37.99	15.30	30.34	29.85
Be	0.11	0.47	0.60	0.39	0.28	0.53	0.36	0.19	0.34	0.18	0.40	0.36
V	4.55	19.80	20.84	15.00	9.62	18.69	14.64	8.76	13.24	8.42	14.31	15.55
Cr	3.94	18.31	19.03	12.61	8.61	16.25	13.47	5.90	11.89	5.64	11.96	12.66
Mn	125.0	215.3	216.9	226.9	390.2	289.7	239.0	148.5	320.6	232.2	270.2	582.9
Co	1.28	2.97	3.24	2.61	2.99	3.21	1.94	1.76	2.48	1.95	2.65	4.90
Ni	6.37	9.08	11.29	8.89	8.31	13.61	7.60	6.85	7.34	7.92	11.83	14.16
Cu	1.47	4.37	6.53	4.44	3.25	4.88	16.23	2.33	4.59	2.64	3.66	5.38
Zn	-0.90	5.34	8.64	8.85	3.40	10.22	12.85	8.26	8.01	6.35	10.40	5.46
Ga	0.80	3.24	4.08	2.58	1.70	3.26	2.79	1.26	2.43	1.19	2.65	2.49
Ge	0.32	0.82	1.00	0.86	0.88	1.13	0.93	0.56	0.77	0.57	1.00	0.87
As	0.88	1.66	1.06	1.78	2.36	3.65	1.93	1.01	1.45	2.27	2.47	3.51
Se	0.98	2.94	0.55	1.96	1.03	0.99	1.15	1.11	0.50	1.42	0.69	1.47
Rb	6.13	25.82	33.12	20.69	11.23	25.07	21.21	9.95	19.28	8.25	20.12	17.04
Sr	441.1	316.6	252.4	253.0	155.4	272.3	231.0	246.0	242.3	241.0	170.8	209.1
Y	2.30	5.30	6.50	7.70	7.00	10.50	5.30	4.40	3.80	4.90	7.10	36.36
Zr	10.17	38.70	47.40	23.70	25.57	31.04	39.90	10.44	20.08	12.19	25.72	24.13
Nb	0.56	2.39	2.79	1.57	1.10	1.97	1.98	0.99	1.37	0.65	1.48	1.34
Mo	0.15	0.14	0.12	0.18	0.16	0.12	0.14	0.15	0.16	0.16	0.19	0.16
Cd	0.02	0.03	0.04	0.03	0.04	0.08	0.08	0.02	0.03	0.04	0.06	0.06
In	-0.85	-0.72	-0.44	-0.49	-0.37	-0.01	-0.11	-0.65	0.27	-0.46	-0.31	-0.35
Sn	0.08	0.55	0.65	0.50	0.28	0.62	0.91	0.14	0.48	0.17	0.51	0.36
Sb	0.06	0.13	0.13	0.11	0.15	0.18	0.19	0.09	0.12	0.13	0.16	0.24
Ba	17.62	49.04	51.94	37.17	66.80	59.77	47.81	16.48	127.62	31.11	47.06	104.75
Hf	0.28	0.99	1.17	0.59	0.59	0.77	0.90	0.25	0.46	0.27	0.59	0.59
Ta	0.05	0.22	0.25	0.13	0.09	0.15	0.15	0.07	0.11	0.05	0.11	0.11
W	0.25	1.44	0.70	0.61	1.14	0.67	0.47	3.31	0.46	0.36	0.73	0.87
Tl	0.08	0.21	0.26	0.16	0.08	0.13	0.12	0.07	0.13	0.07	0.10	0.09
Pb	1.86	5.17	5.57	3.81	3.46	5.43	5.62	3.17	2.69	4.58	3.32	4.49
Bi	0.03	0.06	0.07	0.05	0.03	0.06	0.05	0.03	0.04	0.03	0.03	0.04
S	1012.0	1217.0	2507.0	1903.0	348.7	135.5	581.4	609.1	751.7	121.0	197.9	147.7
Cl	123.0	142.4	156.0	221.7	108.4	62.3	194.0	96.0	254.4	59.1	104.4	158.2
Br	3.00	1.90	2.40	3.20	1.70	2.30	3.00	1.30	2.20	1.90	2.00	3.52
Y	2.30	5.30	6.50	7.70	7.00	10.50	5.30	4.40	3.80	4.90	7.10	36.36
Rare earth elements (ppm)												
La	3.0	5.4	5.9	5.7	5.4	13.4	5.1	3.9	4.0	4.6	7.5	6.3
Ce	6.1	10.4	11.3	12.2	11.1	15.0	9.6	8.9	7.8	10.6	10.7	10.6
Pr	0.7	1.2	1.3	1.5	1.4	2.8	1.1	1.1	0.9	1.2	1.4	1.4
Nd	2.7	4.6	4.8	5.8	5.2	10.3	4.0	4.1	3.4	4.7	5.4	5.3
Sm	0.5	0.9	1.0	1.2	1.1	1.9	0.8	0.8	0.7	1.0	1.0	1.1
Eu	0.1	0.2	0.2	0.2	0.2	0.4	0.2	0.1	0.2	0.2	0.2	0.2

Gd	0.6	1.0	1.0	1.1	1.1	1.9	0.8	0.8	0.7	1.0	1.1	1.1
Tb	0.1	0.1	0.1	0.2	0.2	0.3	0.1	0.1	0.1	0.1	0.1	0.2
Dy	0.4	0.8	0.9	0.9	1.0	1.5	0.7	0.6	0.6	0.8	0.8	0.9
Ho	0.1	0.2	0.2	0.2	0.2	0.3	0.1	0.1	0.1	0.1	0.2	0.2
Er	0.2	0.5	0.6	0.6	0.6	0.8	0.4	0.3	0.3	0.4	0.5	0.5
Tm	0.0	0.1	0.1	0.1	0.1	0.1	0.1	0.0	0.0	0.0	0.1	0.1
Yb	0.2	0.5	0.6	0.5	0.5	0.8	0.4	0.3	0.3	0.3	0.4	0.5
Lu	0.0	0.1	0.1	0.1	0.1	0.1	0.1	0.0	0.0	0.0	0.1	0.1
REE	14.8	26.0	28.1	30.3	28.0	49.6	23.6	21.3	19.1	25.3	29.5	28.3
Eu/Eu*	0.5	0.6	0.6	0.6	0.6	0.6	0.6	0.6	0.7	0.6	0.6	0.6
Ce/Ce*	1.0	1.0	1.0	1.0	1.0	0.6	1.0	1.1	1.0	1.1	0.7	0.8
Er/Nd	0.1	0.1	0.1	0.1	0.1	0.1	0.1	0.1	0.1	0.1	0.1	0.1
Y/Ho	27.6	30.3	34.9	40.0	37.8	35.6	36.6	36.3	33.6	34.1	43.8	197.5

DISCUSSION

The distribution of REEs in calcareous sediments and oceanic water has been discussed by Madhavaraju and Ramasamy (1999). Low concentration of REEs in limestones (average 26.9) is attributed to marine carbonate phase rather than that of clay which generally contains higher average REE concentration as suggested by Piper (1974). CaO. The positive correlation between REEs and P_2O_5 (r = 0.40; Fig. 7a) depicts that in addition to terrigenous origin for REEs in the limestone, the diagenetic fluids also might have played an effective role in their supply. The mean analytical value of Al_2O_3 in the limestone at Girgita mines is 1.87 wt. %, which is greater than the average value of siliciclastic-contaminated limestones (0.42 wt. %; Veizer, 1983). This concentration value shows

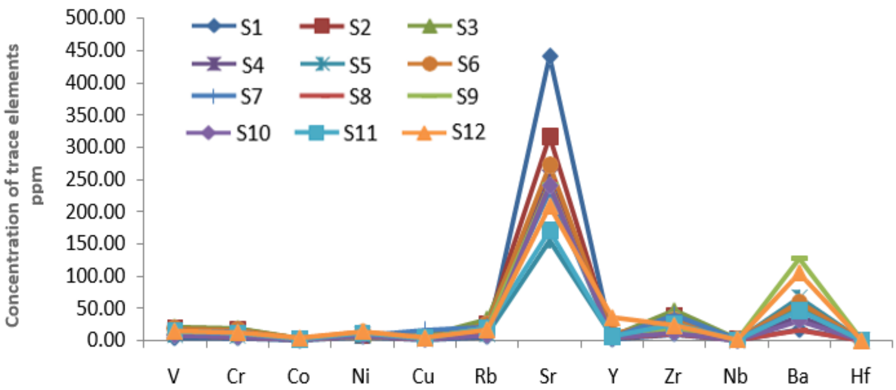

Fig. 5. Distribution patterns of trace elements in the limestone at Girgita mine, Maihar (normalized against UCC).

Bellanca et al. (1997) documented ~ 28 ppm REE average value for marine carbonate rocks. The average REE value of the limestone (26.9) is well comparable with those of Bellanca et al. (1997).

Commonly, REEs with detrital origin have positive correlations with elements such as SiO_2, TiO_2, Al, K, Cr, Co, Rb, Y, V, Ni and Nb, and negative correlation with

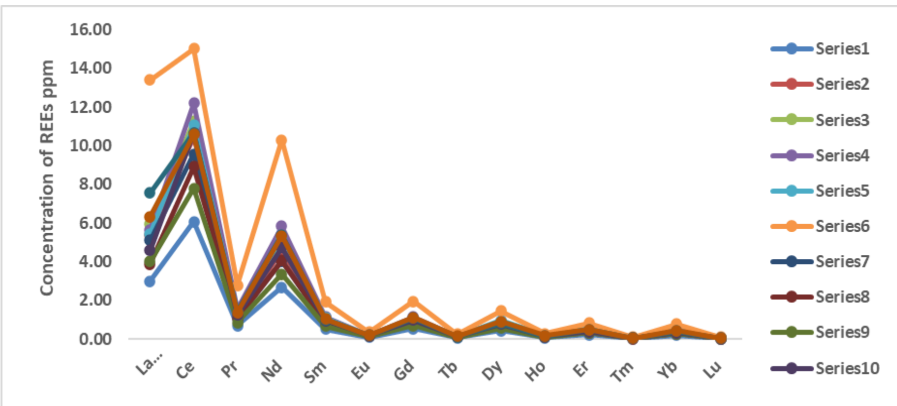

Fig. 6. Distribution patterns of REEs in the limestone at Girgita mine Maihar (normalized against UCC).

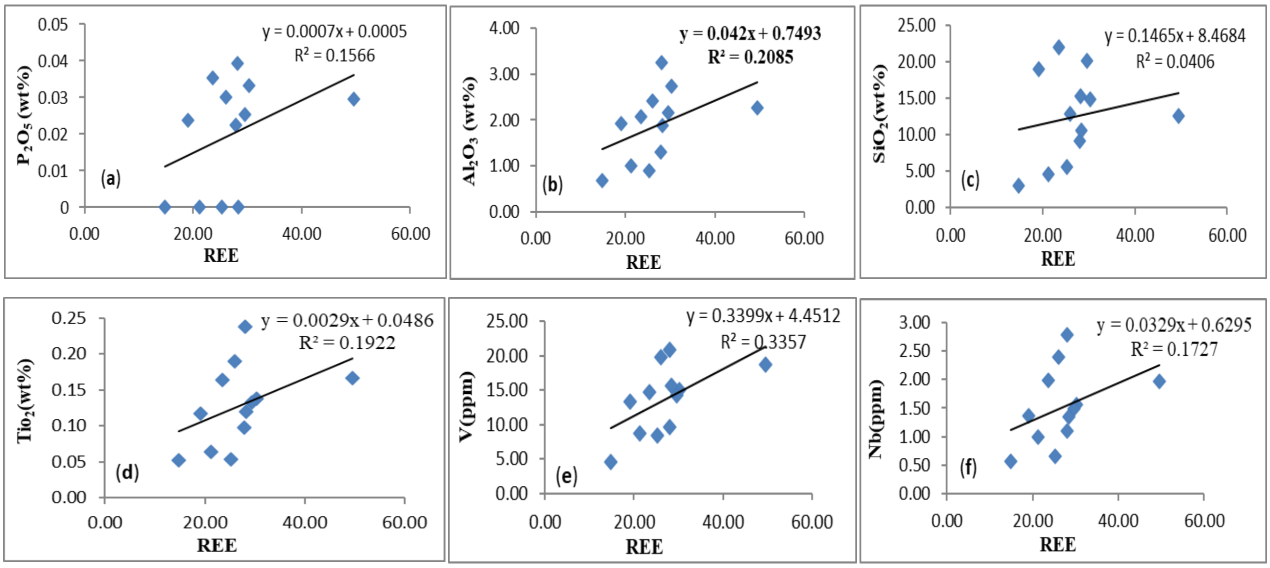

Fig. 7. Bivariate plots between REE and other elements. a) REE-P_2O_5, b) REE-Al_2O_3, c) REE-SiO_2, d) REE-TiO_2, e) REE-V, and f) REE-Nb.

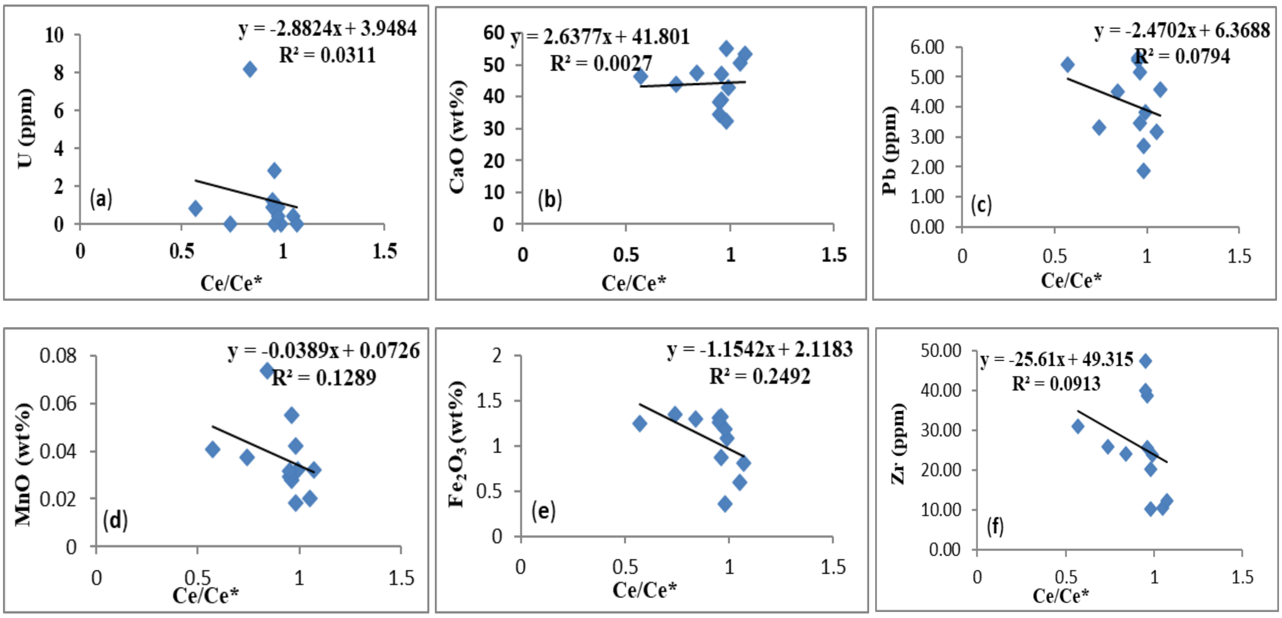

Fig. 8. Bivariate plots: a) Ce/Ce* - U, b) Ce/Ce* – CaO, c) Ce/Ce* – Pb, d) Ce/Ce* – MnO, e) Ce/Ce* – Fe_2O_3, and (f) Ce/Ce* – Zr.

positive correlation with the REE content Al_2O_3 (r = 0.46; Fig. 7b), suggesting an intense contamination (Madhavaraju et al., 2010). This study endorses the terrigenous source for REEs in Nagod limestone by considering the correlation coefficients between REEs and certain major and trace elements.

The Nagod limestone shows that the REEs have a positive correlation with SiO_2 (r = 0.20; Fig. 7c), TiO_2 (r = 0.43; Fig. 7d), V (r = 0.58; Fig. 7e), and Nb (r = 0.42; Fig. 7f). These relations evidently point to a terrigenous derivation of REEs in the Nagod limestone. The positive correlation between MnO and P_2O_5 (r = 0.63) rules out the possibility of significant contamination generated by Mn and Fe oxides in the limestone.

The anomalous values of Ce (Ce/Ce*), in the limestone of the study area, show a narrow range of 0.57–1.07 with an average of 0.92. The Ce anomaly for marine waters ranges from <0.1 to 0.4 (Elderfield and Greave, 1982). Therefore, it appears that the Ce/Ce* values in the Nagod limestone are influenced by the relative proportions of precipitates derived from both pure seawater (carbonates) and suspended fluvial materials. Commonly, the positive anomaly of Ce is generated as a result of influx of terrigenous material (Nath et al., 1992; Madhavaraju and Ramasamy, 1999; Armstrong-Altrin et al., 2003).

Besides, factors like paleo-redox (Liu et al., 1988; German and Elderfield, 1990; Armstrong-

Altrin et al., 2003), fluviatile colloids enriched by Fe-organics (Sholkovitz,1992), and scavenging processes (Masuzawa and Koyama, 1989) could have played crucial role in the occurrence of positive Ce anomalies. The Ce/Ce* values display negative correlation with U (r = –0.2; Fig. 8a) and positive correlation with CaO (r = 0.05; Fig. 8b), indicating that the variations in Ce anomalies are not related to the paleo-redox conditions of the depositional environment. The Ce/Ce* values also have negative correlations with reactive scavenging type particles like Pb, Mn and Fe (r = –0.28 to –0.50; Fig. 8c-8e). These correlations show that the limestone, in question, appears to have been precipitated in a shallow marine environment where the role of scavenging processes is comparatively less than that of deep marine environments. Ce shows positive correlations with elements such as Al (r = 0.53), Ti (r = 0.49), V (r = 0.62), Co (r = 0.51), Ni (r = 0.69), Rb (r = 0.52), Cu (r = 0.09) and Nb (r = 0.47) in the Nagod limestone. The Ce/Ce* values show weak and negative correlations with few major (MnO, CaO, and Fe_2O_3) and trace elements (U, Zr, and Pb; Fig. 8a-f). So, it can be inferred from these correlations that the Ce abundance and Ce anomalies, in the limestone of the study area, might have been controlled by the influx of detrital materials.

Eu ANOMALY

Eu anomaly values are helpful in comprehending the physico-chemical conditions of various geochemical systems operating in the depositional environment of limestones (Derry and Jacobsen, 1990). The Eu anomalies, in the studied limestone are negative ranging from 0.53 to 0.69, with a mean value of 0.58. Commonly, positive Eu anomalies (normalized to PAAS) are observed in limestones influenced by hydrothermal processes, whereas negative Eu anomaly is indicative of high decomposition of minerals and transportation of minerals containing Eu. Because of the negative correlations between Ce/Ce* and by the presence of components like Fe_2O_3 and MnO, the role of hydrothermal activities in the occurrenceof positive Eu anomalies, in the limestone at Girgita mines, may be ruled out. Aeolian materials too, have not been reported so far. The role of diagenetic processes can be postulated by positive correlations between Eu/Eu* and by the concentration of certain immobile elements such as Zr, Y and Hf (Madhavaraju and Lee, 2009). The positive correlations between Eu/Eu* and Zr (r = 0.09; Fig. 9a), Eu/Eu* and Y (r = 0.17; Fig. 9b), Eu/Eu* and Th (r = 0.29; Fig. 9c) and Eu/Eu* and Hf (r = 0.04; Fig. 9d) advocate the effective role of diagenesis in the occurrence of Eu anomalies in the Nagod limestone. Furthermore, the effect of diagenetic alteration can be deduced by the strong positive correlation between Mn and Sr (r = -0.56) (Brand and Veizer, 1980). Inclusion of detrital feldspars in sediments can bring about positive Eu anomalies in limestones. The ratios of oxides like Na_2O/Al_2O_3 and K_2O/Al_2O_3 may help in the recognition of different kinds of feldspars in sediments (Madhavaraju and Lee, 2009; Nagarajan et al., 2011). Therefore, it seems that in addition to diagenetic processes, the presence of K-feldspars appears to have played a significant role in the occurrence of negative Eu anomaly in the Nagod limestone.

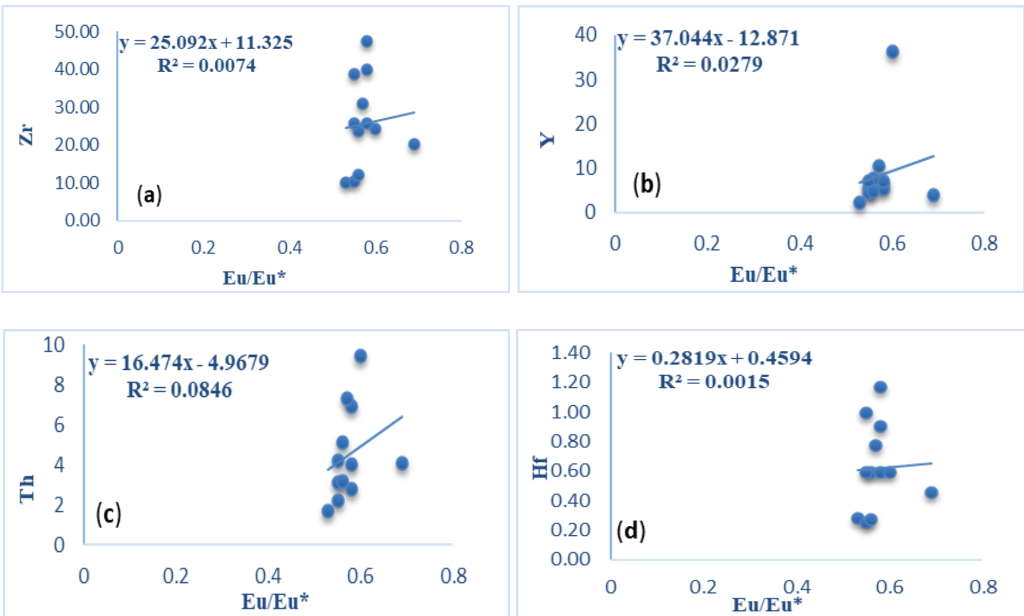

Fig. 9. Bivariate plots: a) Eu/Eu* – Zr, b) Eu/Eu* – Y, c) Eu/Eu* – Th, and d) Eu/Eu* –Hf.

Y / Ho and Er / Nd ELEMENTAL RATIOS

Yttrium(Y) is identical to Ho and Dy in terms of ionic charge and ionic radius. Therefore, in distribution pattern of REEs, it is inserted between Ho and Dy (Bau, 1996). Although Y and Ho have similar geochemical behavior, yet Ho can be removed from sea water twice as fast as Y. This phenomenon is related to the difference in degree of surface complex stabilities, which leads to a notable super chondritic marine ratio of Y/Ho (Bau, 1996; Nozaki et al., 1997). Terrigenous material and volcanic ash have constant chondritic values of Y/Ho (Approximately 28). Seawaters have Y/Ho values greater than those of volcanic ash, ranging from 44 to 74 (Bau, 1996; Nozaki et al., 1997).

In this study, the Nagod limestone has Y/Ho values varying noticeably from 27.62 to 197.46 (mean 49). These values indicate that the limestones are contaminated with terrigenous materials. The ratio value of Er/Nd in normal seawater is ~ 0.27 (De Baar et al., 1988). The Er/Nd value in limestone efficiently indicate the seawater signature. The Er/Nd values, in the studied limestone, display a narrow range of ~ 0.08 - 0.12, which in turn, indicate the effective role of detrital material and diagenetic processes in the occurrence of Er and Nd in the Nagod limestone.

The controlling factor of diagenetic processes in the distribution of REEs in limestones can be established by a negative correlation between Eu/Eu* and Ce/Ce*. The existence of negative correlation between Eu/Eu* and Ce/Ce* (r = 0.006; Fig. 10) demonstrates that the processes during diagenesis are the controlling factor in the distribution of REEs in limestone.

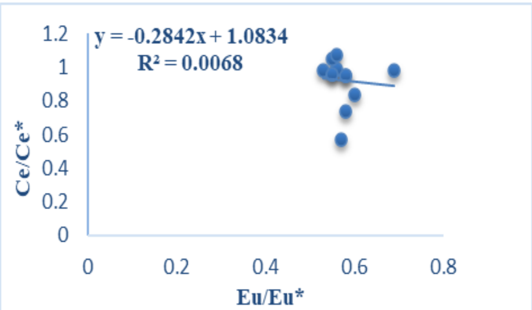

Fig. 10. Bivariate plot between Eu/Eu* and Ce/Ce* ratios for the Nagod limestones.

CONCLUSIONS

Geochemical indicators such as low ratio of Y/Ho and high values of REEs suggest that the concentration of REEs in the limestone is associated with the incorporation of terrigenous material. This can further be supported by the positive correlation of REE with elements such as Si, Al, Ti, V, Co, Ni, Rb, Cu and Nb, and by negative correlation between REE and CaO. The positive correlation between Ce/Ce* and Si, Al, Zr, Hf and Y, and along a negative correlation between Ce/Ce* and CaO, U, Fe_2O_3 and MnO reveal that variation in the values of Ce anomalies in the limestone have substantially been controlled by fluvial detrital material. Besides, the negative correlation furnishes strong evidence for the deposition of limestones in a shallow marine environment.

ACKNOWLEDGEMENTS

The assistance given by the officials from IIT, Kanpur for ICP-MS analysis and Pune University for XRF analysis are thankfully acknowledged. Our sincere thanks to MPCST, Bhopal for providing the facilities to prepare various maps. We are grateful to the Editor and two anonymous reviewers for their comments, which improved our presentation.

REFERENCES

Armstrong-Altrin, J.S., Verma, S.P., Madhavaraju J, Lee YI, Ramasamy S (2003). Geochemistry of Late Miocene Kudankulam Limestones, South India. International Geology Review, 45:16–26.

Bau, M. (1996). Controls on the Fractionation of Isovalent Trace Elements in Magmatic and Aqueous Systems: Evidence from Y/Ho, Zr/Hf and Lanthanide Tetrad Effect. Contributions to Mineralogy and Petrology, 123:323–333.

Bellanca, A., Masetti, D., Neri, R. (1997). Rare earth elements in limestone/marlstone couplets the Albian-Cenomanian Cismon section (Venetian region, from northern Italy): assessing REE sensitivity to environmental changes. Chemical Geology, 141:141–152.

Brand, U., Veizer, J. (1980). Chemical diagenesis of a multi component carbonate system: trace elements. Journal of Sedimentary Petrology, 50:1219–1236.

De Baar, H.J.W., German, C.G., Elderfield, H., Van-Gaans, P. (1988). Rare earth elements distributions in anoxic waters of the Cariaco Trench. Geochimica et Cosmochimica Acta, 52:1203–1219.

Derry, L.A., Jacobsen, S.B. (1990). The chemical evolution of Precambrian seawater: evidence from REEs in banded iron formations. Geochimica et Cosmochimica Acta, 54:2965–2977.

Elderfield, H., Greaves, M.J. (1982). The rare earth elements in seawater. Nature, 296:214–219.

German, C.R., Elderfield, H. (1990). Application of Ce anomaly as a paleo-redox indicator: the ground rules. Paleoceanography, 5:823–833.

Greaves, M.J., Elderfield, H., Sholkovitz, E.R. (1999). Aeolian sources of rare earth elements to the Western Pacific Ocean. Marine Chemistry, 68:31–38.

Liu, Y.G., Miah, M.R.U., Schmitt, R.A. (1988). Cerium: a chemical tracer for paleooceanic redox conditions. Geochimica et Cosmochimica Acta, 52:1361–1371.

Madhavaraju, J., Gonzalez-Leon, C.M., Lee, Y.I., Armstrong-Altrin, J.S., Reyes-Campero, L.M. (2010). Geochemistry of the Mural Formation (Aptian-Albian) of the Bisbee Group, Northern Sonora, Mexico. Cretaceous Research, 31:400–414.

Madhavaraju, J., Lee, Y. (2009). Geochemistry of the Dalmiapuram Formation of the Uttatur Group (Early Cretaceous), Cauvery basin, southeastern India: implications on provenance and paleo- redox conditions. Revista Mexicana de Ciencias Geologicas, 26:380–394.

Madhavaraju, J., Ramasamy, S. (1999). Rare earth elements in limestones of Kallankurichchi Formation of Ariyalur Group, Tiruchirapalli, Tamil Nadu. Journal of the Geological Society of India, 54:291–301.

Masuzawa, T., Koyama, M. (1989). Settling particles with positive Ce anomalies from the Japan Sea. Geophysical Research Letters 16:503–506.

McLennan, S.M. (1989). Rare earth elements in sedimentary rocks: Influence of provenance and sedimentary processes. In: Lipin BR, McKay GA, editors. Geochemistry and Mineralogy of Rare Earth Elements. Chantilly, VA, USA: Mineralogical Society of America, pp. 169–200.

Murphy, K., Dymond, J. (1984). Rare earth element fluxes and geochemical budget in the eastern equatorial Pacific. Nature 307:444–447.

Nagarajan, R., Madhavaraju, J., Armstrong-Altrin, J.S., Nagendra, R. (2011). Geochemistry of Neoproterozoic limestones of the Shahabad Formation, Bhima Basin, Karnataka, southern India. Geosciences Journal, 15:9–25.

Nath, B.N., Roelandts, I., Sudhakar, M., Pluger, W.L. (1992). Rare Earth Element patterns of the Central Indian Basin sediments related to their lithology. Geophysical Research Letters, 19:1197–1200.

Nozaki, Y., Zhang, J., Amakawa, H. (1997). The fractionation between Y and Ho in the marine environment. Earth and Planetary Science Letters, 148:329–340.

Piper, D.Z. (1974). Rare earth elements in the Sedimentary cycle: a summary. Chemical Geology, 14:285–304.

Sholkovitz, E.R. (1992). Chemical evolution of rare earth elements: fractionation between colloidal and solution phases of filtered river water. Earth and Planetary Science Letters, 114:77–84.

Taylor, Y., McLennan, S.M. (1985). The Continental Crust: Its Composition and Evolution. 1st ed. Oxford, UK.

Veizer, J. (1983). Trace elements and isotopes in sedimentary carbonates. In: Reeder RJ, editor. Carbonates: Mineralogy and Chemistry, Vol. 11. Chantilly, VA, USA: Mineralogical Society of America, pp. 265–299.

Received on : *05th Feb 2023*
Revised accepted on : *13th April 2023*

JOURNAL INDIAN ASSOCIATION OF SEDIMENTOLOGISTS ISSN NO 2582 – 2020
Vol. 40, Issue 1, 2023, pp. 29-42
DOI: https://doi.org/10.51710/jias.v40iI.285

Textural characteristics and abundance of microplastics in the Nethravati river estuary sediments, south-west Mangalore beach, India

Darshan, M. S[1]. , K. Siddaraju and P. Madesh
[1]Department of Marine Geology, Mangalagangothri, Mangalore University, Mangalore-574199.
Faculty, Department of Studies in Earth Science, Manasagangothri, University of Mysore, Mysore-570006.
Professor, Department of Studies in Earth Science, Manasagangothri, University of Mysore, Mysore-570006.

ABSTRACT

Microplastics commonly enter the world's sea through rivers and estuaries. Yet somehow, very little is known about what happens to plastic waste in estuaries. This study provides important information on the Microplastics (MP's) distribution and features in the Nethravati estuary. The present level of knowledge on microplastic trash dispersal in estuaries and their intertidal ecosystems. The MPs identified in this were classified as: source (Primary and secondary MPs), size < 1000 µm (78%), followed by >1000 µm (22%), color (coloured plastic (32%) and white plastic (68%), shape (fibre (96%), beads (3%), fragment (1%). The polymer types detected are Polyamide (60%), polyethylene (33%), followed by polypropylene (5%) and polystyrene (2%). We observed that secondary MPs were the most often recovered microplastics in 22 samples, indicating that primary microplastics had been destroyed by photo-degradation, chemical degradation, and biological degradation. According to the FTIR study, polyamide and polyethylene were the most common microplastics, followed by polystyrene and polypropylene. Future research to track MPs abundance along the Netravati estuary's shoreline can utilize the results of this study as guidelines. The best methods to prevent the abundance of MPs in estuary sediments are to manage solid wastes properly, implement laws, and spread awareness about the cause of MPs to the ecosystem.

KEY WORDS: Microplastics (MP's), FTIR, degradation, Netravati estuary, South-west coast.

INTRODUCTION

The plastic products are an excellent packaging material that is ideal for a variety of applications because of its low cost, excellent oxygen and moisture barrier properties, bio-inertness, and light weight. Globally, the amount of plastic manufactured each year has almost doubled since the 1950s, reaching 322 million metric tons in 2015. In the 1970s, a report on ocean plastic pollution was published, bringing it to the attention of the scientific community for the first time (Carpenter et al., 1972; Colton and Knapp, 1974; Coe and Rogers, 1996). About 80% of the plastic garbage is generated on land, including beach debris. Nearly 18% of the marine plastic waste found in the ocean environment comes from the fishing sector. In addition to other things created of land based resources; the aquaculture business can likewise release plastic into the ocean (Hinojosa and Thiel, 2009). MPs size ranges from 0.5 mm to 5 mm were categorised as macro or mesoplastics (Andrady, 2011; Cole et al., 2011). However, the phrases "microplastics" and "microlitter" have been interpreted differently by

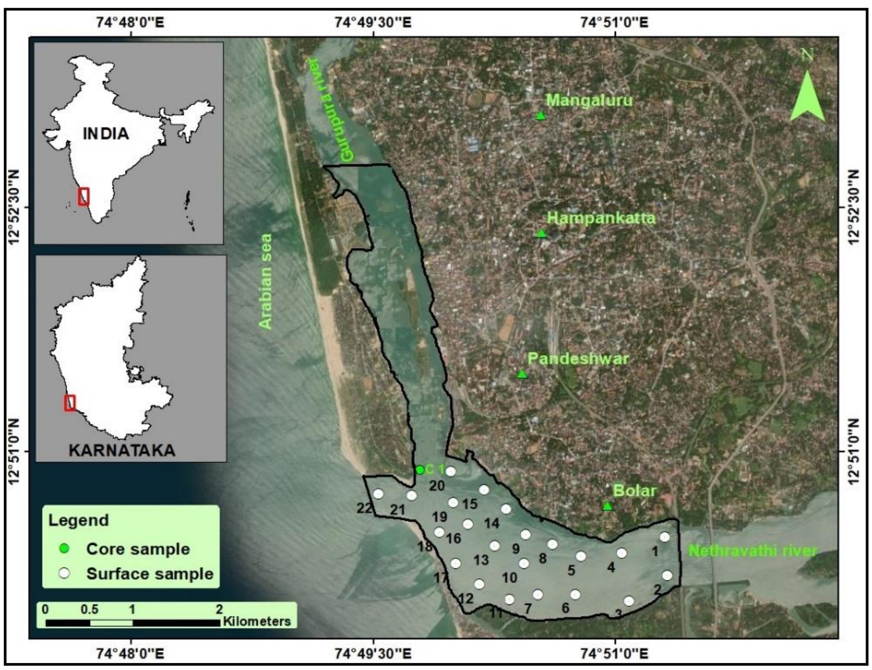

Figure 1. Map showing sample locations in the Nethravati river estuary

Figure 2. Sediment sample collection

Figure 3. Plastic wastes in the Nethravati river estuary

various academics. (Gregory and Andrady 2003) defined microplastics as particles with a diameter between a few µm to 500 µm, while microlitter was defined as practically imperceptible particles that are retained by a 67 µm sieve (≈0.06–0.5 mm in diameter). Microplastics constitute a risk to the aquatic environment due to their prolonged residence periods, tendency for biota eating, and release of hazardous components during decomposition (Andrady, 2011). The Netravati-Gurpur estuary is characterized by a mixed type of semidiurnal tides (Reddy et al., 1979). The Netravati and Gurpur Rivers deliver 12,015 x 106 m^3 and 2,822 x 106 m^3 of fresh water and 14 x 105 and 1 x 105 tons of sediment annually in to the Arabian Sea (Subramanian et al., 1987; Karnataka Irrigation Department, 1986). The mean annual rainfall in the drainage area is 3,954 mm, of which, nearly 87% is received during the southwest monsoon (Murthy et al., 1988). Therefore, currents in the river mouth are controlled by fresh water discharge during the southwest monsoon and by tides during the rest of the year (Reddy et al., 1979). For this reason, ebb flow is

Figure 4. Van Veen grab sampler

Figure 5. Core sample collection

dominant during the southwest monsoon and flood flow during winter and summer. The primary goal of this study is to determine the textural characteristics and the abundance of microplastics in the Netravati River estuary sediments.

Figure 6. River flow direction towards west

STUDY AREA

Dakshina Kannada is a maritime district located in the south-western part of Karnataka state adjoining the Arabian Sea. The geographical area is 4770 sq. km the study area lies in between 12°56'12" - 12° 57' 59" N and 74° 47' 57" - 74°, 48' 09" E. The study area has a tropical climate and the maximum temperature recorded so far is 36° C. The average annual rainfall is 3954 mm out of which 87% is received during the southwest monsoon (Murthy et al., 1988). Wind speed varies from 7.2 to 9.6 km/hr. Mangalore town is the district headquarters, which is divided into five taluks viz. Bantwal, Belthangady, Mangalore, Puttur, and Sulya.

MATERIALS AND METHODS

22 sediment samples were collected using a Van Veen grab sampler and the grid sampling technique. Samples were collected from 400 to 500 m interval and one core sample was collected using PVC pipe measuring 10 feet long. Every 2 inches, the samples were marked, sliced into pieces, and sediment samples were selected randomly for the microplastics analysis. A GPS was used to confirm the sampling locations in the field after being chosen using pre-made grids (Garmin 010-00970-00 eTrex 10 Worldwide Handheld GPS Navigator). To eliminate big debris and retain particles smaller than 5 mm, the wet samples were sieved using a 5 mm screen. The sediment was put in ceramic bowls and dried at a 50° C. To get rid of the big debris and organic plant remnants, the oven dried samples were homogenised and put through a 5 mm testing sieve (Sruthy and Ramasamy, 2017). MPs were recovered from sieved sediment samples in accordance with National Oceanic and Atmospheric Administration (NOAA) guidelines (Masura et al., 2015). To get rid of the organic matter and calcareous component from the surface sediments, 30g of dried sediment was treated with a 30% hydrogen peroxide (H_2O_2) solution followed by 2N HCl. Later, the following density separation technique was used: 50cc of readymade zinc chloride solution (density: 1.58g/cm^3) was thoroughly mixed with the pre-treated estuary sediments. The mixture was filtered using a vacuum pump assembly and 0.45 m of Whatman® nitro-celluloe membrane filter paper. To improve the extraction results, the filtering process was repeated three times. To distinguish between the various polymer compositions in the microplastics, Bruker's Fourier-transform infrared spectroscopy (FTIR) technology was used in conjunction with an attenuated total reflectance (ATR) diamond crystal attachment. Using a setup of instruments and a freely accessible spectrum library, the frequency curve of the microplastic composition was found. Based on the colour, form, and composition of the materials, the recoverable microplastic was categorised using an optical stereo zoom microscope in polarising mode and an online digital camera system (Model: Leica DMC 4500). A pie chart was used to show the distribution of microplastics in terms of colour, shape, size, and composition (Excel, 2007). In order to avoid contamination, all vessels and equipment utilized during MPs extraction were rinsed with distilled water before usage. Similarly, petri dishes used to store the samples were wiped by Kimberly Clark cellulose wipe. All equipment was covered when they were not in use. In addition, the extraction process for a sample was repeated without sediment sample to test the contamination during analysis.

MICRO TEXTURAL STUDIES:

100 g of sediments were socked with H_2O_2 and HCl to remove the organic debris and carbonate coatings, respectively. The samples were sieved at 0.6-Ø interval by using the ASTM sieve setson Ro-tap mechanical sieve shaker. The sand grains of 120 ASTM size were used for the surface micro textural studies. To represent the variability present in a grain (Higgs 1979; Krinsley and Doornkamp, 1973), 3-4 quartz grains in each sample were studied. Quartz grains were examined for their surface microtextural features in Hitachi S-3400N SEM at magnification of ×5 to ×300,000. At the Department of Material science, Vijnana Bhavan, University of Mysore, Karnataka, India.

RESULT AND DISCUSSION

COLOR CLASSIFICATION OF MICROPLASTICS

The MPs are made available to fishes due to its attractive colours, small size, and high buoyancy (Chatterjee and Sharma, 2019). The use of coloured plastic items in daily life, such as clothing, packaging, and fishing equipment, causes MP's of different colours to appear in the silt. (Wang et al., 2017; Zhang et al., 2015). However, weathering during transportation in the surface water can cause the hues to shift (Kalogerakis et al., 2017; Wu et al., 2018). The colour classification of MPs was: coloured plastic (32%) and white plastic (68%) made up the microplastic overall, in core the colour classification is as follows: coloured plastics (97%) and white plastics

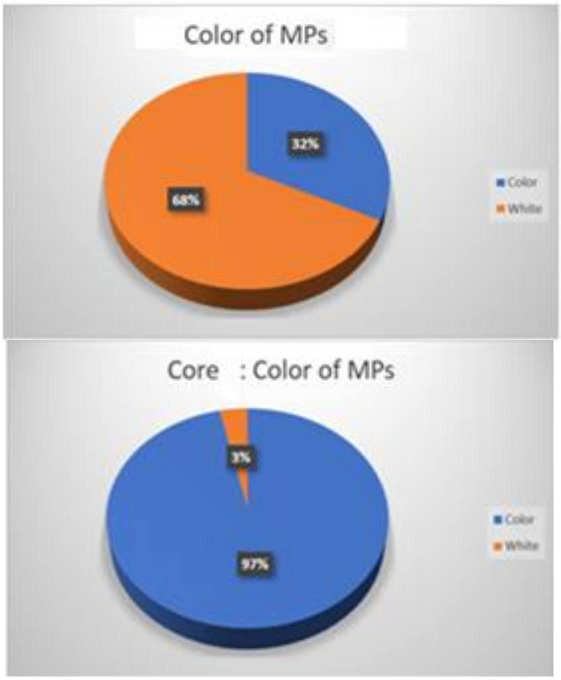

Figure. 7 Pie Chart representing the MPs color towards west

(3%). The transparent variety out numbers the white-colored variety in white plastics and the majority of the fragments were blue and white in colour (Tables 1& 3. Figure.7)

SHAPE OF MICROPLASTICS

Plastics are composed of four main categories: fibres, films, pieces, and pellets (Doyle et al., 2011; Hidalgo-Ruiz et al., 2012) Fibres are likely created by fishing gear and textiles, (Andrady, 2017) and are often poured into drainage canals of the rivers (Peng et al., 2017) both asserted that household waste from using personal care products and washing clothing is a significant contributor to fibre pollution in the environment, and larger plastic items break down in rivers due to mechanical and UV aging (Maes et al., 2017). Figure 8 and Table 1 and Table 3 show the shapes of the MPs. The shapes of MPs are classified as fibre (96%), beads (2%), fragment (1%), and film (1%). In core sediments the MPs are classified as fiber (81%) and fragment (19%) (Table 1 and Table 3; Fig. 8).

SIZE CLASSIFICATION OF MICROPLASTICS

The most popular method for quantifying microplastics is visual counting under an optical microscope, but it is labor-intensive and prone to error. MPs size and distribution are governed by UV light intensity, physical conditions, and plastics durability

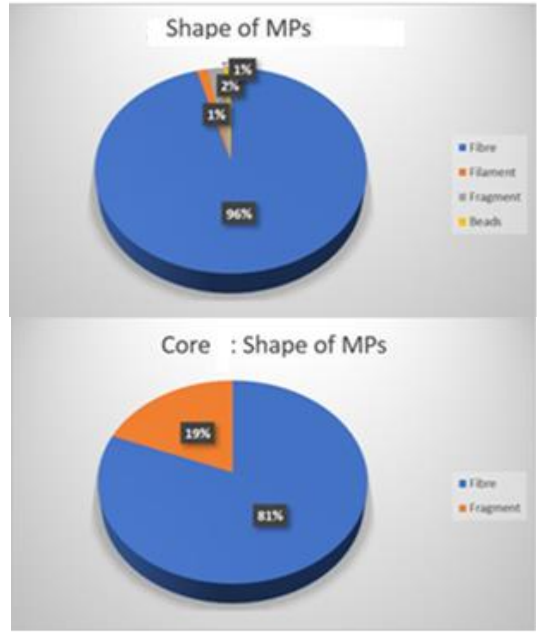

Figure 8. Pie Chart showing the shape classification

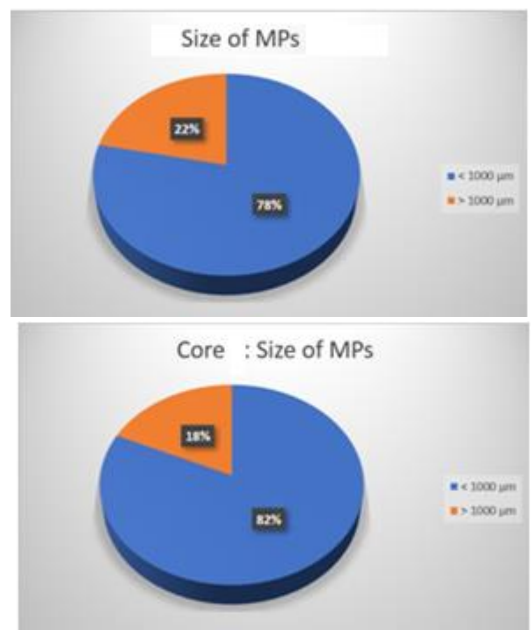

Figure 9. Size classification of MPs

(Thompson et al., 2004; Barnes et al., 2009). The size classification of MPs suggest that the majority of particles fall under < 1000 µm (78%), followed by >1000 µm (22%) in surface sediments. In core sediments MPs are <1000 µm (82%) and >1000 µm (18%). In the sediment core samples the trend of reduced trend of larger microplastics is noted, indicating the difficult vertical mobility capacity of the larger MPs (Fig. 9; Table 1 and Table 3).

COMPOSITION OF MICROPLASTICS

For FTIR analysis, a total of 22 MPs were chosen. Nearly 92.6% to 97.5% of the frequency curve of the MPs composition matched a spectral library for an instrument that is easily available (Fig. 10). The FTIR results revealed that among several types of MPs in surface sediments polyamide, polyethylene, polystyrene, and polypropylene are the predominant polymers. The polymer types in decreasing order are: Polyamide (60%), polyethylene (33%), polypropylene (5%), and polystyrene (2%). Table 2. The polymers in the core samples are: Polyamide (69%) and polyethylene (13%), which are followed by polypropylene (5%) and polystyrene (13%). There are synthetic and natural polyamides. Proteins like those in wool and silk are examples of naturally occurring polyamides. Solid-phase synthesis or step-growth polymerization may be used to create synthetic polyamides, which are then utilized to create products like sodium polyaspartate, nylon, and aramids. Although ethylene may be made from renewable resources, it is often acquired from petroleum or natural gas. Ethylene is the precursor to polyethylene and can be created from these sources as well. Polystyrene have been detected in air, soil, water and sludge. Polystyrene comes from the production of Styrofoam and other products like toys, CDs and cup covers. Polypropylene are the source comes from industries such caps and closures for pallets, crates, bottles, just-in-time storage solutions, bottles and jars for packaging (condiments, detergent, and toiletries), and thin-wall containers (yoghurt cups, disposable hot beverages cups, etc.). Polypropylene is used as rigid packaging.

Figure 10. Pie Chart showing classification of MPs

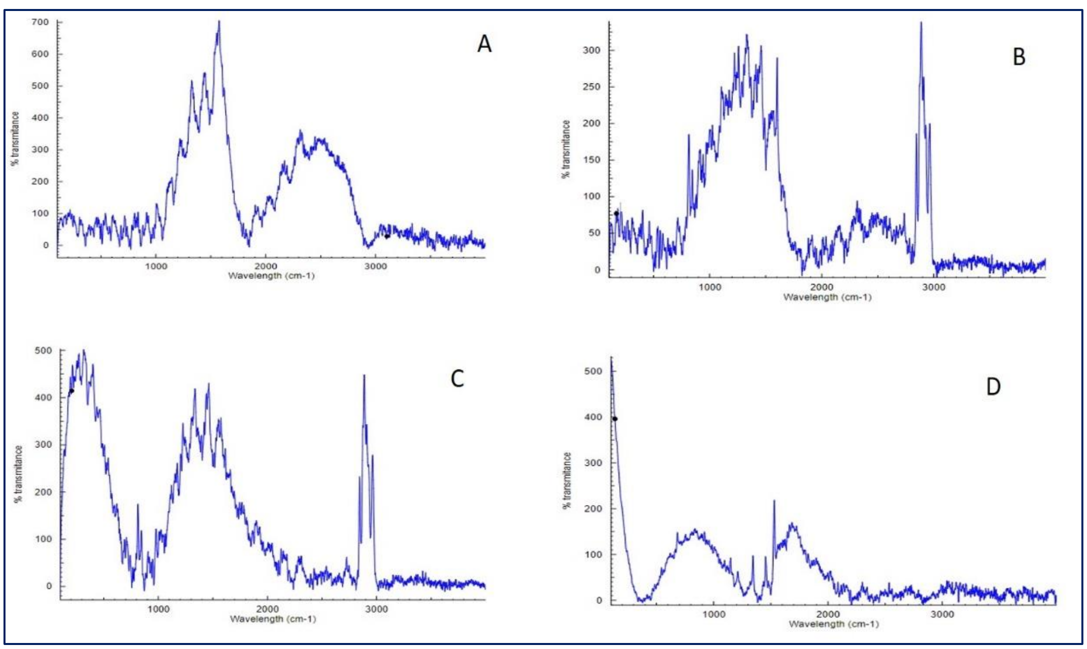

Figure 11. FTIR peaks of MPs: (A) polyamide, (B) polyethylene, (C) polypropylene, and (D) polystyrene

Table 1. Shape and color of microplastics in surface sediments

Shape of MPS	**Fibre**							**Filament**	**Fragment**					**Beads**	**Total**
Colour of (Mps) / S. NO	Transparent	White	Blue	Red	Green	Black	Pink	White	White	Blue	Orange	Pink	Black	Black	
1	2	1	5	6	1	4	0	0	0	0	0	0	0	0	**19**
2	0	1	5	3	1	0	0	0	0	2	0	0	0	0	**12**
3	1	2	9	3	0	1	0	0	0	0	0	0	0	0	**16**
4	0	4	1	4	0	0	0	0	0	0	0	0	0	0	**9**
5	0	9	2	6	1	5	1	2	1	0	0	0	0	0	**27**
6	0	5	3	4	0	0	0	0	0	0	0	0	0	0	**12**
7	0	4	9	5	0	0	0	0	0	0	0	0	0	0	**18**
8	2	5	4	3	1	1	1	2	0	0	0	0	0	2	**21**
9	0	13	5	5	1	0	0	0	0	0	0	0	0	0	**24**
10	1	4	8	5	1	1	0	0	2	0	0	0	0	0	**22**
11	0	1	5	2	1	1	1	0	0	0	0	0	0	0	**11**
12	0	3	7	2	0	2	0	0	0	0	0	0	0	0	**14**
13	1	3	1	3	0	4	3	0	0	0	0	0	0	2	**17**
14	3	0	1	1	3	2	1	0	1	0	0	0	0	0	**12**
15	3	0	4	0	0	4	0	0	2	0	0	1	0	0	**14**
16	1	0	0	4	0	4	0	1	0	0	0	0	0	0	**10**
17	1	0	1	13	1	8	0	0	0	0	0	0	0	0	**24**
18	6	0	8	3	1	1	0	0	0	0	0	0	0	0	**19**
19	6	1	3	2	0	0	0	0	0	0	0	0	0	0	**12**
20	0	0	2	1	2	4	0	0	0	0	0	0	0	0	**9**
21	0	1	1	2	7	7	0	1	0	0	0	0	0	0	**19**
22	2	0	2	5	1	0	0	0	0	0	0	0	0	0	**10**
Total	**29**	**57**	**86**	**82**	**22**	**49**	**7**	**7**	**6**	**2**	**0**	**1**	**0**	**4**	**351**

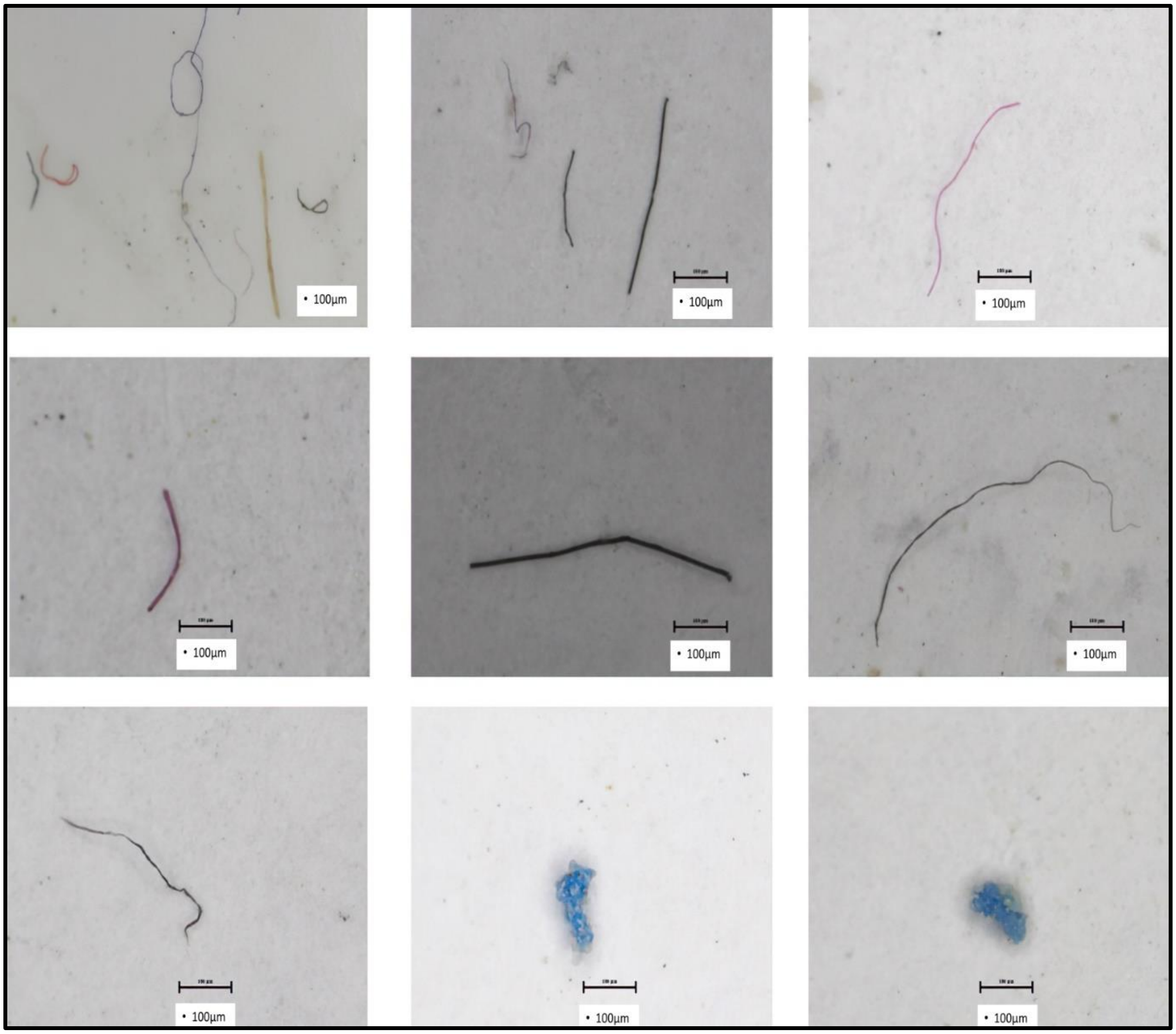

Figure 12. Fibre, filament, and fragments in the Nethravati River estuary sediments

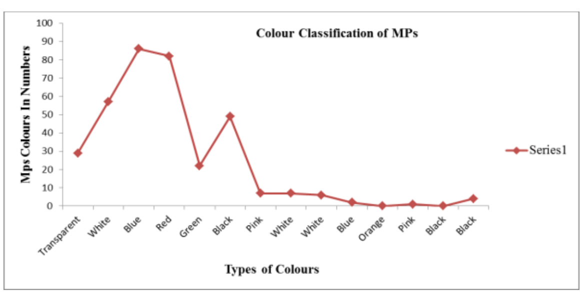

Figure 13. Color versus abundance of MPs

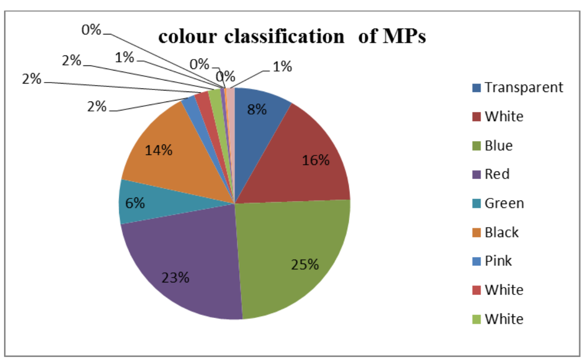

Figure 14. Pie chart showing various colors of MPs

Table 2. Shape and color of microplastics identified in core sediments

Shape of (Mps)	Depth in Inch	**FIBER**					**FRAG MENT**	**Microplastics count in numbers**
Colour of (Mps)		Transparent	Red	Blue	Green	Black	Blue	
S. NO								
1	3.6	5	2	1	0	8	1	**17**
3	10.9	0	0	0	0	3	9	**12**
5	18.15	0	0	0	0	6	7	**13**
7	25.41	0	0	0	0	3	5	**8**
9	32.67	0	3	5	0	7	5	**20**
11	39,93	0	0	3	0	4	0	**7**
13	47.19	0	6	3	2	9	0	**20**
15	54.45	0	2	2	0	5	0	**9**
17	61.71	0	2	1	1	3	0	**7**
19	68.97	0	5	2	0	3	0	**10**
21	76.23	0	2	0	0	2	0	**4**
23	83.49	0	3	0	0	1	0	**4**
25	90.75	0	2	0	0	1	0	**3**
27	98.01	0	1	0	0	0	0	**1**
29	105.27	0	2	0	0	0	0	**2**
31	112.53	0	1	0	0	2	0	**3**
33	119.79	0	2	1	0	0	0	**3**
Total		**5**	**33**	**18**	**3**	**57**	**27**	**143**

MICROTEXTURAL FEATURES OF SAND GRAINS

Quartz, being a common rock-forming mineral, which is resistant to weathering. The sediment grain transportation and depositional processes are reflected by the type of microtextures preserved on quartz grain surfaces (Margolis and Kennett, 1971; Krinsley and Doornkamp, 1973). The mechanical and chemical processes affect sediments during transport and thus the grain surfaces are modified (Al-Saleh and Khalaf, 1982; Armstrong-Altrin, 2020; Armstrong-Altrin et al., 2021, 2022). The quartz surface microstructure of sand grain reflects the depositional environment and differentiates the fluvial, marine, aeolian and glacial environments (Chakroun et al. 2009; Newsome and Ladd 1999). Geologically, Netravathi River basin consists of gneisses, charnockites, felsic and mafic dykes, meta sediments, laterites, alluvium and sand deposits of marine and fluvial origin (CGWB, 2012). Different types of microtextures with mechanical, chemical, and morphological characteristics were identified in this study.

Table 3. Size and polymer types of MPs in surface sediments

S.No	< 1000 µm	> 1000 µm	(PA) polyamide	(PP) polypropylene	(PE) polyethylene	(PP) polypropylene	Total
1	15	4	13	1	5	0	**19**
2	9	3	8	1	3	0	**12**
3	12	4	11	0	5	0	**16**
4	8	1	7	0	2	0	**9**
5	22	5	15	2	9	1	**27**
6	8	4	8	0	3	1	**12**
7	13	5	8	2	7	1	**18**
8	17	4	11	2	7	1	**21**
9	19	5	12	1	11	0	**24**
10	18	4	15	0	7	0	**22**
11	8	3	6	1	4	0	**11**
12	11	3	8	2	4	0	**14**
13	13	4	11	1	5	0	**17**
14	11	1	7	1	5	0	**12**
15	10	4	10	0	4	0	**14**
16	9	1	8	1	1	0	**10**
17	20	4	12	3	7	2	**24**
18	11	8	9	2	7	0	**19**
19	10	2	6	1	5	0	**12**
20	7	2	5	0	4	0	**9**
21	14	5	11	1	7	0	**19**
22	7	3	8	0	2	0	**10**
Total	**272**	**79**	**209**	**22**	**114**	**6**	**351**

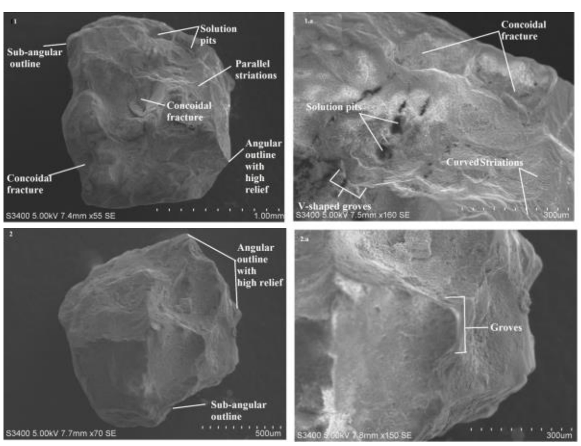

Figure 15. 1 and 1a) Surface micro textures of sand grains showing sub-angular outline, solution pits, parallel striations, and conchoidal fracture. 2) Angular out line with high relief and curved striations. 2a) V-shaped grooves. 3) Angular outline with high relief, sub-angular outline, grooves, chemical solution pit, angular out line, solution pit, sub-rounded outline. 3a) arc shaped steps and V-shaped pit.

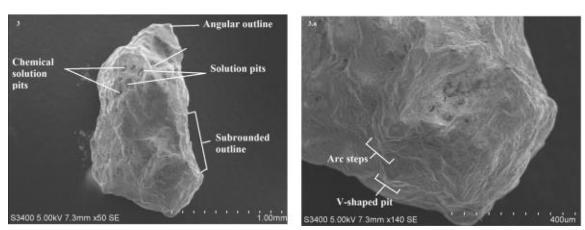

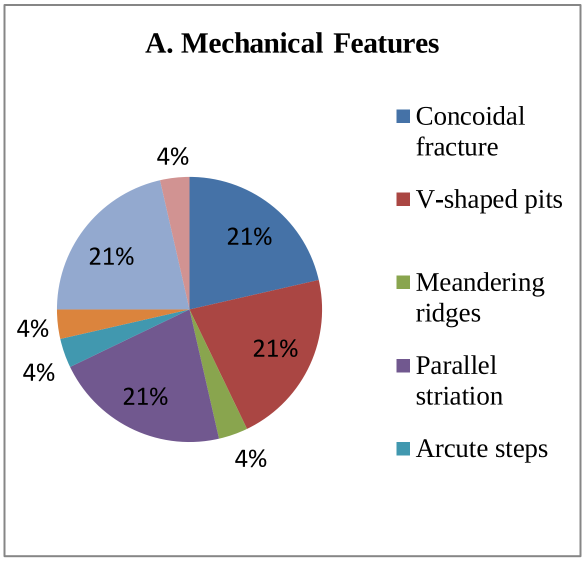

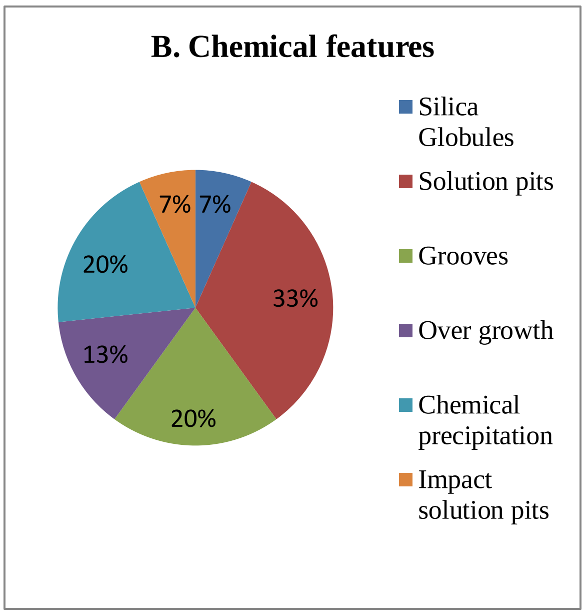

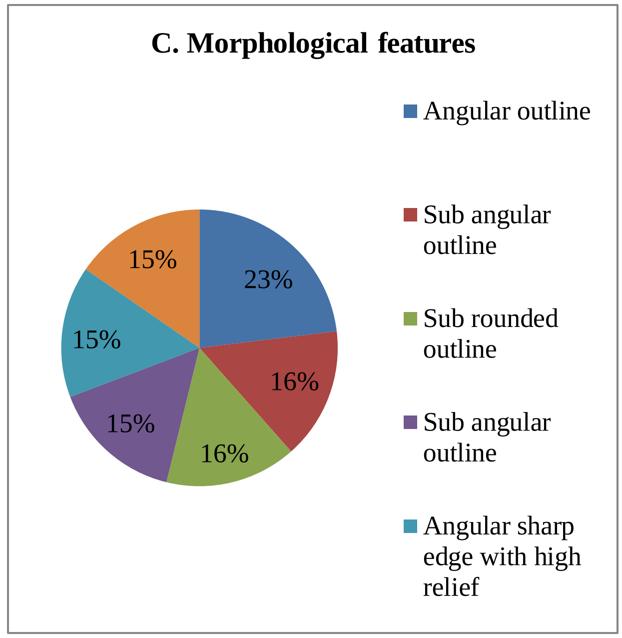

Figure 16. Microtexture types and morphology of quartz grains. A) Mechanical features, B) chemical features, and C) morphological features

MECHANICAL FEATURES

The mechanical features like conchoidal fractures, V-shaped pits, meandering ridges, parallel straight, V-shaped striations, linear fracture line, curved arcuate, arc-shaped and irregular-stepped furrows are recognized on quartz grain surfaces. These features are formed during erosion or weathering processes, grain to grain abrasion and collision during transportation of sediments from their source to the depositional basin. Irregular steeped furrows and meandering ridges are derived from the crystalline source rocks, particularly the straight scratches produced by the high energy environment (Krinsley and Margolis, 1969; Krinsley and Doornkamp, 1973; Krinsley and Marshall, 1987). The V-shaped features are formed by the grain-to-grain collision (Manickam and Barbaroux, 1987) and parallel orientation of groove features might have been caused by collision between two grains during transportation (Krinsley and Donahue 1968; Armstrong-Altrin, 2020). The abundance and size of the V-shaped pits are attributed for long duration with high intensity of subaqueous agitation (Manickam and Barbaroux, 1987). These features are associated with straight and curved scratches suggesting that quartz grains are transported by the fluvial environment (Krinsley and Takahshi, 1962; Krinsley et al., 1964; Madhavaraju et al., 2022) (Fig. 15 and Fig. 16a).

CHEMICAL FEATURES

The chemical precipitation features are associated with silica globules in the sand and are formed by the precipitation of silica from chemical solution due to the long residence of sediments in the depositional basin (Udayaganeshan et al., 2011) under a silica saturated environment (Armstrong-Altrin and Natalhy-Pineda, 2014). The sands of variable grain size with rounded and sub-rounded shapes are attributed to the influence of contaminated sea water (Krinsley and Doornkamp, 1973; Armstrong-Altrin and Natalhy-Pineda 2014). The parallel- grooves on quartz grains are formed by a chemical process at reduced water velocity (Joshi 2009). Over growth, chemical Precipitation features and impact solution pits are derived from the source rock by an action of weathering process (Bull 1977; Bull et al., 1980; Orr and Folk, 1983; Ramos-Vázquez and Armstrong-Altrin, 2020, 2021) (Fig. 15 and Fig. 16b).

MORPHOLOGICAL FEATURES

The quartz grains are showing angular and sub-angular outlines (Fig. 15). Showing angular sharp edges with high relief arcuate steps suggest that the sediments have undergone short transportation and rapid deposition, as a result of which, angular outline is gradually decreased by the action of transportation resulting in downstream rounding of quartz grains.

SOURCE OF MICROPLASTICS

The two main categories of microplastics are microscopic commercially produced particles, including those found in cosmetics, and fibres shed from garments and other materials like fishing nets. Due to the breakdown of larger plastic objects such as water bottles, secondary MPs are created. The primary cause of this breakdown is exposure to external factors, particularly sun radiation. In the present study, all the samples were secondary MPs, indicating that the MPs are the degraded remains of primary microplastics through various degradation processes such as photo-degradation, chemical-degradation, and biological degradation.

CONCLUSIONS

White colored MP's are most common in Nethravati estuary. In core sediments, the shape classification of MPs indicates that the dominant shape is fibre followed by fragment in core. The abundance of fibre indicates the degradation of fishing nets and long transport due to its morphology and the hydrodynamics of the estuary. The size classification of the MPs denotes that the smaller MPs are dominant (<1000 µm) compare to larger MPs. This is due to the greater accumulation capacity of the smaller MPs in the interstitial spaces of a sandy substrate than the inefficiency of the larger microplastics to accommodate them. Polyamide and polyethylene are the most abundant polymer types, followed by polystyrene and polypropylene. Samples numbers 5 and 9 have a greater number of microplastics; in 30 g of sediments, there are 24 to 27 MPs are identified, which is due to fishing and industrial operations. The proximity of metropolitan areas and the sampling location distance from the coast contributed MPs in sediments. The best way to solve this issue is to manage solid waste properly, implement laws that may be adopted, and create an awareness about the defect of MPs to the ecosystem.

REFERENCE

Abayomi, Oyebamiji Abib, Pedro Range, Mohammad A. Al-Ghouti, Jeffrey Philip Obbard, Saeed Hashim Almeer, and Radhouane Ben-Hamadou (2017). Microplastics in coastal environments of the Arabian Gulf. Marine Pollution Bulletin, volume 124, no. 1, pp.181-188.

Andrady and Anthony L. (2011). Microplastics in the marine environment. Marine Pollution Bulletin, volume 62, no. 8, pp.1596-1605.

Al-Saleh S. and Khalaf F.I. (1982) Surface textures of quartz grains from the various recent sedimentary environments in Kuwait. Journal of Sedimentary Petrology, volume 52, pp. 215–225.

Armstrong-Altrin, J.S. (2020). Detrital zircon U-Pb geochronology and geochemistry of the Riachuelos and Palma Sola beach sediments, Veracruz State, Gulf of Mexico: a new insight on palaeoenvironment. Journal of Palaeogeography, vol. 9 (4), article no. 28. DOI: https://doi.org/10.1186/s42501-020-00075-9.

Armstrong-Altrin, J.S. and Natalhy-Pineda, O. (2014). Microtextures of detrital sand grains from the Tecolutla, Nautla, and Veracruz beaches, Western Gulf of Mexico. Mexico: implications for depositional environment and paleoclimate. Arabian Journal of Geosciences, 7, 4321-4333.

Armstrong-Altrin, J.S., Ramos-Vázquez, M.A., Hermenegildo-Ruiz, N.Y. and Madhavaraju, J. (2021). Microtexture and U-Pb geochronology of detrital zircon grains in the Chachalacas beach, Veracruz State, Gulf of Mexico. Geological Journal, 56 (5), 2418-2438.

Armstrong-Altrin, J.S., Ramos-Vázquez, M.A., Madhavaraju, J., Verma, S.K., Macías-Martínez, K. and Martínez-Ruíz, D. (2022). Quartz grain microtextures in the Boca del Cielo and Chocohuital beaches in the Mexican Pacific, Chiapas state: implication on palaeoenvironment. Arabian Journal of Geosciences, 15:1086.

Barnes, David KA, Francois Galgani, Richard C. Thompson, and Morton Barlaz (2009). Accumulation and fragmentation of plastic debris in global environments. Philosophical transactions of the royal society B: biological sciences, volume 364, no. 1526, pp.1985-1998.

Bull, P.A. (1977). Glacial deposits identified by chatter mark trails in detrital garnets: comment. Geology, pp. 5:248.

Bull, P.A., Culver, S.J. and Gardner, R. (1980). Chatter mark trails as paleo environmental indicators. Geology, pp. 318–322.

Carpenter, Edward J., Susan J. Anderson, George R. Harvey, Helen P. Miklas, and Bradford B. Peck (1972). Polystyrene spherules in coastal waters. Science, volume 178, no. 4062, pp.749-750.

CGWB (2012). Central Groundwater information booklet Dakshina Kannada District, Karnataka.

Colton, John B., Frederick D. Knapp, and Bruce R. Burns (1974). Plastic particles in surface waters of the northwestern Atlantic. Science, volume 185, no. 4150, pp.491-497.

Chakroun, A., Miskovsky, J.C. and Zaghbib-Turki, D. (2009). Quartz grain surface features in environmental determination of Aeolian Quaternary deposits in north eastern Tunisia. Mineralogical Magazine, volume 73 (4), pp. 607–614.

Doyle, Miriam J., William Watson, Noelle M. Bowlin, and Seba B. Sheavly (2011). Plastic particles in coastal pelagic ecosystems of the Northeast Pacific Ocean. Marine Environmental Research, volume 71, no. 1, pp.41-52.

Eriksson, Cecilia, and Harry Burton (2003). Origins and biological accumulation of small plastic particles in fur seals from Macquarie Island. AMBIO: A Journal of the Human Environment, volume 32, no. 6, pp. 380-384.

Fendall, L.S. and Sewell M.A. (2009). Contributing to marine pollution by washing your face. Microplastics in facial cleansers. Marine Pollution Bulletin, volume 58, Issue 8, pp. 1225-1228.

Gregory, Murray R., and Anthony L. Andrady (2003). Plastics in the marine environment. Plasticsand the Environment, pp. 379-401.

Hinojosa, Iván A., and Martin Thiel (2009). Floating marine debris in fjords, gulfs and channels of southern Chile. Marine Pollution Bulletin, volume 58, no. 3, pp. 341-350.

Higgs, R. (1979). Quartz grain surface features of Mesozoic-Cainozoic's and from the Labrador and Western Greenland continental margins. Journal of Sedimentary Petrology, volume 49 pp. 599–610.

Hall, N.M., K.L.E. Berry, Llew Rintoul, and M.O. Hoogenboom (2015). Microplastic ingestionby scleractinian corals. Marine Biology, volume 162, no. 3, pp.725-732.

Hankins, Cheryl, Allyn Duffy, and Kathryn Drisco (2018). Scleractinian coral microplastic ingestion: potential calcification effects, size limits, and retention. Marine Pollution Bulletin, volume 135, pp.587-593.

Hidalgo-Ruz, V., Gutow, L., Thompson, R.C. and Thiel, M. (2012). Microplastics in the Marine Environment: A Review of the Methods Used for Identification and Quantification. Environmental Science & Technology, 46, 3060-3075.

Kalogerakis, N., Karkanorachaki, K., Kalogerakis, G., Triantafyllidi, E.I., Gotsis, A.D., Partsinevelos, P., Fava, F. (2017). Microplastics generation: onset of fragmentation of polyethylene films in marine environment mesocosms. Frontiers in Marine Sciences, volume 4, pp.84.

Karnataka Irrigation Department (1986). River Discharge Data. No. 5, Gauging Sub-division, Shimoga, India

Krinsley DH. and Doornkamp, JC (1973). Atlas of quartz sand surface textures. Cambridge University Press, Cambridge, pp. 91.

Krinsley DH, Marshall JR (1987). Sand grain textural analysis: an assessment. In: Marshall JR (ed) Clastic particles: scanning electron microscopy and shape analysis of sedimentary and volcanic clasts. Van Nostrand-Reinhold, New York, pp 2–15.

Krinsley DH, Takahshi T (1962). Applications of electron microscopy to geology. Transactions of the New York Academy of Sciences. Transactions of the New York Academy of Sciences volume 25 pp. 3–22.

Lusher, Amy L., Matthew Mchugh, and Richard C. Thompson (2013). Occurrence of microplastics in the gastrointestinal tract of pelagic and demersal fish from the English Channel. Marine Pollution Bulletin, volume 67, no. 1-2, pp. 94-99.

Masura, Julie, Joel Baker, Gregory Foster, and Courtney Arthur (2015). Laboratory Methods for the Analysis of Microplastics in the Marine Environment: Recommendations for quantifying synthetic particles in waters and sediments.

Murthy, T.R.S.; Madhyastha, M.N.; Rao, I.J., and Chandrasek- Harappa, K.N. (1988). A study of physical determinants of natural environments and their impact on land use in Netravati and Gur- pur river basins of Western Ghat region, Karnataka. Department of Environment and Forest, Government of India, New Delhi, Project Report, pp 60.

Madhavaraju, J., Armstrong-Altrin, J.S., Selvaraj, K. and James, R.A. (2022). Microtextures on quartz grains from the Gulf of Mexico and the Mexican Pacific coastal sediments: Implications for sedimentary processes and depositional environment. Journal of Palaeogeography, 11(2): 257-275.

Manickam S, Barbaroux (1987). Variations in the surface texture of suspended quartz grains in the Loire River: an SEM study. Sedimentology, volume 34 pp. 495–510.

Naidu, S.A. (2019). Preliminary study and first evidence of presence of microplastics and colorants in green mussel, Perna viridis (Linnaeus, 1758), from southeast coast of India. Marine Pollution Bulletin, volume 140, pp. 416-422.

Neves, Diogo, Paula Sobral, Joana Lia Ferreira, and Tânia Pereira (2015). Ingestion of microplastics by commercial fish off the Portuguese coast. Marine Pollution Bulletin, volume 101, 1, pp. 119-126.

Newsome D. and Ladd P. (1999). The use of quartz grain microtextures in the study of the origin of sand terrains in Western Australia. Catena, volume 35 pp. 1–17.

Nor and Obbard, (2014). Microplastics in Singapores coastal mangrove ecosystems Marine Pollution Bulletin, volume 79 (1–2) (2014), pp. 278-283.

Peng, Guyu, Bangshang Zhu, Dongqi Yang, Lei Su, Huahong Shi, and Daoji Li. (2017). Microplastics in sediments of the Changjiang Estuary, China. Environmental Pollution, volume 225, pp. 283-290.

Ramos-Vázquez, M.A. and Armstrong-Altrin, J.S. (2020). Provenance and palaeoenvironmental significance of microtextures in quartz and zircon grains from the Paseo del Mar and Bosque beaches, Gulf of Mexico. Journal of Earth System Science, 129:225 https://doi.org/10.1007/s12040-020-01491-0.

Ramos-Vázquez, M.A. and Armstrong-Altrin, J.S. (2021). Provenance of sediments from Barra del Tordo and Tesoro beaches, Tamaulipas State, northwestern Gulf of Mexico. Journal of Palaeogeography, 10:20, 1-17. https://doi.org/10.1186/s42501-021-00101-4

Reichert, Jessica, Johannes Schellenberg, Patrick Schubert, and Thomas Wilke (2018). Responses of reef building corals to microplastic exposure. Environmental Pollution, volume 237, pp. 955- 960.

Reddy, M.P.M.; Hariharan, V., and Kurian, N.P. (1979). Sediment movement and siltation in the navigational channel of Old Man- galore Port. Proceedings of Indian Academy of Sciences, volume 88 (Part II), pp 121-130.

Sruthy, Shini, and E.V. Ramasamy (2017). Microplastic pollution in Vembanad Lake, Kerala, India: the first report of microplastics in lake and estuarine sediments in India. Environmental Pollution, volume 222, pp. 315-322.

Subramanian, V Biksham, G, and Ramesh, R. (1987). Environmental geology of peninsular river basins of India. Journal of Geological Society of India. volume 30 pp 393 -401.

Syakti, Agung Dhamar, Rafika Bouhroum, Nuning Vita Hidayati, Chandra Joei Koenawan, Abdelaziz Boulkamh, Isdy Sulistyo, Stephanie Lebarillier, Syafsir Akhlus, Pierre Doumenq, and Pascal Wong-Wah-Chung, (2017). Beach macro-litter monitoring and floating microplastic in a coastal area of Indonesia. Marine Pollution Bulletin, volume 122, no. 1-2, pp. 217-225.

Tamminga, Matthias, Elena Hengstmann, and Elke Kerstin Fischer, (2018). Microplastic analysis in the South Funen Archipelago, Baltic Sea, implementing manta trawling and bulk sampling. Marine Pollution Bulletin, volume 128, pp. 601-608.

Thompson, Richard C., Ylva Olsen, Richard P. Mitchell, Anthony Davis, Steven J. Rowland, Anthony WG John, Daniel McGonigle, and Andrea E. Russell, (2004). Lost at sea: where is all the plastics? Science, volume 304, no. 5672, pp. 838-838.

Udayaganeshan P, Angusamy N, Gujar AR, and Rajamanickam GV (2011). Surface microtextures of quartz grains from the central coast of Tamil Nadu. Journal of the Geological Society of India, volume 77. pp. 26-34.

Vidyasakar, A., K. Neelavannan, S. Krishnakumar, G. Prabaharan, T. Sathiyabama Alias Priyanka, N. S. Magesh, Prince S. Godson and S. Srinivasalu, (2018). Macrodebris and microplastic distribution in the beaches of Rameswaram Coral Island, Gulf of Mannar, Southeast coast of India: a first report. Marine pollution bulletin, volume 137, pp. 610-616.

Wang, J., Tan, Z., Peng, J., Qiu, Q. and Li, M. (2016). The behaviors of microplastics in the marine environment. Marine Environmental Resource. volume 113, pp no 7–17.

Wang, J., Peng, J., Tan, Z., Gao, Y., Zhan, Z., Chen, Q. and Cai, L. (2017). Microplastics in the surface sediments from the Beijiang River littoral zone: Composition, abundance, surface textures and interaction with heavy metals. Chemosphere, volume 171, pp. 248-258.

Wright, S. L., Rowe, D., Thompson, R. C. and Galloway, T. S. (2013). Microplastic ingestion decreases energy reserves in marine worms. Current Biology, volume 23(23), pp. 1031–1033.

Wu, Chenxi, Kai Zhang, and Xiong Xiong (2018). Microplastic pollution in inland waters focusing on Asia. In Freshwater microplastics 85-99.

Xiong, Xiong, Kai Zhang, Xianchuan Chen, Huahong Shi, Ze Luo, and Chenxi Wu, (2018). Sources and distribution of microplastics in China's largest inland lake–Qinghai Lake. Environmental pollution, volume 235, pp. 899-906.

Zhang, Jian-Dong, You-Shao Wang, Hao Cheng, Zhao-Yu Jiang, Cui-Ci Sun, and Mei-Lin Wu. (2015). Distribution and sources of the polycyclic aromatic hydrocarbons in the sediments of the Pearl River estuary, China. Ecotoxicology, volume 24, no. 7, pp.1643-1649.

Received on : *27th March 2023*
Revised accepted on : *11th May 2023*

JOURNAL INDIAN ASSOCIATION OF SEDIMENTOLOGISTS ISSN NO 2582 – 2020
Vol. 40, Issue 1, 2023, pp. 43-54
DOI: https://doi.org/10.51710/jias.v40iI.284

Reservoir characterization and rock eval pyrolysis of clastic sedimentary rocks in the Geku Formation, Arunachal Pradesh, North-eastern India

Anannya Bordoloi[1], Ananya Chutia[1], and Chaitra Dhar Taye[2]

[1] Department of Geology, Cotton University, Guwahati, Assam-781001
[2] Department of Geology, Jagannath Barooah College (Autonomous), Jorhat, Assam-785001
E-mail: GLY1891002_anannya@cottonuniversity.ac.in

ABSTRACT

The present investigation aims to decipher the reservoir quality and source rock potential of the sandstones and shales of the Geku Formation of the Yinkiong Group, Eastern Himalaya, NE India. To achieve the goal, sandstone petrography and rock-eval pyrolysis of shale aided with X-Ray diffraction have been employed. A petrographic study revealed that the detrital constituent of the sandstones is mainly quartz, feldspar, and lithic fragments. Authigenic cements such as carbonate and clay bind the detrital materials as indicated by petrographic as well as X-Ray diffraction study. Clay minerals include illite, smectite-montmorillonite and kaolinite. The studied sandstones underwent compaction as evidenced by the formation of concavo-convex and sutured grain contacts, which also suggest its phyllomorphic stage of diagenesis. The presence of calcite and clay cement has led to reduction of the porosity and permeability of sandstones, which is also substantiated by sorting and irregular grain shapes such as sub-angular, angular, and sub-rounded, thereby affecting reservoir quality. The rock eval pyrolysis data suggests that the Yinkiong shales have poor source rock potential with dominantly kerogen type III. The geochemical parameters of the studied shales suggest mostly immature and postmature organic matter and the very low TOC values indicate poor organic richness.

Keywords: Geku Formation, Petrography, Reservoir characterisation, Diagenesis, Rock eval pyrolysis

INTRODUCTION

Rift basins are known to bear abundant hydrocarbon reservoirs and source rocks worldwide (Morley, 1999). But structural deformations and basin fill stratigraphy also comes into play while determining whether it has hydrocarbon bearing potential or not (Lambiase and Morley, 1999). The stratigraphic succession in the syn- and post-rift phases of basin evolution is largely responsible for the presence and distribution of hydrocarbons in rift basins. The kind of post-rift tectonics and whether marine or non-marine strata predominate in basin fill are important factors (Lambiase and Morley, 1999).

The Paleogene sediments of Eastern Himalaya have been deposited in a rift basin, which developed after the north-eastern edge of the Indian plate separated and begun to rotate clockwise during India-Asia collision (Beaumont et al., 2001; Cook and Royden, 2008; Houseman and England., 1993; Sarma et al., 2020). The Himalayan orogenic movement began as a result of north-south compressional forces caused by the India-Asia collision. As the Burmese Plate continued to converge further, which deformed the rift basin sediments (Sarma et al., 2020). After the development of the rift basin, the Yinkiong Group rocks were thrusted and hence intensely deformed due to a WNW-ESE compressional force which was created when the Indian plate started colliding with the Burmese plate (Sarma et al., 2020). Moreover, the Geku Formation sediments have been found to be of continental facies which deposited in a terrestrial environment, although there was a shift in provenance and the depositional environment in the foreland basin changed to marine which could be the

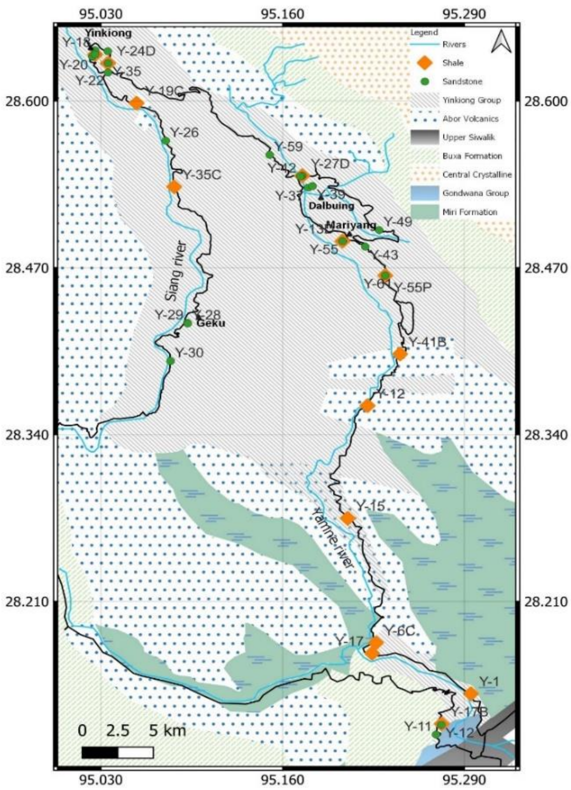

Fig. 1: Geological map of study area (Modified after Acharyya, 2007; Taye, 2015; Taye & Bhattacharyya, 2017)

result of the collision between the Indian and Asian plates (Baral et al., 2019; Bordoloi et al., 2022). One significant factor that contribute to rift-basin stratigraphy, and hence, hydrocarbon potential, are whether the syn- and post-rift basin fill is dominantly marine or non-marine sediment. It has been found that rifts with marine fills are more prolific hydrocarbon reserves than those with non-marine rifts (Lambiase and Morley, 1999).

Tripathi and Mamgain (1986) compared the larger foraminiferal assemblage record from Subathu Formation with that from Yinkiong Group of Eastern Himalaya in similar stratigraphic/tectonic setup and suggested the continuity of Subathu sea all along the Himalayan frontal zone up to Arunachal Pradesh (Tripathi et al. 1981; Tripathi and Mamgain, 1986; Chutia et al. 2019; Jafar and Singh, 1992). Similar Palaeocene to Miocene marine strata has been reported from Gamba, Tingri and Yadong sections in southern Tibet and throughout the Himalaya and were correlated with the Yinkiong and Subathu Formation (Jiang et al., 2016). Organic geochemical analysis of Subathu Formation has suggested the prevalence of Type III (gas prone) kerogen with high TOC content (average 7.5%). These rocks have been found to exhibit poor to excellent hydrocarbon potential with Tmax and Ro (vitrinite reflectance) values indicating wet gas to dry gas generation window (Hafiz et al., 2022). Hydrocarbon potential study of Subathu Formation sediments based on palynofacies analysis and Thermal Alteration Index values has indicated that these sediments display moderate to good gaseous hydrocarbon generation (Thakur and Dogra, 2011).

In Holocene stratigraphic division, the prospect of sedimentary environment and coal accumulations has been accomplished by a few scholars but there hasn't been a significant development in Palaeocene-Eocene oil and gas exploration. The Yinkiong Group of the Eastern Himalayas, due to its unique stratigraphic position, has been a topic of discussion lately. Few scholars (Tripathi et al., 1979; Singh.,1984; Chutia et al., 2019; Baral et al., 2019; Sarma et al., 2020; Bordoloi et al., 2022) have extensively studied the eastern Himalayan Cenozoic sediments with the help of geochemistry, petrography, clay mineralogy and tectonics to evaluate the depositional environments. But no detailed reports on hydrocarbon potential of the Yinkiong Group in terms of reservoir quality and source rock potential have been found. Hence, the proposed study is encouraged by the lack of hydrocarbon potential study of sediments in the Eastern Himalaya (Fig-1). The present study encompasses the characterization of reservoir and source rock potential of sandstones and shales based on petrography, X-Ray diffraction, and rock eval pyrolysis data.

REGIONAL GEOLOGY AND TECTONICS

The Geku formation of Yinkiong Group comprises sedimentary rocks consisting of variegated shale (grey, green and purple) with sandstone of Palaeocene-Eocene age and are exposed along the Siang and Yamne river sections. The rocks of these areas are intensely deformed with complex folding and varies in age from Late Palaeocene to early Eocene. These Paleogene rocks have been believed to hold the record of events that occurred during India-Asia collision. The Main Central Thrust (MCT) and the Main Boundary Fault (MBT) are two major tectonic features of Eastern Himalayas as it is in the western Himalayas. The MBT marks the boundary between the Palaeocene-Eocene Yinkiong Group and the Siwalik Group, where the Siwalik sediments have been thrusted over by the older sediments in the Siang valley and is of ENE-WSW trend (Kumar, 1997). These rocks have undergone intense deformation and have been faulted and folded into anticlines and synclines with axial planes dipping towards north west of the Siang valley. The Himalayan orogeny had quite a significant influence on the sedimentation of Siang valley. The India-Asia collision took place during the Palaeocene-Eocene at ~65 Ma resulting in the separation of the north-eastern edge of the Indian plate and this portion underwent a clockwise tectonic rotation due to compression and commenced the development of a rift basin, where Yinkiong Group sediments were deposited during Late Palaeocene-Early Eocene (Beaumont et al., 2001; Cook and Royden, 2008; Houseman and England, 1993; Sarma et al., 2020). The India-Asia collision gave rise to N-S compressional forces and this marked the beginning of Himalayan orogeny (Sarma et al., 2020). Later, the Indian plate converged with the Burmese plate to produce WSW-ENE compressional forces and due to these two compressions, thrusting took place over Palaeocene-Eocene sediments and gave rise to a number of faults and tight folds and deformation of Yinkiong Group sediments took place (Sarma et al., 2020). At the centre of the Siang Window in the Eastern Himalayan Syntaxis, a deep sequence of fossiliferous Paleogene sediments interbedded with the Abor Volcanics is exposed beneath up-arched MBT (Acharyya, 1994; Sengupta et al., 1996). Although these sediments tectonically hidden in the foothills of Bhutan and Arunachal Pradesh, the Palaeogene sediments are well exposed at the centre of the Siang Window at the Eastern Himalayan Syntaxis. (Acharyya, 2007). In the upper and east Siang districts of Arunachal Pradesh, there is a laterally continuous exposure of Yinkiong Group of rocks along Mariyang-Yinkiong and Yinkiong-Geku road sections (Chutia et al., 2019; Bordoloi et al., 2022). The Yinkiong Group is divided into the late Palaeocene to early Eocene lower Geku Formation consisting of fine-medium grained sandstone and variegated shale (purple, grey, and green) associated with basic volcanics and early to middle upper

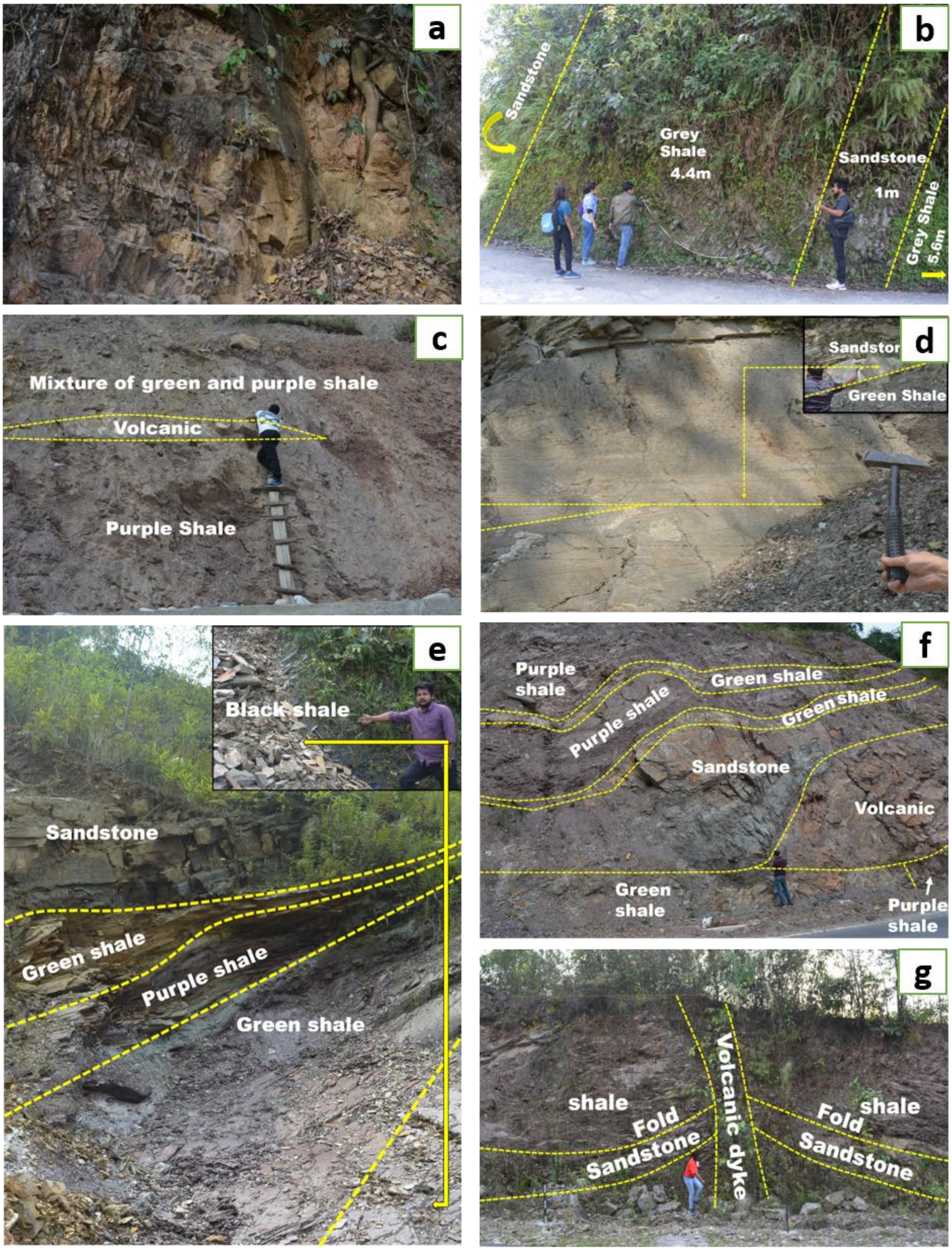

Fig. 2: (a) Well bedded sandstone Geku type section sandstone, (b) An outcrop of shale-sandstone alteration; The sandstone exposed here is fine to medium-grained exhibiting thin laminae, (c) An outcrop of purple and green shale with a band of intermixed volcanics in between the shale beds, (d) Sandstone and shale exposures with sandstone exhibiting ripple marks and current beddings, (e) An exposure of Sandstone-green shale-purple shale-green shale-black shale alteration, (f) Large exposure of green shale-purple shale-sandstone alternations with volcanic below and above green shale, and (g) A folded sandstone-shale outcrop intruded by volcanic dyke.

Eocene Dalbuing Formation comprising of shale, sandstone and limestone. The Geku Formation comprises of massive well jointed sandstones which are well exposed in and around Geku Town (Fig. 2a). The outcrop along Yinkiong-Geku road section, laterally along the left bank of Siang river with frequent sandstone-shale alterations (Fig. 2b) indicating a transitional environment of deposition. The concordant relationship between the volcanics and the folded and thrusted Yinkiong Group of rocks further points to syn-sedimentary volcanism in the shale-sandstone sequence (Fig. 2c). Cross bedded white to pale sandstones also exhibiting ripple marks are present near Mariyang on the way out of Dalbuing village (Fig. 2d). The Gondwana Group comprising of quartzite, sandstone and grey to black shale is thrusted over by the Yinkiong Group rocks and this contact is evident from the carbonaceous black shale in contact with the variegated shales of Geku Formation (Fig. 2e). The Abor volcanic rocks also show discordant relationship with Geku Formation in the form of dyke cutting across a sandstone and shale outcrop near Mariyang (Fig. 2f & 2g).

MATERIALS AND METHODS

Fresh samples belong to Yinkiong Group were collected along the Mariyang-Yinkiong and Yinkiong-Geku road section for a consolidated petrographic and rock eval pyrolysis study. Twenty-two fresh sandstone samples have been selected for petrographic investigation and studied under optical microscope at Department of Geology, Cotton University in order to examine the reservoir characteristics. During this procedure, detrital and diagenetic minerals and properties such as porosity and sorting were determined.

In order to detect the source rock potential of Yinkiong Group, a total of 15 shale samples were selected in order to obtain the pyrolysis data from which the kerogen type and maturity were determined. The samples were powdered and the pyrolysis was carried out as described by Hunt (1995) nd Lafargue et al. (1998). The geochemical data obtained from this analysis is then plotted to determine the maturation level and quality of kerogen. To determine TOC and Tmax, selected shale samples were examined using a Rock-Eval 6 instrument using the Basic/Bulk-Rock programmed pyrolysis procedure for source rocks at Indian Institute of Technology, Bombay (IIT). The clay mineralogical composition (including non-clay minerals) has been studied using X-Ray Diffraction (XRD) analysis. Pulverised fine bulk powder samples were considered for the XRD analysis, which was performed using Philips X'Pert Pro, a fully automated computerized powdered XRD technology (using Cu Kα radiations) at the Department of Instrumentation and USIC, Gauhati University and obtained X-Ray diffractogram patterns have been identified by following the published data (Tucker, 1988).

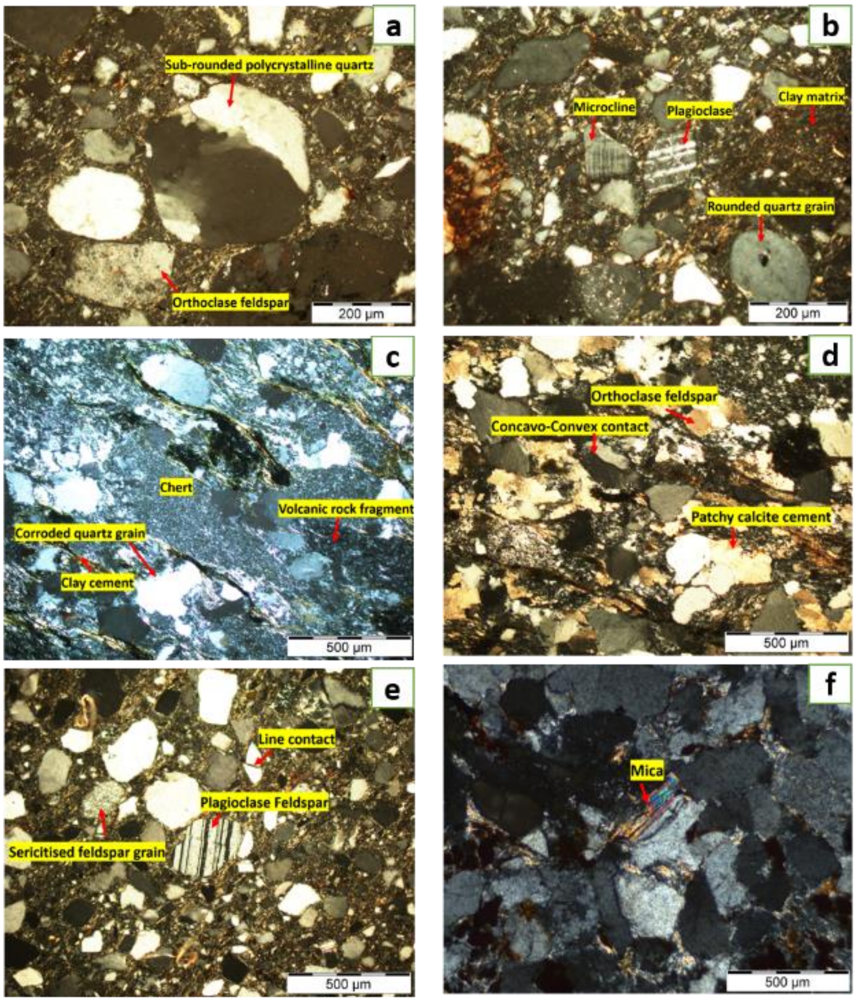

Fig. 3: Photomicrographs of sandstones showing: (a) Sub-rounded polycrystalline quartz and orthoclase feldspar in poorly sorted framework, (b) Microcline, plagioclase feldspar and a rounded monocrystalline quartz grain, (c) Intense deformation characterized by corroded quartz grain and stretched alignment of cement and grains, (d) Intergranular spaces occupied by calcite cement blocking almost all porosity, (e) Sericitized feldspar and another feldspar grain with prominent twinning; also displaying line contact owing to compaction, and (f) Bending of mica flakes, angular quartz grains and clay cement dominating a moderately sorted sandstone.

RESULTS

PETROGRAPHY

The petrographic study of sandstones reveals that they are fine to medium-grained comprising mostly of sub-angular to angular and sub-

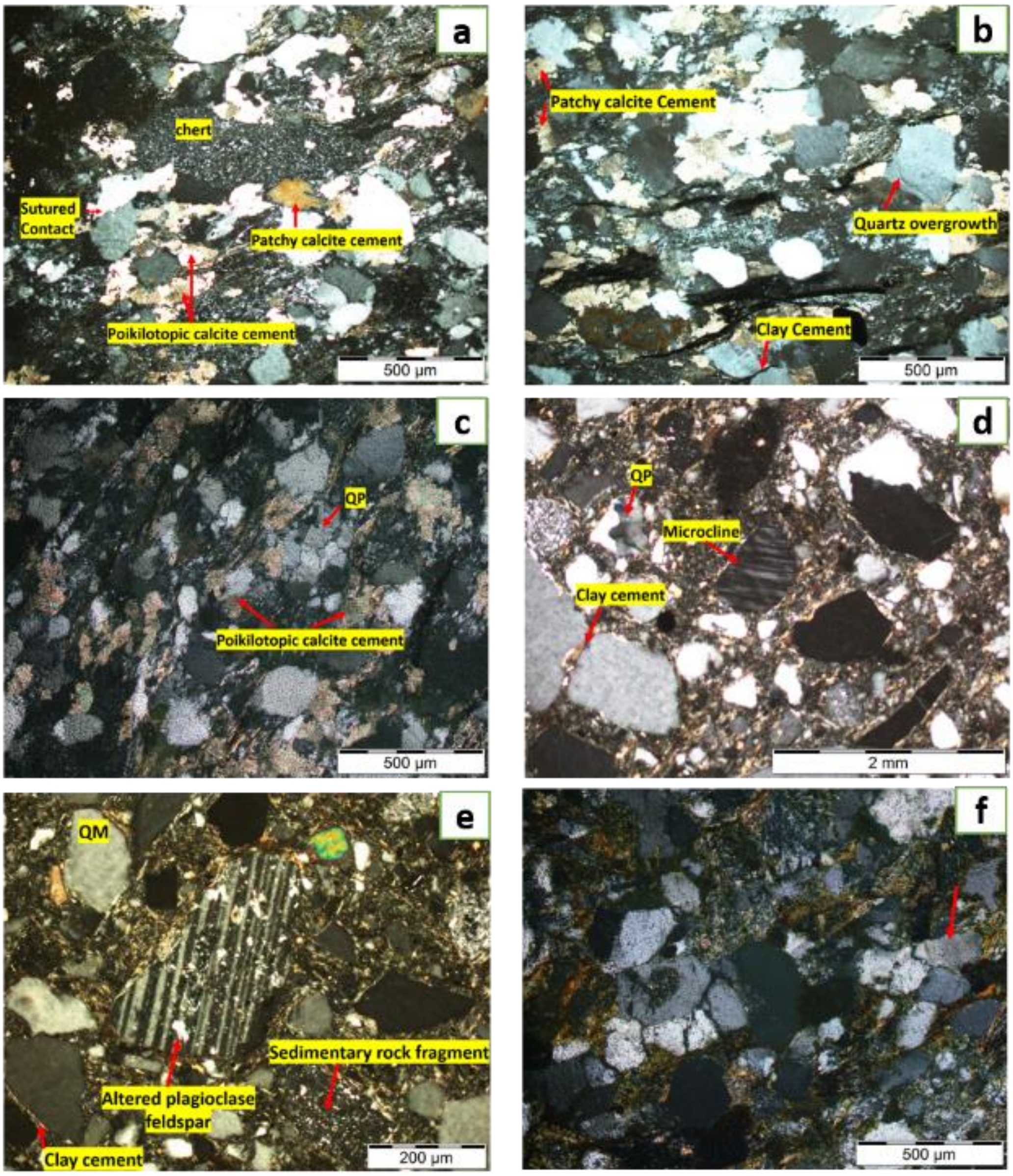

Fig. 4: Photomicrographs of sandstones of Geku Formation. (a) Typical calcite cemented sandstone with sutured grain contacts all indicating signs of compaction and cementation, (b) Patchy calcite cement and quartz overgrowth, (c) Poikilotopic calcite cement engulfing several quartz grains at a time. Also showing polycrystalline quartz (Qp) and quartz overgrowth, (d) Polycrystalline quartz and microcline, (e) Partially altered plagioclase feldspar, grain coating clay cement and sedimentary rock fragment in a poorly sorted sandstone, and (f) Partially albitized K-feldspar grains.

rounded quartz grains (Fig. 3a). Few rounded grains are also observed which are quartz and feldspar (Fig. 3b). All the sandstone samples are moderate to poorly sorted. Quartz grains present are both monocrystalline and polycrystalline, with an average quartz percentage 70 %. Some quartz grains have a relatively dense contact relationship such as line, concavo convex and sutured, because of which pores are significantly less (3d, 3e and 4a). Most of the quartz crystals are deformed and a few have undergone corrosion (Fig. 3c). The feldspar content in these sandstones is low and averages about 11.5%. Commonly found feldspar are orthoclase, microcline and plagioclase (Fig. 3d and 3e). The different feldspar grains vary in size from fine to coarse with subhedral shape. A few feldspars have also been sericitized (Fig. 3e). The mica grains present are bended (Fig. 3f) and platy and a few have been deformed when sandwiched between quartz grains and cement. Minor amounts of lithic fragments are also present. The main diagenetic elements found in the studied sandstones are cementation, compaction, alteration and development of different grain contacts. Cement types identified are mainly calcite, clay and silica (in the form of quartz overgrowths). Calcite occurs as patches as well as poikilotopic pore filling cement (Fig. 4a, 4b, and 4c). The mechanical compaction as a result of increased burial during diagenesis indicated by development of authigenic

TABLE 1: Results of rock eval pyrolysis of studied shales of Geku Formation

Sample no.	Qty - (mg)	S1 (mg/g)	S2 (mg/g)	S3 (mg/g)	S1+S2 (GP)	S1/S1+S2 (PI)	Tmax (˚C)	HI	OI	TOC (%)
Y2-17B	60.75	0.01	0.01	0.27	0.02	0.5	488	100	2700	0.01
Y2-41B	60.23	0.01	0	0.14	0.01	1	581	0	1400	0.01
Y2-61B	60.76	0.01	0	0.14	0.01	1	283	0	1400	0.01
Y2-19C	60.92	0.01	0	0.11	0.01	1	301	0	1100	0.01
Y2-35C	60.46	0.02	0	0.07	0.02	1	326	0	24	0.29
Y2-24D	60.86	0.01	0	0.08	0.01	1	499	0	0	0
Y2-27D	60.33	0.02	0.03	0.18	0.05	0.4	356	150	900	0.02
Y2-13D	60.67	0.02	0	0.06	0.02	1	549	0	300	0.02
Y2-27M	60.68	0.04	0.01	0.15	0.05	0.8	327	100	1500	0.01
Y2-55P	60.31	0.01	0	0.04	0.01	1	440	0	0	0
Y-1	60.56	0.02	0.12	0.1	0.14	0.13	433	133	111	0.09
Y-6C	60.61	0.01	0.05	0.11	0.06	0.2	449	83	183	0.06
Y-12	60.36	0.01	0.05	0.03	0.06	0.17	595	15	9	0.34
Y-15	60.71	0.01	0.03	0.19	0.04	0.19	450	7	41	0.46
Y-17	60.75	0.02	0.04	0.02	0.06	0.36	486	200	100	0.02
Average	60.59	0.015	0.023	0.11	0.038	0.65	437.53	52.53	651.2	0.09

quartz in the form of quartz overgrowths (Fig. 4c) and bending of mica flakes have greatly affected the reservoir quality of the studied sandstones. Calcite cement is fairly abundant in the sandstones blocking almost all of the porosity thereby controlling reservoir quality.

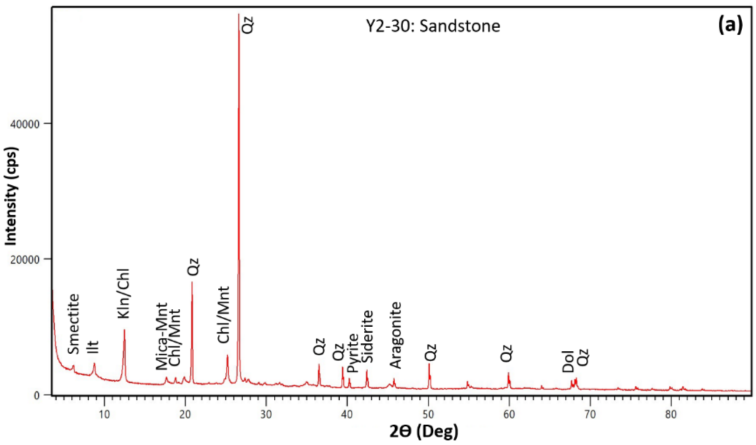

ROCK EVAL PYROLYSIS

The rock eval pyrolysis data are reported in Table 1. Tmax average value is about 437.5, which ranging from 283 to 595°C. The results show very erratic Tmax and PI (Production Index) values and low pyrolysis values such as S2 about 0.023 mg HC/g rock, S3 about 0.11 mg HC/g rock,

TOC about 0.09 wt. %, HI about 52.5 mg HC/g TOC and highly variable OI about 0-2700 mgHC/gTOC. Total organic carbon (TOC) content of the shale samples ranges from 0 to 0.46 and averages 0.09 %. Maximum TOC value is 0.46, which suggest poor organic richness. The studied samples show poor hydrocarbon generation potential, GP (S1+S2) with values ranging from 0.01 to 0.14 mg HC/g rock. The Production Index (PI) is an indication of the amount of hydrocarbon, which has been produced geologically relative to the total amount of hydrocarbon, the sample can produce. The PI (=S1/(S2+S3)) (Peters and Cassa, 1994) value of the studied shales, which is also an indication of thermal maturity, range from 0.13 to 1.0, which indicates immature to mature

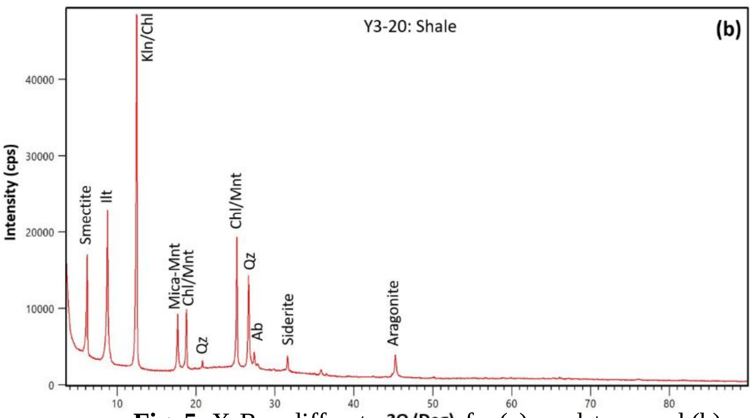

Fig. 5: X-Ray diffractograms of a (a) sandstone and (b) shale of the Geku Formation

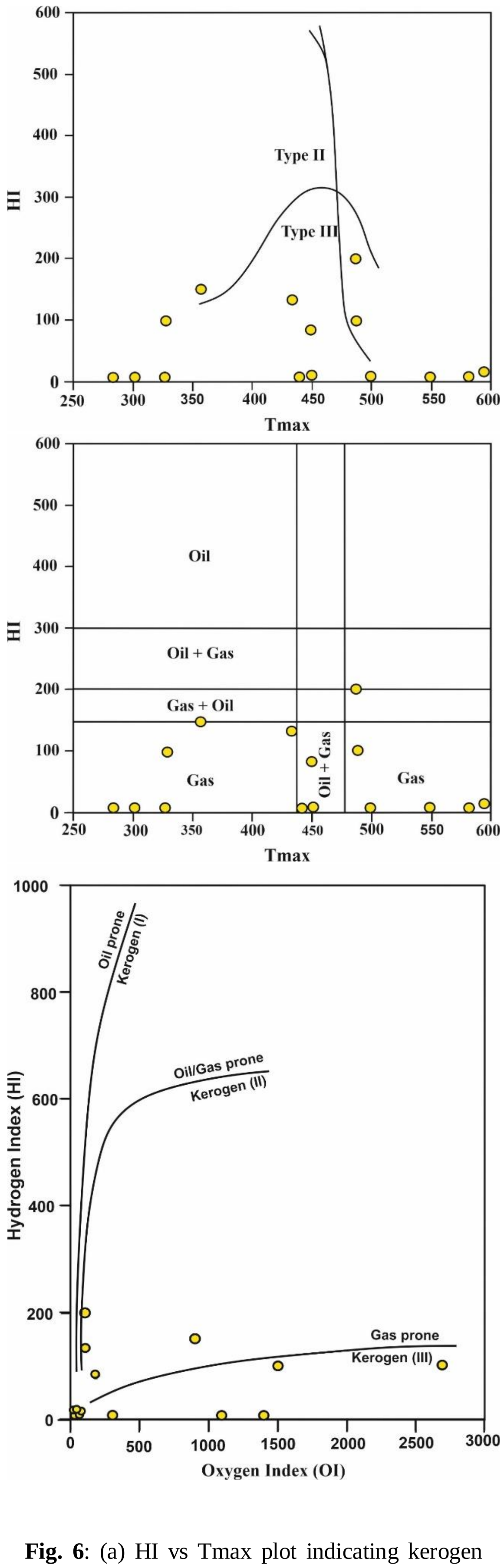

Fig. 6: (a) HI vs Tmax plot indicating kerogen type, (b) HI vs Tmax plot indicating whether it is gas prone or oil prone source rock, (c) HI versus OI plot showing the type of kerogen, and (d) HI vs Tmax plot showing the maturity level of kerogen

as well as postmature organic matter. HI value for most of the samples is less than 100 mg HC/g TOC with an average value of 52.5 indicating a gas generative type of kerogen (Type III). The geochemical data obtained from rock eval pyrolysis have been plotted on the kerogen classification diagram (Fig. 6c) where HI is plotted against OI in the Pseudo Van Krevelen diagram (Van Krevelen, 1961; Tissot et al., 1974) for delineating kerogen type and it suggests the abundance of Type III (gas prone) organic matter. The Tmax values of these rocks range from 283 to 595 °C, which suggests immature to postmature gas generation stage. Although some of them fall under the immature field and some others in the postmature or overmature organic matter in the HI vs Tmax plot (Fig. 6d), only three of them falls in the mature field. The HI vs Tmax is also plotted for kerogen type and for identifying oil prone/gas prone source rock (Fig. 6a and 6b), which indicates mainly type III kerogen and mostly gas prone source rock. The Oxygen Index (OI) results for samples with less than 0.5 wt.% TOC may be anomalous due to carbon dioxide or oxygen adsorption (Nuñez-Betelu and Baceta, 1995). So, both the HI vs OI and HI vs Tmax diagrams provides a reliable comparison of results that helps detecting the anomalies.

DISCUSSION

MINERALOGICAL COMPOSITION OF SANDSTONES

The studied sandstones are moderate to poorly sorted and are medium to fine-grained. The effect of mechanical compaction is quite evident from the sutured and straight contacts between grains, corroded quartz grains and alignment of the grains to each other. Monocrystalline quartz is abundant and is the main detrital component with relatively lesser amount of polycrystalline quartz indicating a cratonic or recycled source (Al-Harbi and Khan, 2008; Bordoloi et al., 2022; Chutia et al., 2019). Potassium feldspar is more abundant than plagioclase feldspar. Lithic fragments include mainly sedimentary with minor amount of igneous and metamorphic fragments, chert and trace amounts of heavy minerals. Detrital clay and calcite are mainly present as pore lining and grain coating cements. The relatively lesser amounts of feldspars and lithic fragments in these sandstones also indicates a cratonic source as well as a moderate degree of chemical weathering (Chutia et al., 2019; Bordoloi et al., 2022). In addition to this, smectite, illite and kaolinite are the main clay minerals found in the studied rocks as indicated by the X-Ray diffractograms (Fig. 5a). The porosity and permeability of sandstones with moderate sorting and varying grain sizes are expected to be lower, which has an impact on the reservoir parameters. Based on the petrographic study, these sandstones exhibiting sub-rounded to sub-angular shapes have undergone extensive reworking as indicated by the transportation history, which reveals that the source of the sediment is cratonic or recycled (Al-Harbi and

Khan, 2008; Bordoloi et al., 2022; Chutia et al., 2019).

DIAGENESIS AND RESERVOIR CHARACTERISTICS OF SANDSTONES

Numerous parameters affect the quality of sandstone reservoirs including (i) depositional porosity and permeability governed by grain size, sorting, and grain morphology, (ii) degree of mechanical and chemical compaction, and (iii) quantity and kind of pore filling cement (Worden and Morad, 2000). The most important diagenetic processes that have an impact on reservoir quality include cementation, dissolution, compaction and clay mineral authigenesis. Diagenesis is significantly governed by depositional environment and the diagenetic changes that occur during post depositional processes greatly control the distribution of porosity in sandstone reservoirs (Olaussen et al.,1984). The sandstones of the Geku formation have undergone diagenesis leading mainly to reduction of feldspars and unstable lithic fragments forming new clay minerals. Carbonate cement is more abundant than other cements and are the main cause of permeability and porosity reduction (Akinlua et al., 2016; Al-Ramadan et al., 2012; Shar et al., 2021). Calcite cement has the tendency to fill the intergranular pore space thereby affecting the reservoir quality. Calcite is present as patchy cement as well as poikilotopic cement in the intergranular pore spaces. Mechanical compaction is one such diagenetic process that begins right after the sediments are deposited and continues throughout the entire diagenetic history of the rock (Worden and Burley, 2009). Mechanical compaction appears to have very significant effect on these rocks as evident from the sutured and concavo convex grain contacts. The sandstones have undergone strong mechanical compaction, because of which most of the primary pores have disappeared. There has been observed an absence of secondary porosity indicated by the presence of abundant calcite and argillaceous cements. Compaction has also led to the deformation of lithic fragments and micas resulting in further loss of porosity in sandstone. Though it's possible that pseudoplastic deformation and the creation of a pseudomatrix can increase the development of secondary porosity but the low percentage of lithic grains in the studied sandstones did not significantly contribute to the formation of secondary porosity (Ramadan et al., 2004).

The studied sandstones of Geku Formation have undergone phyllomorphic / mesogenetic stage of diagenesis as indicated by the diagenetic changes observed during petrography such as precipitation of cements, sericitization of feldspars, authigenesis of secondary minerals such as chert, mica and quartz overgrowths all of which are responsible for porosity reduction (Dapples, 1962; Chima et al., 2018). Sandstone porosity is reduced by quartz cements, which form as syntaxial, euhedral grain overgrowths that frequently interlock within pores (Borgohain et al., 2010; Shar et al. 2021). Also, the concavo-convex and line contacts, which later forms sutured contacts between grains during increased stages of burial also suggest mesogenetic stage. The mechanical compaction as a result of increased burial during diagenesis indicated by bending of mica flakes substantiates a similar stage of diagenesis. And these processes have greatly affected the reservoir quality of the studied sandstones. Leaching or sericitization of feldspars does create secondary porosity but when it is in minor amount just like in the studied sandstones, it doesn’t seem to play a significant role in porosity development. Cement types identified are mainly calcite, clay and silica (in the form of quartz overgrowths). Low porosity sandstones contain either abundant authigenic kaolinite in isolated secondary pores or widespread carbonate grains and cement that have undergone little or no dissolution (Goodchild and Whitaker, 1986; Pitman et al,1989; Al-Ramadan et al, 2012). In areas where fractures are filled by carbonate cement, the carbonate may act as a barrier to fluid flow and greatly reduce permeability.

The variations in grain sizes and sorting leading to lower porosity and permeability in sandstones is also controlled by the sediment’s transportation history (Akinlua et al., 2016). The degree to which the sediments were transported, however, is what distinguishes these variations (Hussain et al., 2006). Generally, well rounded and sorted grains indicate that the sediments were transported for a long distance from its source, whereas the sub-rounded and poorly sorted grains imply short distance of transportation (Hussain et al. 2006). Earlier studies suggest recycled orogenic and craton interior sources with quartzose recycled and transitional recycled type sources for sandstones of Geku Formation (Chutia et al., 2019; Bordoloi et al., 2022). This is indicated by the sub- rounded and sub-angular grains, the abundance of monocrystalline quartz and minor amounts of feldspar and lithic fragments. The minor amount of feldspars is attributed to the diagenetic processes that the rocks have undergone leading to the formation of clay cements, which in turn have reduced the porosity and permeability of these rocks. Because clay and calcite obstruct the build-up and flow of fluids in pore spaces, they completely negate the potential of a good reservoir. It is important to note here that the Geku Formation belongs to continental facies and have been intensely deformed by post rift tectonics due to the WNW-ESE compressional force which was created when the Indian plate started colliding with the Burmese plate, as evident from the numerous folds and faults present in the study area. Since rifts with marine fills are more prolific hydrocarbon reserves than those with non-marine rifts with little or no post tectonic deformations, so the Geku Formation sediments might have limited distribution of good seals and the absence of seals in turn might have prevented the hydrocarbon accumulations thereby affecting their reservoir quality.

SOURCE ROCK POTENTIAL OF SHALE

The ability of a source rock to generate hydrocarbons is determined by the quantity (TOC), quality (Hydrogen Index) and maturity of kerogen present in the rock (Hunt, 1995). It has been found that rocks containing organic matter significantly influenced by continental sediments has very little contribution to oil generation potential due to the abundance of hydrogen poor organic matter (Gordon, 2021).

Rock eval pyrolysis has been used to determine the organic matter type, their distribution, hydrocarbon potential and the source rock type. The quantity and maturity of organic matter are expressed as TOC and Tmax, respectively. In general, Tmax values lower than 435 ºC indicate immature organic matter (Nuñez-Betelu and Baceta, 1995). TOC and Tmax values obtained for the studied rocks indicate immature to mature to postmature organic matter. Standard plots of Rock-Eval pyrolysis data have been used to determine source rock richness, quality, maturity and kerogen type.

Maturity stage determination plot of HI vs Tmax indicates mostly immature or post mature organic matter barring three samples, which falls in the mature field with Tmax values 486 °C, 488 °C, and 499 °C. Yinkiong shales are mainly oil/gas prone and gas prone (GP). On the assessment of GP (Generation Potential), all samples show poor potentiality for generating hydrocarbons. When compared to the pyrolysis of pure kerogen, low TOC samples from whole-rock pyrolysis frequently have lower HI and greater OI values (Hunt, 1995). This is worsened by the presence of smectite and illite (Fig. 5b) in immature low TOC rocks as the hydrocarbons, which released during thermal cracking of kerogen is adsorbed on clay mineral surfaces. A portion of the carbon in S2 never leaves the rock due to the adsorption of oil on clay minerals, which causes subsequent cracking to gas at higher temperatures (Hunt 1995). For shales, usually a TOC of 2.0% is considered to be good, and a TOC value higher than 4% is considered as very good (Nuñez-Betelu and Baceta, 1995; Espitalie et al., 1985). The studied rocks containing TOC averaging 0.09% indicates poor organic richness.

The generation potential of source rock can be delineated using the pyrolysis data. According to Hunt (1995), source rocks with GP <2, 2 to 5, 5 to 10, and >10 are considered to be poor, fair, good and very good, respectively (Espitalie et al., 1985). The average generation potential of the studied shales is 0.02. Hence, the generation potential of shales of Geku Formation is poor. The Production Index (PI) is also in part indicative of the degree of thermal maturity. In general, PI values below 0.4 indicate immature organic matter; PI values between 0.4 and 1.0 indicate mature organic matter; and PI values above 1.0 are indicative of overmature organic matter (Nuñez-Betelu and Baceta, 1995; Espitalie et al., 1985). The PI value of the studied shales ranges from 0.13 to 1.0 which indicates immature to mature as well as postmature organic matter.

The amount and type of organic matter preserved in sediments is controlled in part by the depositional environment but also by the productivity of the waters, sediment grain size, physical conditions in the area of deposition, and mineralogy of sediments. Sedimentary rocks deposited in deltaic environment tend to have low TOCs and mostly exhibits type III kerogen with some type II, which is most likely to produce gas rather than being an oil source (Hunt, 1995). Also, the type of organic hydrogen is controlled by the nature of the organic matter. The low hydrogen content (HI) and a variable high oxygen content (OI) indicates that the organic matter is derived from terrestrial sediments (Nuñez-Betelu and Baceta, 1995; Hunt, 1995). Rocks containing immature kerogen with TOC < 1% and HI values 150-400 indicate terrestrially derived organic matter (Davis et al., 1989). These data coincide with the results obtained from pyrolysis of shales of Geku Formation in the present study. Type III kerogen corresponds to terrestrially produced organic matter, especially material from higher plants. Terrestrial organic matter has a low HI value, because of its nature and damage it suffers during transport. Instead of being an oil source, this sort of kerogen typically produces gas (Nuñez-Betelu and Baceta, 1995). The most common form of organic matter decomposition is oxidation. In contrast to fresh core samples, outcrop samples often have lower HI values and higher OI values due to the removal of hydrogen and addition of oxygen during oxidation (Nuñez-betelu and Baceta, 1995). Generally, surface samples always appear with low TOC and other rock eval parameters. Considering this, it is believed that the Geku shales of the study area negates all the geochemical parameters of being a good oil prone source rock and can effectively act as Type III gas prone source rock, which is capable of producing gas.

CONCLUSION

The integrated petrographic and rock eval pyrolysis study of sandstones and shales of Yinkiong Group, the following conclusions can be drawn:

1. The Geku sandstones are mainly fine to medium-grained, moderate to poorly sorted quartz arenite and quartz wacke, which have suffered porosity loss due to precipitation of mainly calcite cement.

2. The studied sandstones are texturally immature to sub-mature as reflected by their grain size, particle shape, and degree of sorting, which contributed to their poor reservoir quality.

3. The sandstones have undergone strong mechanical compaction as evident from the long,

concavo-convex and sutured grain contacts responsible for their porosity reduction.

4. The source rock characterization of Geku Shale suggests Type III kerogen, suitable for gas production. All the samples are organic poor and do not constitute a potential source rock. Only small amounts of gas may have originated from these rocks.

5. The low hydrogen content (HI) and a variable high oxygen content (OI) indicate that the organic matter is derived from terrestrial sediments.

ACKNOWLEDGEMENTS:

We are grateful to Cotton University for providing ample laboratory facilities to carry out the present work. We also extend our heartfelt gratitude to Dr. Suryendu Dutta and Tanu Priya from Department of Earth science, IIT Bombay for processing our samples at their rock eval pyrolyzer facility. We thank the Sophisticated Analytical Instrument Facility (SAIF), Department of Instrumentation & USIC, Gauhati University, Guwahati for providing their XRD lab facility. One of us is extremely grateful to DST-INSPIRE for the financial assistance in the form of INSPIRE Fellowship/2018/IF180616. Finally, we appreciate the non-anonymous reviewers for their comments on the original version, which helped us to improve our presentation.

DECLARATION OF CONFLICTING INTEREST

The authors declare that they have no competing interests in this manuscript.

AUTHOR CONTRIBUTIONS

All the authors were actively involved in the field study for the proposed work. AB carried out the petrographic study, analysed the data and drafted the manuscript. AC helped supervise the experiment, analysis and interpretation of results. CDT edited and coordinated the manuscript. All authors reviewed the results and approved the final version of the manuscript.

FUNDING

Author Anannya Bordoloi has received financial support from DST-INSPIRE for pursuing Ph.D having order number INSPIRE Fellowship/2018/IF180616.

REFERENCES:

Acharyya, S.K. (1994). The Cenozoic foreland basin and tectonics of the Eastern Sub-Himalaya: problems and prospects. Himalayan Geology, v.15, p.3–21.

Acharyya, S.K. (2007). Evolution of the Himalayan Paleogene foreland basin, influence of its litho-packet on the formation of thrust-related domes and windows in the Eastern Himalayas – A review. Journal of Asian Earth Sciences, v.31, p.1–17.

Akinlua, A., Ngola, A., Fadipe, O.A., and Adekola, S.A. (2016). Petrography and geochemistry of sandstone samples of Vischkuil formation, Karoo Supergroup, South Africa. Petrol Explor Prod Technol, v.6, p.159-167, https://doi.org/10.1007/s132 02015-0199-1

Al-Harbi, O.A., and Khan, M. (2008). Provenance, diagenesis, tectonic setting and geochemistry of Tawil sandstone (Lower Devonian) in Central Saudi Arabia. Journal of Asian Earth Sciences, v.33, p.278-287.

Al-Ramadan, K., Morad, S., and Plink-Bjorklund, P. (2012). Distribution of diagenetic alterations in relationship to depositional facies and sequence stratigraphy of a wave- and tide-dominated siliciclastic shoreline complex: Upper Cretaceous Chimney Rock Sandstones, Wyoming and Utah, USA. Int. Assoc. Sediment. Spec. Publ., v.45, p.271–296.

Baral, U., Lin, D., Goswami, T.K., Sarma, M., Qasim, M., and Bezbaruah, D. (2019). Detrital zircon U–Pb geochronology of a Cenozoicforeland basin in Northeast India: Implications for zircon provenance during the collision of the Indian and Asian plates. Terra Nova, v. 31, p. 18–27. https://doi.org/10.1111/ter.12364

Beaumont, C., Jamieson, R.A., Nguyen, M., and Lee, B. (2001). Himalayan tectonics explained by extrusion of a low viscosity crustal channel coupled to focused surface denudation. Nature, v.414, p.738–742.

Bordoloi, A., Chutia, A., Taye, C., and Gogoi, M.P. (2022). Petrography and geochemistry of palaeogene sandstones of Geku Formation, Yinkiong Group, Arunachal Pradesh, NE India: implications on provenance and tectonic setting, Journal of Sedimentary Environments. v. 7(4), p. 691-709. https://doi.org/10.1007/s43217-022-00116-4

Borgohain, P., Borah, C., and Gilfellon, G.B. (2010). Sandstone diagenesis and its impact on reservoir quality of the Arenaceous Unit of Barail Group of an oilfield of Upper Assam Shelf, India. Current Science, v.98(1), p.82-88.

Chima, P., Baiyegunhi, C., Liu, K., and Gwavava, O. (2018). Diagenesis and rock properties of sandstones from the Stormberg Group, Karoo Supergroup in the Eastern Cape Province of

South Africa. Open Geosciences, v.10, p.740–771. https://doi.org/10.1515/geo-2018-0059

Chutia, A., Taye, C. D., Nath, D., and Chutia, D. (2019). Provenance of the Yinkiong Group exposed along Pasighat-Mariyang road section, East Siang District, Arunachal Pradesh: A petrographic, heavy mineral and clay mineralogical approach. Indian Journal of Geosciences, v.73(4), p.253–264.

Cook, K.L., and Royden, L.H. (2008). The role of crustal strength variations in shaping orogenic plateaus, with application to Tibet. Journal of Geophysical Research, Solid Earth, v.113.

Dapples, E.C. (1962). Stages of Diagenesis in the Development of Sandstones. GSA Bulletin, v.73 (8), p.913-934.

Davis, H.R., C.W. Byers., and Pratt, L.M. (1989). Depositional Mechanisms and Organic Matter in Mowry Shale (Cretaceous), Wyoming, AAPG Bulletin, v.73(9), p.1103-1116.Espitalie, J., Deroo, G., and Marquis, F. (1985). Rock–Eval pyrolysis and its application. Rev. Inst. Fr. Petrol., v.72.

Goodchild, M.W., and Whitaker, J.H.McD. (1986). A petrographic study of the Rotliegendes sandstone reservoir (Lower Permian) in the rough gas field. Clay Minerals, v.21, p.459-477.

Gordon, J.B. (2021). Geochemistry, Diagenesis and Secondary Porosity Development of Late Jurassic strata, Offshore Newfoundland, Canada. University of Calgary. Ph.D thesis.

Hafiz, M., Hakhoo, N., Bhat, G., Kanungo, S., Thusu, B., Craig, J., Ahmed, W., and Magotra, R. (2022). An assessment of the source potential and reservoir characterization for tight gas exploration in the Subathu Formation shale, Himalayan Foreland Basin, Northwestern India. Journal of Asian Earth Sciences, v.230, https://doi.org/10.1016/j.jseaes.2022.10520

Houseman, G., and England, P. (1993). Crustal thickening versus lateral expulsion in the Indian–Asian continental collision. Journal of Geophysical Research Solid Earth, v.98, p.12233–12249.

Hunt, M. (1995). Petroleum Geochemistry and Geology. Chapter-10, p.322-353.

Hussain, M., El Hassan, W.M., and Abdul Raheen, A. (2006). Control of grain size distribution on geochemical properties of reservoir rocks—a case study: Cretaceous Kahafji member, Zuluf field, offshore Arabian Gulf. Marine and Petroleum Geology, v.23, p.703–713

Jafar, S. A. and Singh, O. P. (1992). K/T boundary species with Early Eocene nannofossils discovered from Subathu Formation, Shimla Himalaya, India. Current Science, v.62(5), p.409-413.

Jiang, T., Aitchison, J. C. and Wan, X. (2016). The youngest marine deposits preserved in southern Tibet and disappearance of the Tethyan Ocean. Gondwana Research, v.32, p.64-75.

Kumar, G. (1997). Geology of Arunachal Pradesh. Geological Society of India, p. 217.

Lafargue, E., Espitalie, J., Marquis, F., and Pillot, D. (1998). Rock-Eval 6 Applications in Hydrocarbon Exploration, Production and Soil Contamination Studies, In Rev. Inst. Fr. Pétrol., v.53(4), p.421-437. DOI: 10.2516/ogst:1998036

Lambiase, J.J., and Morley, C.K. (1999). Hydrocarbons in rift basins: the role of stratigraphy. Philosophical Transactions of The Royal Society A, Mathematical Physical and Engineering Sciences, v.357 (1753).

Morley, C. K. (1999). Comparison of hydrocarbon prospectivity in rift systems. In Continental rifting in East Africa, structural and sedimentary geometries, processes and evolution: as revealed by hydrocarbon exploration (ed. C. K. Morley), American Association of Petroleum Geologists Special Publication.

Nuñez-betelu., and Baceta, J.I. (1995). Basics and Application of Rock-Eval/TOC Pyrolysis: an example from the uppermost Paleocene/lowermost Eocene in The Basque Basin, Western Pyrenees. MUNIBE (Ciencias Naturales - Natur Zientziak),p.43-62.

Olaussen, S., Dalland, A., Gloppen, T.G., and Johannesen, E. (1984). Depositional environment and diagenesis of Jurassic reservoir sandstones in the eastern part of Troms I area. In Spencer, A.M., Holter, E.,Johnsen, S.O., Mørk, A., Nysaether, E., Songstad, P. and Spinnangr, Å. (Eds.), Petroleum geology of the North European Margin. NorwegianPetroleum Society (NPF), Graham and Trotmanp, p.61-79.

Peters, K.E., and Cassa, M. R. (1994). Applied source rock geochemistry, in Magoon, L. B. and W. G. Dow, Eds. The petroleum system — from source to trap, AAPG Memoir, v.60, p.93–120.

Pitman, J.K., Spencer, C.W., and Pollastro, R.M. (1989). Petrography, Mineralogy, and Reservoir Characteristics of theUpper Cretaceous Mesaverde Group in the East-Central Piceance Basin, Colorado, USGS bulletin 1787, Evolution of sedimentary basins- Uinta and Piceance basins, Chapter-G, https://doi.org/10.3133/b1787G

Ramadan, K.A., Hussain. M., Badrul, I., and Salih. S. (2004). Lithologic characteristics and diagenesis of the Devonian Jauf sandstone at Ghawar Field, Eastern Saudi Arabia. Marine and Petroleum Geology, v.21, p.1221–1234.

Sarma, M., Bezbaruah, D., Goswami, T.K., and Baral, U. (2020). Geologic and Tectonic Evolution of the Yinkiong Group and Abor Volcanic Rocks in the Eastern Himalaya: An Overview of Geologic Data. Geotectonics, v.54(3), p.395–409.

Sengupta, S., Acharyya, S.K., and Smeth, B.D. (1996). Geochemical characteristics of the Abor volcanic rocks, N.E. Himalaya, India: nature and Early Eocene magmatism, Journal of Geological Society of London, v.153, p.695–704.

Shar, A.M., Mahesar, A.A., Narejo, A.A., and Fatima, N. (2021). Petrography and Geochemical Characteristics of Nari Sandstone in Lower Indus Basin, Sindh, Pakistan, Mehran University. Research Journal of Engineering and Technology, v.40 (1), p.82-92, DOI: 10.22581/muet1982.2101.08

Singh, S. (1984). A reappraisal of Yinkiong Formation with reference to Dalbuing area, East Siang district Arunachal Himalaya. Indian Minerals, v.38(2), p.34–38.

Taye, C. D. (2015). Petrography and Geochemistry of the Volcanic and Metavolcanic Rocks of Siang Valley, Arunachal Pradesh, India (Ph.D. Thesis, Dibrugarh University), p.34, http://hdl.handle.net/10603/212919.

Taye, C. D., and Bhattacharyya, P. (2017). Mineral chemistry and thermobarometry of the Mafic Igneous Rocks of Yamne Valley, Arunachal Pradesh India. Journal of Applied Geochemistry, v.19(4), p.400–415.

Thakur, O.P. and Dogra, N.N. (2011). Palynofacies characterization for hydrocarbon source rock evaluation in the Subathu Formation of Marhighat, Sirmaur district, Himachal Pradesh. Journal of Earth System Science, v.120(5), p.933. DOI: 10.1007/s12040-011-0110-5.

Tissot, B. P., Durand, B., Espitalie, J. and Combaz, A. (1974). Influence of nature and diagenesis of organic matter in formation of petroleum. AAPG Bull. v.58, p.499 506.

Tripathi, C., Dungrakoti, B. D., and Ghosh, R. N. (1979). Note on discovery of Nummulites from Dihang Valley, Siang district Arunachal Pradesh. Indian Minerals, v.33(1), p.43–44.

Tripathi, C., Gaur, R. K. and Singh, S. (1981). A note on the occurrence of Nummulites in East Siang district, Arunachal Pradesh, Indian Minerals, v.35 (1), p.36-38.

Tripathi, C. and Mamgain, V. D., 1986: The larger foraminifera from the Yinkiong Formation (Early Eocene) of East Siang district, Arunachal Pradesh, Journal of the Palaeontological Society of India, v.31, p.76-84.

Tucker, M. (1988). Techniques in sedimentology. Blackwell Scientific Publication, Ch-7, p.206-208.

Van Krevelen, D.W. (1961). Coal Typology - Physics - Chemistry – Constitution. Elsevier Publishing Company, New York, p.113 120

Worden, R. H. and Morad, S. (2000). Quartz cementation in oil field sandstones: a review of the key controversies. In: Quartz cementation in sandstones. Special publications of International Association of Sedimentologists, v.29, p.1-20.

Worden, R.H., and Burley, S.D. (2009). Sandstone Diagenesis: The Evolution of Sand to sandstone, In book: Sandstone Diagenesis. Recent and Ancient, Chapter: 1. DOI: 10.1002/9781444304459.

Received on : *21st March 2023*
Revised accepted on : *16th May 2023*

JOURNAL INDIAN ASSOCIATION OF SEDIMENTOLOGISTS ISSN NO 2582 – 2020
Vol. 40, Issue 1, 2023, pp. 55-72
DOI: https://doi.org/10.51710/jias.v40iI.292

Tectonic setting of Kaladgi-Badami basin and its possible connection with adjacent Proterozoic basins, Karnataka, India

Sukanta Goswami[1], Suman Das[2], Prathamesh S. Samant[3], T. Vijaya Kumar[1], B. G. Prakash[3], Kalyan Chakrabarti[1]

[1]Atomic Minerals Directorate for Exploration and Research, Hyderabad, Telangana-500016.
[2]Geological Survey of India, CHQ, Kolkata, West Bengal-700016.
[3]Atomic Minerals Directorate for Exploration and Research, Bangalore, Karnataka-560072.
E-mail: sukantagoswami.amd@gov.in

ABSTRACT

Sedimentary rock types and basin geometries are interrelated with characteristic tectonic settings. In fact, sedimentation pattern at central stable cratonic areas are not same as that on continental margins. Kaladgi-Badami (KB) basinal feldspathic arenite (i.e., arkose) dominated rocks contain more plagioclase than potassium feldspar unlike the opposite scenario of Phanerozoic sandstones. Tectonic history of the KB basin has been interpreted since basin development, sedimentation through interrupting hiatus, tectonic reworking, redeposition at later developed depocenters and later exhumation, erosion, tectonism till Deccan volcanism and finally latest configuration. As per the International commission of Stratigraphy (ICS), principles of stratigraphic classification and usages of terminology of fundamental lithostratigraphic unit 'Formation' is reexamined in this paper. The definition of Formation as "smallest mappable rock unit with a definite lithologic characteristic that allow it to be distinguished from other such units" is improperly used because without mentioning a specific scale every unit is mappable or traceable. Therefore, the minimum mappable unit means the unit which can be at least visible in a scale in which entire basin can be seen. Based on this slight modification is proposed in the stratigraphy of KB basin. Geochronology based radiometric stratigraphy is best tool for determination of time sequence of geological events. However, it is always a matter of concern that dating methods and materials are often not suitable in sedimentary geology. In case of passive rifted sedimentary basins like Kaladgi, Badami and Bhima of the Dharwar Craton, there is negligible igneous events and indirect dating methods are mostly available. Detrital zircon dating can give maximum age or provenance age, which cannot be of much use. However, there are other indirect tools, which are already utilized by several workers earlier and based on the reviews and present observation and mapping compilation it is proposed that KB and Bhima basins used to be a single basin, and later tectonism followed by Deccan volcanism affected the present geographic continuity. Since the distance between westernmost Bhima basinal rocks and easternmost KB basinal rocks near Mudhebihal is nearly around 15km, it is logical to consider that these were geographically connected, because there is an intense faulting near to these basin margins.

KEY WORDS: Kaladgi-Badami basin, Bhima basin, Tectonic setting, stratigraphy, Karnataka.

INTRODUCTION

Cratonic basins are characterized by their typical shallow (up to a few km thick sediments at max) and bowl-shaped basins with continental granitoid-greenstone belts as basement rocks. The sedimentary units get thickened gradually toward the center of the basin (Prothero and Schwab, 2014). Kaladgi-Badami (KB) basin is one of the major Proterozoic basins in the Dharwar Craton (DC) (Fig 1). KB basin is a tectonically affected Proterozoic sediment depocenter with long geological history ranges from ~1.86 Ga (lower part i.e., Bagalkot Group) to ~0.8Ga (upper part i.e., Badami Group) (Joy et al., 2019). Basinal sedimentary rocks cover about 8,300 km^2 areas. Typical discontinuous patchy occurrences of sedimentary rocks are characteristic of this basin.

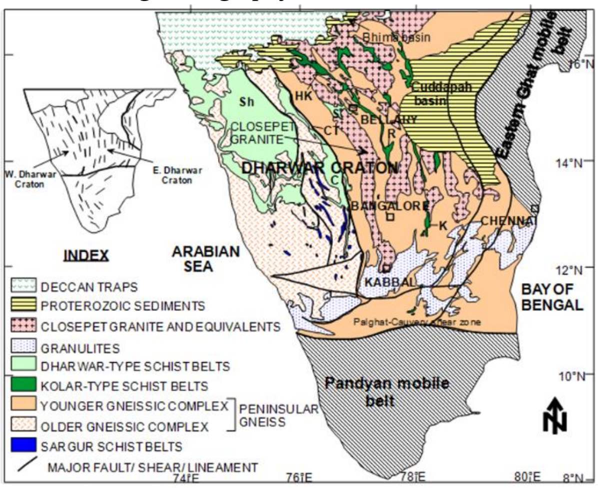

Fig 1. Geological map of Southern India shows the Dharwar Craton (DC) and adjacent units, Proterozoic basins and mobile belts (after GSI, 1994).

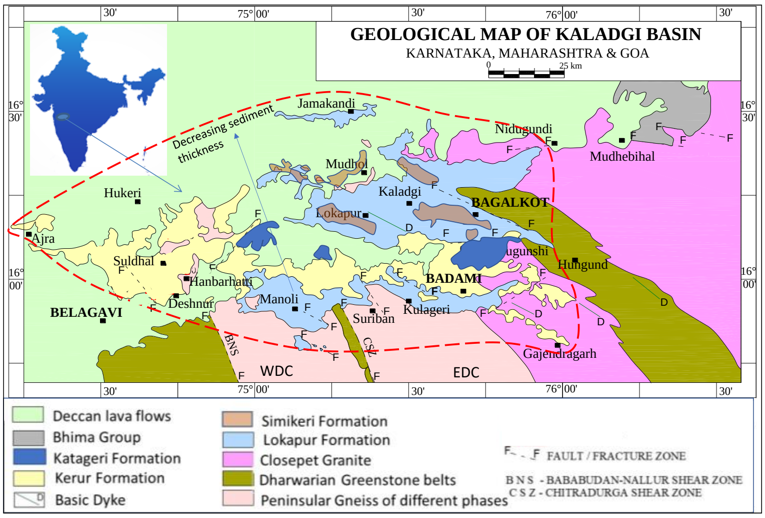

Fig 2. Geological map of Kaladgi-Badami basin (after Jaya Prakash et al., 1987).

The sedimentary patches are spreaded over a cumulative area of ~14000km^2 (i.e., ~175km along E-W and ~80km along N-S). In the southern part near Gajendragarh, Suriban and Manoli area, outliers of Kaladgi Supergroup are observed on basement (Fig 2). On the other hand, possibility of continuation of sediments below the Deccan Trap is very high at least up to Jamakandi area in the northern extreme, where inlier of Kaladgi Supergroup is found to be surrounded by Deccan trap. Similarly, in the western extreme near Ajra area inlier is present. The sub-trappean sediments were well confirmed by heliborne time domain electromagnetic data analysis (Sridhar et al., 2017). The easternmost extension is defined by the midway between Tugunshi and Hungund areas (Fig 2). The continuous geographic basin margin is affected by tectonism, differential weathering-erosion and Deccan volcanism. However, after connecting surface outcrops of sedimentary rocks from northern, southern, eastern and western extreme, it is possible to demarcate an approximate sub-elliptical outline of the basin. Most interestingly, this basin lies over both of the so called Eastern Dharwar Craton (EDC) and Western Dharwar Craton (WDC). The Suture Zone between EDC and WDC called Chitradurga Suture Zone (CSZ) passes below the basin. From the basic fundamental geology, term like "inter cratonic basin" is not so far introduced. Moreover, two cratons are usually separated by mobile belts in between. There is no such mobile belt between EDC and WDC. Therefore, as par the Goswami et al. (2023) EDC and WDC are not separate cratons but these are parts of same craton with slightly different geological development and evolution timing. Hence Kaladgi is intra Dharwar cratonic basin.

In this paper we review the entire tectonic history of the Kaladgi-Badami basin from relief difference creation and basin development through long lasting sedimentation and tectonic interaction to post diagenesis exhumation and volcanism. Therefore, as per geological time scale this review compiles major tectonic imprints of late Archaean to early Tertiary time frame.

GEOLOGY OF KALADGI-BADAMI BASIN

According to the latest stratigraphic column after Jaya Prakash et al. (1987), Kaladgi Supergroup is divided into older Bagalkot Group and younger Badami Group. Further, each of the Groups is subdivided into several Sub-group, Formation and Members (Table 1). Generally, Bagalkot Group (consists of quartzite, shale and limestone with stromatolitic dolomite and chert breccias) is highly deformed and often tightly folded especially along the mid-axial region of the basin like Lokapur, Kaladgi areas. Badami Group is not deformed in general and comprises mostly horizontal to gently dipping feldspathic conglomerate, arenite shale and minor limestone. The Digital elevation map (DEM) of KB basin (Fig. 3) is presented to visualize the range of elevation from ~ 40m to ~ 950m. However, the average elevation inside the basin is ~ 800m in the west and ~ 450m in the east. Thus, a gentle easterly slope is recognizable within the basin. Since the

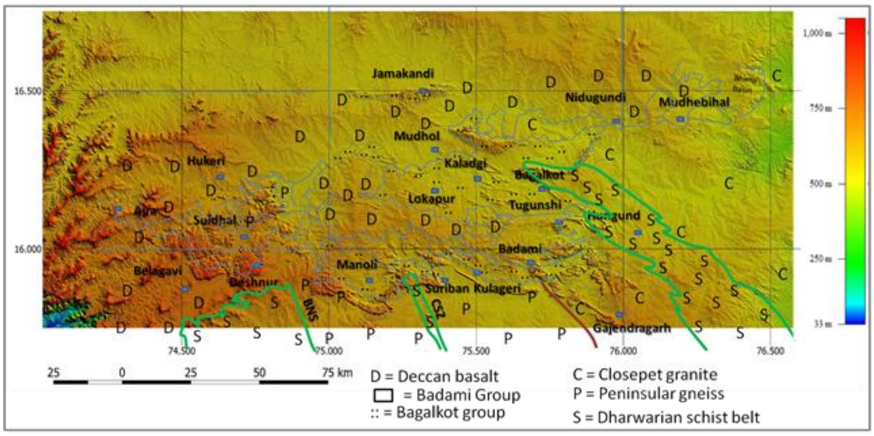

Fig 3. Digital Elevation Map (DEM) of Kaladgi-Badami basin. Litho-contacts are drawn as per the map in Fig. 2.

sub-horizontal undeformed Badami Group is topmost unit (mostly occur about ~ 650-680m RL i.e., elevation), it is not available in the eastern part where average RL is less than 650m. Thus, as per the principle of horizontality and lateral continuity of strata, Badami cannot be expected as such. Hence lower unit, i.e., Bagalkot Group occurs in the central and eastern part. Regional structural lineament plot over DEM and frequency as well as length based rose diagrams suggest that NW-SE trend is the most frequent as well as most continuous in terms of length (Fig 4a-d). This is due to the Krishna river system with its tributaries like Malaprabha, Ghatprabha, and Ilkal rivers.

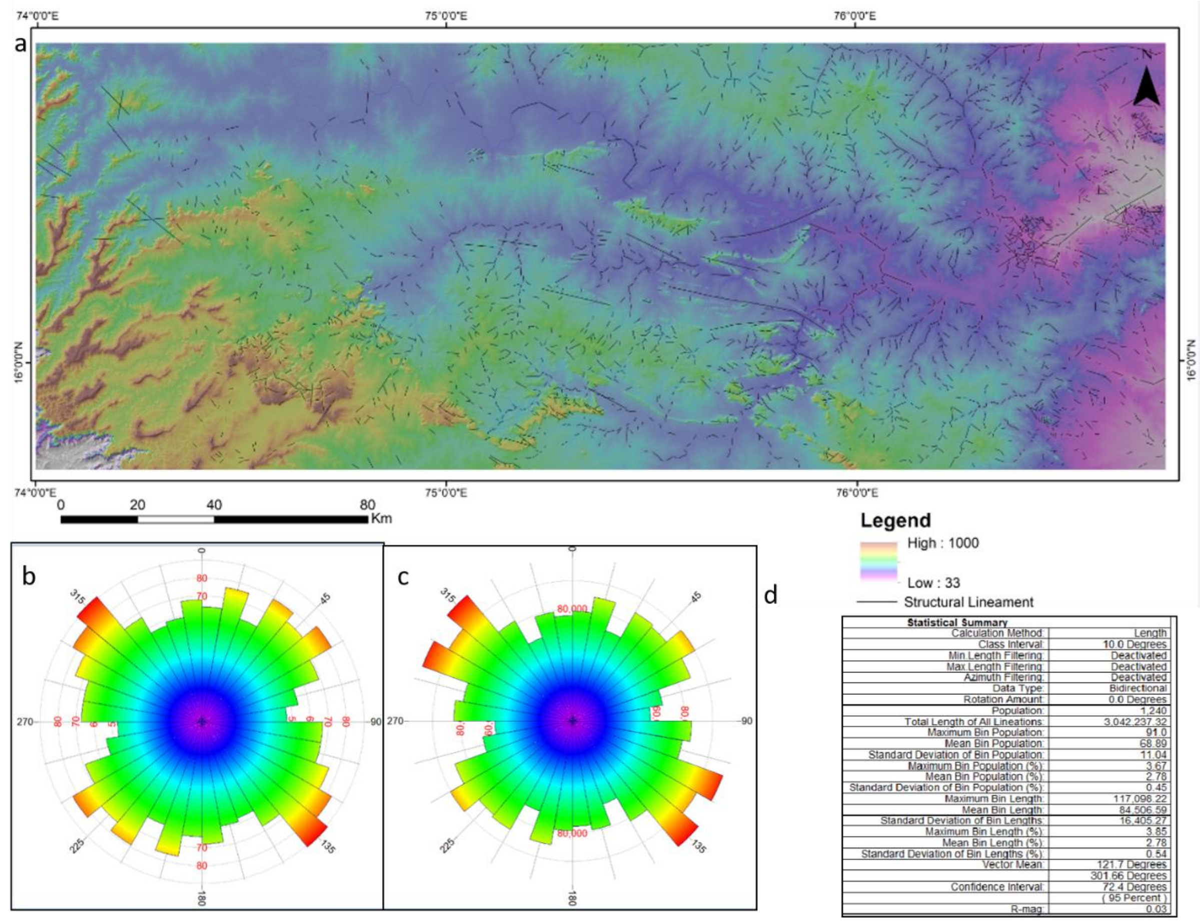

Statistical Summary	
Calculation Method:	Length
Class Interval:	10.0 Degrees
Min.Length Filtering:	Deactivated
Max.Length Filtering:	Deactivated
Azimuth Filtering:	Deactivated
Data Type:	Bidirectional
Rotation Amount:	0.0 Degrees
Population:	1,240
Total Length of All Lineations:	3,042,237.32
Maximum Bin Population:	91.0
Mean Bin Population:	68.89
Standard Deviation of Bin Population:	11.04
Maximum Bin Population (%):	3.67
Mean Bin Population (%):	2.78
Standard Deviation of Bin Population (%):	0.45
Maximum Bin Length:	117,098.22
Mean Bin Length:	84,506.59
Standard Deviation of Bin Lengths:	16,405.27
Maximum Bin Length (%):	3.85
Mean Bin Length (%):	2.78
Standard Deviation of Bin Lengths (%):	0.54
Vector Mean:	121.7 Degrees
	301.66 Degrees
Confidence Interval:	72.4 Degrees
	(95 Percent)
R-mag:	0.03

Fig 4. a). Regional structural lineament plot over DEM. b). Frequency based rose diagram for lineaments. c). length based rose diagram suggest that NW-SE trend is the most frequent as well as most continuous in terms of length. d). parameters for rose diagram.

Despite having established stratigraphy (Jaya Prakash et al., 1987) with minute details up to member level, the fundamental unit (i.e., Formation) fails to represent presently defined Formations because they are not as distinct and large enough to be mappable in the surface or traceable in the sub-surface in the basinal scale. In fact, if the geological map of entire Kaladgi basin is observed it is found that in the basinal scale there are only four mappable units. However, at present these four units are given different lithostratigraphic status viz., Lokapur Sub-group, Simikeri Sub-group, Kerur and Katageri Formation. Although the entire stratigraphy is correctly established, the units are required to be reassigned especially in Lower Group. Lokapur, Simikeri should be kept under Formation. Any lithostratigraphic unit is mappable or traceable depending up on the scale. However, when fundamental lithostratigraphic unit (i.e., Formation) is defined it must represent the minimum mappable or traceable unit in a scale in which entire basin is covered. Thus, Kaladgi Supergroup comprises two groups viz., Bagalkot and Badami. Further, Bagalkot Group comprises Lokapur and Simikeri Formations. Badami Group is already properly assigned to comprise Kerur and Katageri Formations. The existing Formations like Ramdurg, Malaprabha, Yargatti, Yendigere, Muddapur, Yadhalli, Kundargi, Arlikatti and Hoskatti are actually Members, which comprises different marker beds of variable thickness (i.e., existing Members of Bagalkot Group are actually Beds). It is beyond any doubt that presently proposed revised stratigraphy (Table 2) is more

Table 1. Stratigraphy of Kaladgi-Badami basin (after Jaya Prakash et al., 1987)

	Group	**Sub Group**	**Formation**	**Member**	**Thickness (m)**
KALADGI SUPER GROUP	Badami Group	-	Katageri Formation	Konkankoppa Limestone	**85**
				Halkurki Shale	**67**
			Kerur Formation	Belikhindi Arenite	**39**
				Halgeri Shale	**3**
				Cave – Temple Arenite	**89**
				Kendur Conglomerate	**3**
	Angular Unconformity				
	Bagalkot Group	Simikeri Sub-group	Hoskatti Formation	MallapurIntrusives	**7**
				Dadanhatti Argillites	**695**
			Arlikatti Formation	Lakshanhatti Dolomites	**87**
				Kerkalmatti Haematite schist	**42**
				Niralkeri Chert Breccia	**39**
			Kundargi Formation	Govindkoppa Argillite	**80**
				Muchkundi Quartzite	**182**
				Bevinmatti Conglomerate	**15**
		Disconformity			
		Lokapur Sub-group	Yadhalli Formation	Argillite	**58**
			Muddapur Formation	Bamanbundi Dolomite	**402**
				Petlur Limestone	**121**
				Jalikatti Argillite	**43**
			Yendigeri Formation	Nagnur Dolomite	**93**
				Chikkashellikeri Limestone	**883**
				Hebbal Argillite	**166**
			Yaragatti Formation	Chitrabhanukot Dolomite	**218**
				Muttalgeri Argillite	**502**
				Mahakut Chert Breccia	**133**
			Ramadurg Formation	Manoli Argillite	**61**
				Saundatti Quartzite	**383**
				Salgundi Conglomerate	**31**
		Non-conformity			
		Granitoids, Gneisses and Metasedimentary rocks			

comprehensive, representative and coherent as per the definition. Due to the fluvio-marine transitional environment for sedimentation with cyclic transgression and regression events, simple lithostratigraphic correlation is not easy in this setting. The present problem with lithostratigraphic approach is due to the fact that the contacts between different lithofacies (lithostratigraphic unit) are diachronous, i.e., same litho-unit occur at different time at different parts of the basin. Hence strict lithological interpretation must be done with concept of sequence stratigraphy, which help in correlating coeval units, which may be of different lithology but formed at same time in different parts of the basin (Fig. 5).

Geological setting of KB basin is represented with a simple schematic model (Fig. 6) for better visualization. Basement complex comprises Tonalite Trondhjemite Granodiorite (TTG) i.e., Peninsular Gneissic Complex (PGC), Greenstone belt i.e., Hungund Schist Belt (HSB) and granite plutons i.e., Closepet granite (CG). Initially developed accommodation space was occupied by the Bagalkot Group of rocks, which got folded and tectonically affected by subsequent orogeny associated deformation events. During the later tectonics and non-deposition or hiatus period some dyke was intruded and then newly created accommodation space become depocenter of Badami Group above the angular unconformity plane. Later uplift, exhumation and faulting followed by Deccan volcanism gives present

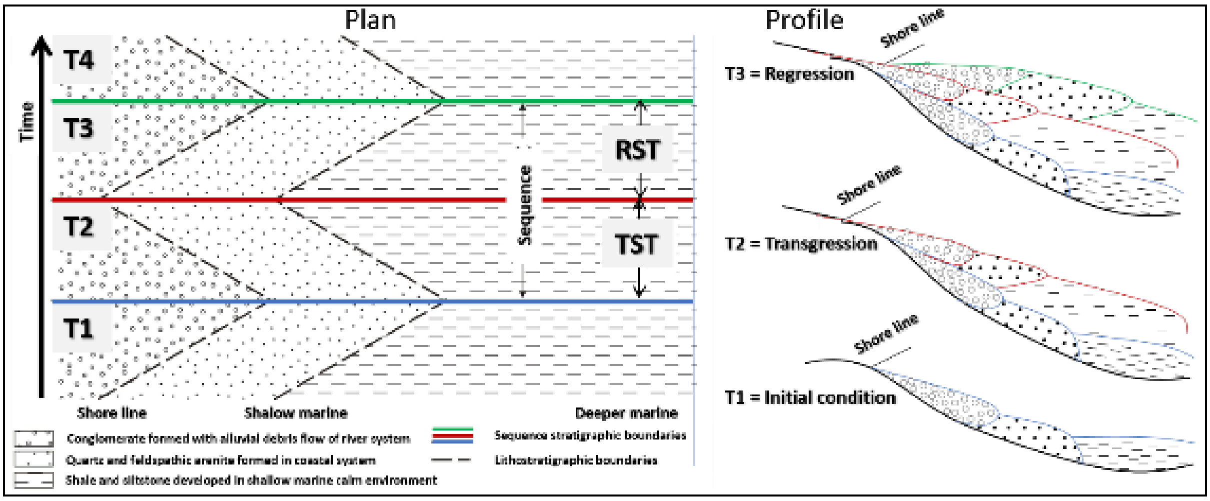

Fig 5. Diagram prepared to show the difference between sequence stratigraphy and lithostratigraphic concept. The dashed lines in the plan indicate lithocontacts without any time significance but the solid lines (blue, maroon and green) are sequence boundaries, which indicate a particular event at particular time. This can be understood from profile view of fluvio-marine (alluvial fan coast setting) environment of epeiric sea setting as observed in present area. During T1 profile across shoreline show progressive change in lithology from shallow to deeper part. After marine transgression during T2 followed by regression during T3, the depocenter of different lithounit changes. Therefore, simple lateral correlation of same lithounit cannot give any additional information, rather sequence boundaries (implying a particular episode, i.e, time line) are more meaningful. Hence, instead of lithology, it is better to use systems tract to describe a particular event. For example, the combined lithounit of T2 will be transgressive systems tract (TST) and similarly for T2 it will be regressive systems tract (RST). A complete cycle of regression and transgression form a sequence, which comprises several small episodes called systems tract e.g., transgressive systems tract (TST), high stand (HST) and low stand systems tract (LST) and falling stage systems tract (FSST).

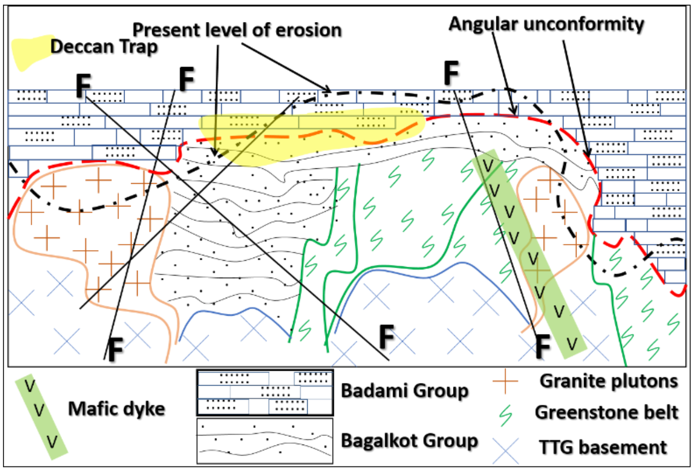

Fig 6. Comprehensive diagram section (not to scale) representative of geological disposition of different units.

geological configuration of the KB basin. Sedimentary rocks are dominated by feldspathic arenite to arkosic with plagioclase as more common than K-feldspar clasts. This is just like typical Precambrian arenites unlike Phanerozoic sandstones.

TECTONICS RELATED TO KB BASIN CREATION

According to Joy et al. (2019), 1,861 ± 4 Ma U–Pb baddeleyite age of dolerite dyke intruding the lowermost part of Kaladgi Supergroup indicate minimum age of the basin. This age is closely supporting the late Paleoproterozoic age (Sharma and Pandey, 2012) based on bio-stratigraphic marker stromatolites. Further, shales from Bagalkot Group in the lower stratigraphic part of basin indicated 1,800 ± 100 Ma of Rb–Sr isotopic ages with respect to chondritic Earth model (CHUR) (Padmakumari et al., 1998). Considering all these works it is safely predictable that the basin development is related to late Archaean Trans Hudsonian Orogeny (THO) during about 2Ga ago, which is related to development of a supercontinent called Columbia. This supercontinent is also known as Nuna or Hudsonland (Stauffer, 2006; Rogers and Santosh, 2002). During this time the amalgamation between south and north Indian cratonic blocks along the Central Indian Tectonic Zone (CITZ) causing northerly tilt of Dharwar cratonic block for about

1.9^0 angle (Goswami et al., 2023). This tilting event was also related to contemporaneous obduction of Dharwar cratonic block in the southern part along the Palghat Cauvery Suture Zone (PCSZ). Due to this block tilting southern part was uplifted and northern part were submerged to form depression in the form of proto basin. The deeper high-grade rocks were exhumed due to erosion in the southern part and the eroded materials were accommodated in the newly created KB basin. The Archaean basement of KB basin comprises Peninsular Gneissic Complex (PGC), Hungund Schist Belt (HSB) and Closepet granite (CG).

Post sedimentation deformation as well as volcanism imprints are directly visible from map and manifestations are already extensively studied by several authors (e.g., Awati and Kalaswad, 1978; Jadhav, 1987; Nair and Raju, 1987; Pillai and Kale, 2011; Mukherjee et al., 2016; Pillai et al., 2018). Detail studies on multistage deformation mechanism in basement along with the Bagalkot Group of sedimentary rocks by Mukherjee et al. (2016) give significant insights in this context and

Table 2. Revised Stratigraphy of KB basin (proposed in this work)

	Group	Formation	Member	Thickness (m)	Depositional environment
KALADGI SUPERGROUP	Badami Group	Katageri Formation	Konkankoppa Limestone	**85**	Dominantly fluvio-lacustrine deposit (**Jaya Prakash 2007; Mukhopadhyay et al. 2013**). Evidenced minor transgression-regression cycle
			Halkurki Shale	**67**	
		Kerur Formation	Belikhindi Arenite	**39**	
			Halgeri Shale	**3**	
			Cave – Temple Arenite	**89**	
			Kendur Conglomerate	**3**	
	Angular Unconformity				
	Bagalkot Group	Simikeri Formation	*Mallapur Intrusives*	**7**	Terrestrial fluvial fan deposits overlain by high-energy beach deposits grading upwards to tidal flats **(Kale and Phansalkar 1991; Jaya Prakash 2007; Mukhopadhyay et al. 2013**).
			Hoskatti Member Dadanhatti Argillite beds	 **695**	
			Arlikatti Member Lakshanhatti Dolomite beds, Kerkalmatti Haematite schist, Niralkeri Chert Breccia	 **87** **42** **39**	
			Kundargi Member Govindkoppa Argillite beds, Muchkundi Quartzite beds, Bevinmatti Conglomerate beds	 **80** **182** **15**	
		Disconformity			
		Lokapur Formation	**Yadhalli Argillite**	**58**	Transgressive deposits with fluvial sediments at the base followed by beach and intertidal suite and grades upward in to cycles of alternating carbonate and muddy tidal flat deposits **(Kale and Phansalkar 1991; Kale et al. 1996; Bose et al. 2008).** Regression initiate at the top.
			Muddapur Member Bamanbundi Dolomite beds, Petlur Limestone beds, Jalikatti Argillite beds	 **402** **121** **43**	
			Yendigeri member Nagnur Dolomite beds Chikkashellikeri Limestone beds Hebbal Argillite beds	 **93** **883** **166**	
			Yaragatti Member Chitrabhanukot Dolomite beds Muttalgeri Argillite beds Mahakut Chert Breccia	 **218** **502** **133**	
			Ramadurg Member Manoli Argillite beds, Saundatti Quartzite beds, Salgundi Conglomerate beds	 **61** **383** **31**	
		Non-conformity			
		Granitoids, Gneisses and Metasedimentary rocks			

also indicated about the initiation of younger Badami sub-basin creation.

CONTEMPORANEOUS SEDIMENTATION AND TECTONICS

Between Bagalkot and the overlying Badami Group there is a hiatus of ~1Ga. Thus, extensional and contractional domains of continuous single event deformation (Mukherjee et al., 2016) took place after Bagalkot sedimentation is pre Badami. Southerly-directed gravity gliding of the Bagalkot Group over nonconformity was related to a tectonic uplift of the basement as a consequence of Grenville orogeny. This Mesoproterozoic orogeny is related to the creation of new sub-basin for accommodating newer Badami sediments. Moreover, this globally known Grenville orogeny is also related to assembly of continents to form Supercontinent called Rodinia (Tollo et al., 2004). This is also supported by the 1154±4Ma age from $^{40}Ar/^{39}Ar$ dating of an intrusive mafic dyke emplaced along the axial plane of the fold in Bagalkot Group (Pillai et al., 2018).

KB SEDIMENT DEPOSITIONAL ENVIRONMENT

Average total thickness of Badami and Bagalkot Groups are ~286m and ~4241m respectively. Hence cumulative thickness is approximately about 4.55km. However, from the sub-surface exploratory drilling data of Atomic Minerals Directorate for Exploration and Research, India it is found that Badami Group comprises >400m sediment thickness with substantial lithofacies variation (Varshanay et al., 2022). The cyclic transgressive and regressive nature of sedimentation was explained to be near-shore, shallow marine condition with individual marker litho horizons indicative of fluvial, lagoonal, beach and littoral-tidal flat environments (Jaya Prakash et al., 1987; Kale and Phansalkar, 1991; Sathyanarayana, 1994; Kale et al., 1996; Bose et al., 2008; Dey et al., 2009; Dey, 2015).

BAGALKOT DEPOSITIONAL ENVIRONMENT

Present observation supports the view of (Bose et al., 2008) and based on distinguishable lithological attributes in this fluvio-marine set up sequence stratigraphic approach is essential with characterization of facies association with suitable scale. Sedimentation starts with a coarsening-upward fan succession in a low-stand systems tract (LST) which corresponds to approximate bottom part of Ramdurg Member. This followed by the fining-upward transgressive systems tract (TST) equivalent to the upper Ramdurg to upper Muddapur Member. There were minor fluctuating events within major systems tracts. After TST, high-stand systems tract (HST) is evidenced by Yadahalli Member. Subsequently, there was a regressive event lead to creation of apparent disconformity (i.e., sub aerial unconformity with correlative conformity) defined as falling stage systems tract (FSST). Next cycle again starts with another LST with conglomerate horizon in the bottom part of Kundargi member of Simikeri Formation. Here, LST and FSST are also called as normal and forced regression, respectively. This LST was again followed by TST (~ Arlikatti Member) and HST (~Hoskatti Member). After this HST basin completely filled up and further accommodation space could not be created. Thus, a break in sedimentation with prolonged non-deposition and erosion occur along with intrusive and tectonic events after diagenesis. As such there is no evidence of syn sedimentary tectonism during Bagalkot Group sedimentation. Detail facies studies are not made in this context as there are already numerous works done by sedimentologists of the country. Moreover, availability of subsurface drill cores would have given more insights. Since fresh cores of Badami Group are available the Badami Group has been studied in more details.

BADAMI DEPOSITIONAL ENVIRONMENT

The Kerur Formation occupies much larger areas than the overlying Katageri Formation. Dominance of SW directed palaeocurrent implies a braided fluvial system at the lowermost Kerur Formation and Katageri Formation is interpreted to be of fluvio-lacustrine origin (Jaya Prakash, 2007; Mukhopadhyay et al., 2013).

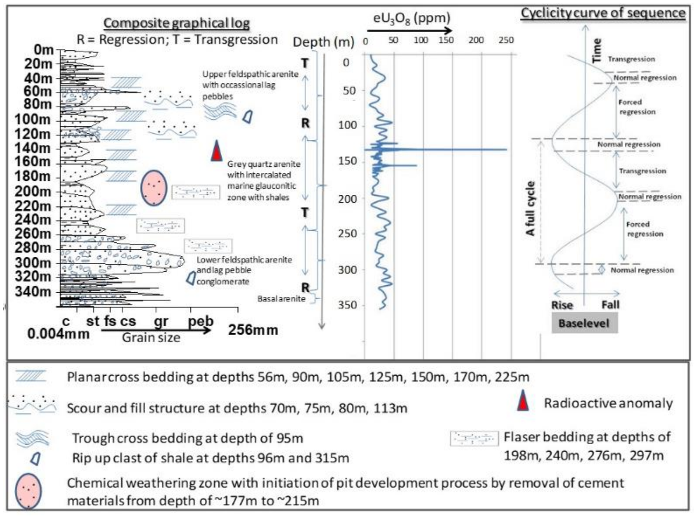

Fig 7. Composite litholog based on subsurface drill core suggests the lithofacies variation and changes in sequence with depth with uranium content variation.

Systematic sedimentary facies analysis is carried out from borehole core studies. Logging of vertical borehole cores for about 360m from entire Kerur Formation up to the basement unconformity contact suggests broadly 4 major lithofacies (e.g., 1. upper feldspathic arenite with lag pebble conglomerate, 2. grey quartz arenite, 3. lower feldspathic arenite with lag pebble conglomerate and 4. Basal arenite). These facies categorization is made based on distinguishable lithological attributes with sequence stratigraphic approach at uniform scale (Fig. 7). The basal sequence of coarse matrix supported fluvial conglomerate and feldspathic arenite starts above a thin shale indicate a regressive event, when the river enters much inside the shallow epeiric sea. However, for better and detailed understanding subdivision into sub-facies are also useful to describe the systems tract. Following basis are standardized in the present study:

SCALE OF OBSERVATION:

It is very important to consider a practical and optimum useful scale in defining particular facies. Because microfacies are not at all relevant in studying about 360m depth ranges, presently macroscopic observations are taken into consideration. Thus, a thin shale lamina (~1mm or less thick) within consistent arenite (~100m) is not considered as separate facies in macroscale but that may be considered as separate facies in microscopic scale (if detailed study is performed). Thus, only selective portions can be studied for detailed facies analysis at microscale. For radioactive intervals especially for uranium exploration such detailed analysis may be taken up exclusively. Present context is not relevant to uranium related studies. For representing about 360m thick sedimentary column in a single sheet resolution cannot be less than 1m, which restricts depiction of thin unit (<1m) as separate unit/facies.

COLOUR, COMPOSITION AND FREQUENCY OF LITHO-UNITS:

These properties are given most importance in characterizing macro facies. There are certain zones where frequency of shale laminations is higher and often depending up on the composition and Eh-pH condition variation in colour is differentiable (such as greenish grey, purple, black, brick red etc). Grain size variation (ranging from clay to pebble) is well represented in this graphical log, in which entire spectrum from 0.004mm to 256mm is kept to easily demarcate the rock types visually at a glance.

PRIMARY SEDIMENTARY STRUCTURES:

This may not be always useful as fundamental criteria of facies classification from litho-core. However, primary sedimentary structures may often give useful information on depositional environments if accurate identification is made. For detailed analysis in understanding the depositional condition structures give valuable insights. For example, cross bedded sandstone may be differentiated from planar bedded sandstone. Shale can show typical tool marks or scour and fill structures at the top, cross bedded sandstone may be sub-divided into trough, hummocky, heringbone and planar tabular cross bedded facies. Presently we have studied only those structures clearly interpretable from core along with their significance. The studied litho-log represents a complete cycle and a partial cycle of sequence (Fig. 7), which starts with a regression when river went much inside the Epeiric Sea. Thus, thin marine shale is immediately overlain by conglomerate, which are not well sorted but matrix supported, sub-angular with moderate to low order sphericity. This implies about low transportation by debris flow from nearby highlands through small river channels into the inland sea. Presence of such conglomerates at different portions of the log suggest about its diachronous nature with variable timing and places of deposition as per the relative advancement and/or retreat of palaeo-shore line. Unlike present day rivers these rivers were of restricted length and such alluvial fan coast were common in Precambrian terrain along with shallow epeiric sea. After the regression transgression were initiated with sea level rise and marine encroachment and landward retreat of river mouth to give rise arenite facies with feldspar rich followed by feldspar poor quartz rich arenite and then heterolithic units of frequent shale bands. These rock types are implying a progressive transgression with characteristic sedimentary structures like wave ripples and associated cross stratifications of various types like tabular and trough. After this transgression another regression phase is identified from facies assemblage and significant structures. Thus, a complete sequence stratigraphic cycle is possible to visualize from a regression followed by transgression and again regression. After the regressive stage another incomplete transgression stage is preserved. This new sequence starts possibly with Belikhindi unit of feldspathic arenite in the log and cycle would have been completed after logging Katageri Formation. However, Katageri Formation is exposed at different areas (Fig. 2).

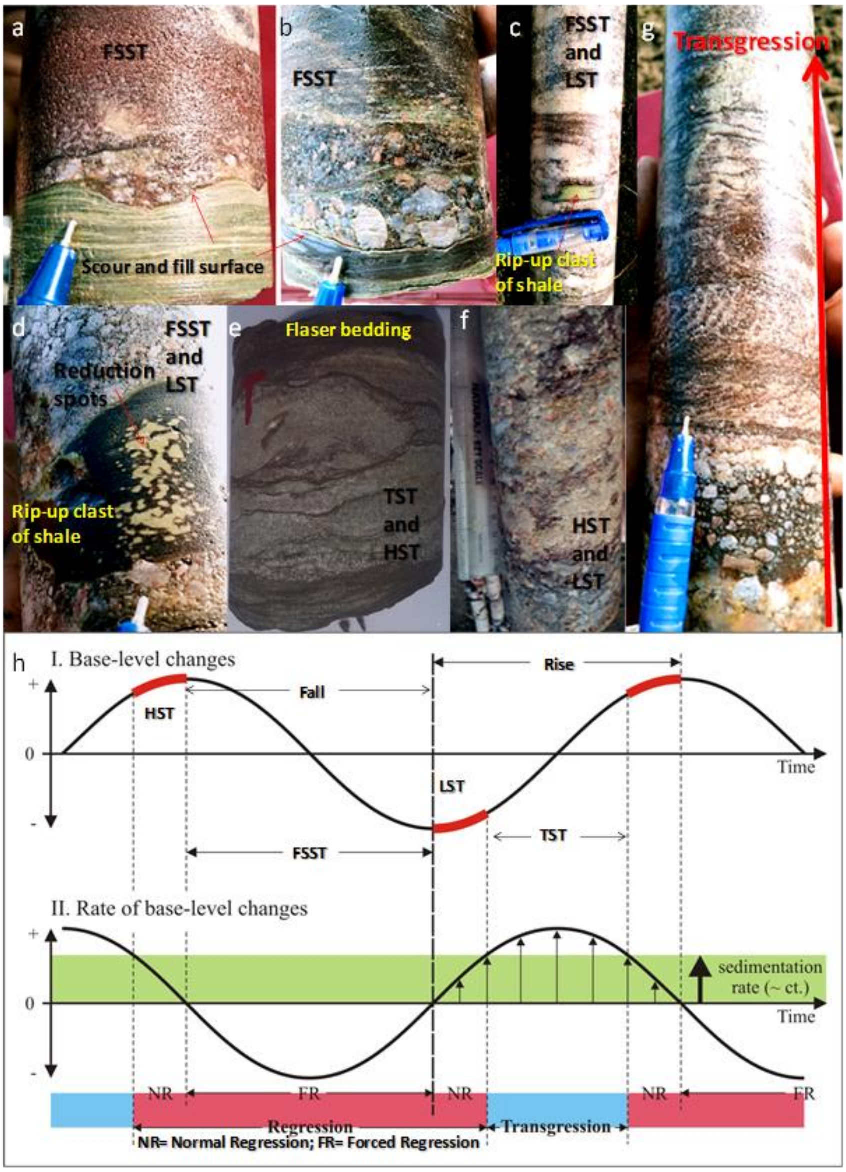

Fig 8. a-b. Scouring of shale bed top and later infilling of scoured portions by coarse grains. c-d. rip up shale clasts implying the transported chips of shale during scouring process of forced regression (FSST) and later settlement as fill structures along the LST. e. flaser bedding indicates marine transgression with thin shale laminae within sandstone (TST to HST). f. feldspathic arenite implying rapid terrestrial input with low transportation during normal regression when rate of sedimentation is higher than base level rise, i.e., either the post transgression HST or LST stage after FSST. g. transgressive facies association with fining upward sequence. h. standard sequence stratigraphic curves to substantiate the transgression - regression cycles.

The implications of sedimentary structures and grain size variation are significant in recognizing the systems tract. Presence of scour and fill structures, rip-up clasts of shale, matrix supported lag pebble conglomerate indicate regression stage and flaser bedding, quartz arenite and frequent shale indicate transgression event. Further details are discussed below for understanding the systems tracts with specific events, corresponding lithofacies and structures.

The initial marine sediments are overlain by forced regressive facies of conglomerate with typical rip-up clasts of shale, which were removed by erosive river current flow during regression and subsequently preserved within lag conglomerate. Such clayey sediments are highly cohesive and during sub-aerial exposure the dried-up chips often form flat tabular clasts of clayey sediment, which can be ripped up when scouring of such shale bed top take place by high velocity stream flow inside the regressive sea. Thus concave-upwards erosion surface of shale bed top implies excavation by aggrading stream. Further, during the waning stage of river flow intensity the scour gets filled by coarser sediments (Fig. 8a-d). Thus, the FSST and LST can be interpreted from such structures, which are produced during forced regression followed by normal regression. Transgressive facies are mostly characterized by quartz arenites with wave ripples (observed in outcrop but not in core), cross beds, flaser beds with overall fining upward grain size variation (Fig. 8e, g). However, increase in feldspar content in the arenite gives clue towards a significant event, i.e., normal regression, when the rate of sedimentation is more than the rate of creation of accommodation space, which is more prominently indicated from feldspar from nearby lands through minimum transportation along stream channels into the sea. Thus, the feldspathic arenite repeatedly occurs due to normal regression before and after transgression corresponds to LST and HST respectively (Fig. 8f, h). A brief overview of significant events with reference to marker surface, lithofacies association and condition of sea-level and/or river system is summarized in Table 3.

Table 3. The fingerprint features used as diagnostic criteria of significant stratigraphic surfaces (after Catuneanu, 2002)

Significant event marker surface	Nature of the plane	Facies		Depositional trend	
		Below	Above	Below	Above
Subaerial unconformity	Scoured or bypass	Not specific	Nonmarine	NR, FR	NR, T
Correlative conformity	Conformable	Coarsening upward marine	Coarsening upward marine	FR	NR
Basal surface of forced regression	Conformable or scoured	Coarsening upward marine	Coarsening upward marine	NR	FR
Regressive wave ravinement	Scoured	Coarsening upward shelf	Coarsening upward shore	NR, FR	FR, NR
Maximum regressive surface	Conformable	Coarsening upward	Fining upward	NR	T
Maximum flooding surface	Conformable or scoured	Fining upward	Coarsening upward	T	NR
Transgressive wave ravinement	Scoured	Coarsening upward	Fining upward	NR, T	T

TECTONIC IMPRINTS ON SEDIMENTATION

According to Gallagher and Lambeck (1989) subsidence of a basin can be reconstructed from the analysis of the accumulated sediments in a basin. Basically, strata get preserved in any basin due to tectonic subsidence of basin floor and such creation of accommodation spaces are syn-sedimentary phenomenon along with other processes like rise in absolute base level. From the analyses of aeromagnetic data basement structures was determined by Sridhar et al. (2018). According to Chaturvedi et al. (2012) there are complex N-S, WNW-ESE and NE-SW fault pattern noted along southern margin of the Kaladgi-Badami basin and the adjacent crystalline basement and also a distinct NE-SW structural zones in the eastern part of basin is interpreted to act as a facilitating factor in creating local depocenter for sediments. The heliborne geophysical data also gave insights on the fact that the entire basin is divided into several sub-basinal segments separated by fault-affected NE-SW and NW-SE oriented basement ridges. Further, sediment thickness was also estimated from the difference between digital elevation model and magnetic basement elevation grid. According to this study after Chaturvedi et al. (2012), average thickness of basin fill sediment is 400 m and at places about 800m thick pockets were also reported. In case of rift basin several fault segments are observed to act as depocenter (Leeder, 1995) and sedimentary fill deposits are wedge shaped with increased thickness nearby the active marginal parts. Exact basin configuration remains doubtful so far due to Deccan flood basalt coverings. However, attempt of mapping the sub-trappean sediments was taken by Sridhar et al. (2017) using heliborne time domain electromagnetic data. It was also observed from the sediment thickness map (Sridhar et al., 2018) that thickness reduce towards north and hence supports wedge like sediment body as typically expected in case of rift basin. Pillai et al. (2018) interpreted sediment accumulation curves (SAC) and explained that during the Bagalkot sedimentation basin floor subsidence rate was more than that during the Badami Group sedimentation. syn-sedimentary reactivation of basement faults is well explained from Bagalkot Group as a supportive tool of rifting (Kale et al., 1998; Kale and Pillai, 2011).

Badami Group also provides syn sedimentary normal faulting evidences in favour of rifting. Based on borehole data from Suldhal and adjacent areas (Figs. 1 and 9) sediment thickness is observed to be different across the fault which records the differences in the elevation of the depositional surface on the footwall and hanging wall sides. In fact, the Bababudan-Nallur Shear (BNS) zone passes below the sediment in this area.

PRESENT BASIN CONFIGURATION AND ARCHITECTURE

From the geological observations it is clear that sedimentation took place in passive rift setting in the Kaladgi-Badami basin. There is signature of depressed graben without igneous activity unlike active rift areas where presence of active volcanoes, elevated heat flows, high seismicity, thinner crust with elevated Moho beneath the rift zones are common (Hochstein, 2005; Kandie, 2015; Goswami et al., 2020).

There is unknown extension of sediments concealed below the vastly spreaded basaltic Deccan Trap flows. In fact, the present KB basin configuration is very much irregular because of

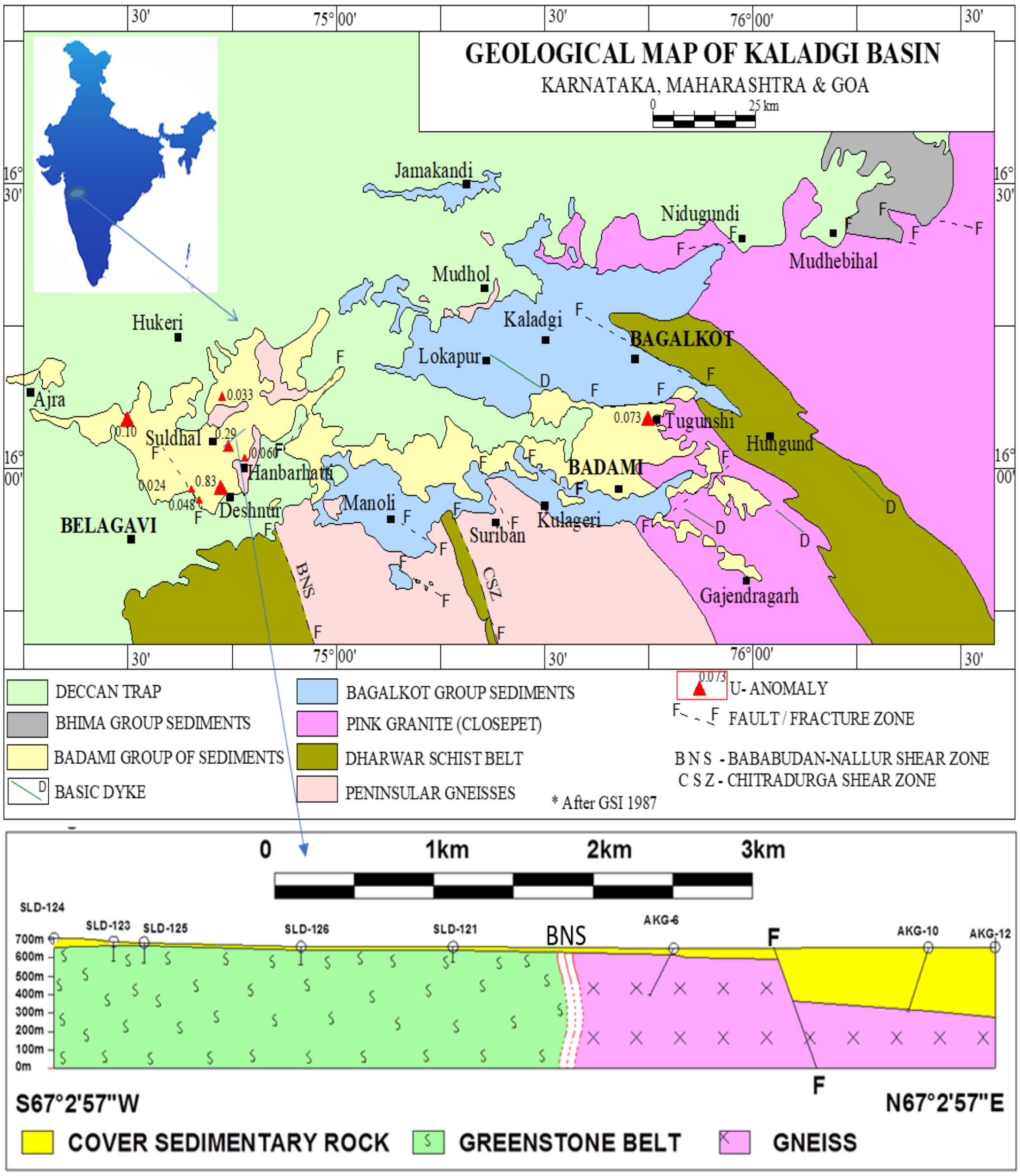

Fig 9. Transverse section along ~ENE-WSW based on sub-surface drilling data along the BNS contact between greenstone belt and gneiss

such extensive overlapping by the younger Deccan volcanism. As physiographically this southern part of Deccan plateau exhibits actual basin margin by forming typical rift shoulder with elevated topography (Goswami et al., 2016), later developed fault affected basement sediment contact should not be confused with actual basin margin. According to Jaya Prakash et al. (1987), sudden topographic rise of ~50m with reference to the surrounding granitoid-greenstone basement complex is noteworthy along the southern, eastern and western margins. Later developed depocenter for Badami Group of sediments was also created by subsequent reactivation of normal fault as a continuation of rifting after a prolonged time gap. Hence these younger rocks lie over the Kaladgi Group and also over the basement complex with distinct angular unconformity. The sedimentary rocks of KB basin are affected by several faults with different dimensions with trends varies among E-W, NE-SW and NW-SE. However, most widely visible fault set can be recognized as E-W trending Sirur-Katageri fault, Saundatti fault, B.N. Jalihal fault, Bilgi-Nidgundi fault and Bisnal-Mantur fault. Therefore, from the analysis of reported diastrophic features it is beyond doubt that Badami Group could not be affected by folding as such but extensively affected by faulting with dominant vertical displacements indicative of normal extension faulting. It can be confirmed that ductile folding event is older than the brittle faulting. Hence older Bagalkot rocks are affected by both folding and faulting. It is also understood from this structures that the entire system got exhumed gradually with time and shallow level deformation imprints could not affect the Badami sediments intensively and almost sub-horizontal to low dipping beds could be preserved.

DISCUSSION

PROBLEM WITH BASIN DIMENSION AND MARGIN DEMARCATION

The basement schist and gneiss of the sedimentary basinal rock indeed indicate shallow intra continental basin i.e., epeiric sea unlike normal marine basin of present-day sea floor with typical basaltic and gabbroic oceanic crust. For any basin of geological past the margin or deeper part is not easy to recognize at a glance because the geographical and geological basin margin is not same thing (Fig. 10). The actual geographic margin rarely remains intact but mostly eroded and removed after affected by tectonism and the preserved remnants of the sedimentary basin margin may not be actual margin. Therefore, depending upon the tectonic history, the Proterozoic basinal sedimentary rock map and contact relationships can give ideas on depth of sedimentation, which in turn give clues on sedimentation history. At places inside the basin only deeper basinal chemical sediments may be directly preserved above nonconformity on basement and at shallow level different clastic rocks may lie above basement. Therefore, even in undeformed basin also stratigraphic correlation must be made carefully after considering unconformity and correlative conformity. Transgressive and regressive events are also significant as already described. Field outcrop and subsurface borehole core lithology in Badami Group suggests clastic sediments dominated and shallow fluvio-marine transitional environment prevailed with transgressive systems tract above basement at apparent geographic basin margin. However, as per stratigraphic position of these horizontal beds this represent topmost part.

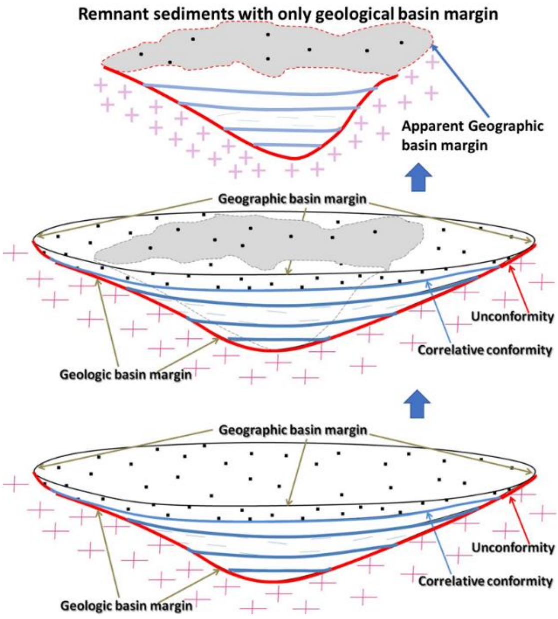

Fig 10. Progressive changes in basin margin with time. These continental basements imply shallow nature. Geographic (black surficial margin) and geologic basin margin (red sub-surface margin and crustal sedimentation above geologic margin indicates eventually preserve geologic margin only.

Now, the importance of scale and basin size come into the discussion because entire understanding is dependent up on the scale of observation. The first relevant question is what should be a minimum size of depression to qualify geologically as basin? Of course, very small depression sites with sedimentation cannot be preserved but there must be some quantification. It is also true that sediment thickness can give an idea on basin size because large basin size may have larger depth to accommodate more and more sediments. It is observed in general that sediment thickness is varying in between the maximum and minimum surface radius of basin (Fig. 11a). Thus, it is important to judiciously estimate the dimension of basin from sediment thickness. Although there may be exception and accuracy may vary, but definitely an isolated patch of ~1km thick sedimentary rock of 1 km^2 area cannot be a basin but it is expected to be a remnant part of earlier existing basin. Similarly, if there is very close proximity of two separately preserved sedimentary sequence and the terrain is intensely affected by faults it is naturally expected that the two sedimentary rock outcrops were part of same basin which got tectonically separated. In this context, time correlation and spatial correlation should be taken into consideration carefully. Depending up on the scale, for smaller area same litho-contacts can be correlated and can indicate same time but when broader area is studied then different litho-units can be deposited at different part of same basin at the same time. Thus, litho-contact tracing cannot give fruitful result of correlation (Fig. 11b). So, different lithology does not always mean different episode of deposition. In Figure 11b, a smaller part is enlarged to show the importance of scale in Figure 11c, in which lithostratigraphic correlation is well applicable. The carbonate dominated Bhima Group and clastic Badami Group are related with time correlatability, which is explained in details with sketches in Figure 5.

It can be seen from the combined map of the Kaladgi-Badami and Bhima basins that the distance between these two basins are only about

10-15 kms near Mudhebihal (Fig. 12). This clue gives enough scope of arguments that Kaladgi-Badami and Bhima basins were geographically connected before tectonism and these were part of a single basin. Therefore, principle of lateral continuity can be applied in correlating the sedimentary rocks between adjacent outcrops.

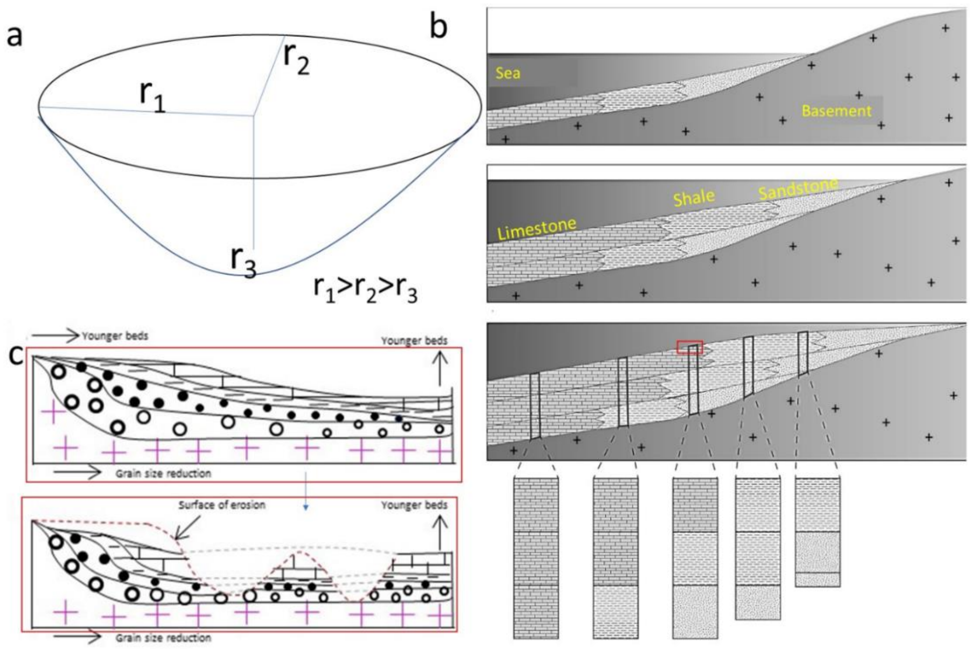

Fig 11.a. Proterozoic rift basin size and depth relation and broadly sub-elliptical geometry due to crustal tilting or stretching. b. lateral and vertical relations with changing sea level. Importance of scale of observation can be visualized in case of correlation of lithounits. c. for detail large scale over small area litho correlation is possible but for small scale over large are time correlation i.e., sequence boundaries are more important.

STRATIGRAPHIC CORRELATION BETWEEN KB BASIN AND BHIMA BASIN

Age data from the KB basin as well as Bhima basin are not sufficiently available. Based on chemo-stratigraphy and carbon isotope composition analysis Neoproterozoic age was proposed (Kumar et al., 1999; Nagarajan et al., 2008) for the Shahabad limestone of Bhima Group. Hence most widely accepted age is Neoproterozoic based on fossil evidences as well (Mishra et al., 1987; Maithy and Babu, 1996; Sharma and Shukla, 2012; Kale and Phansalkar, 1991; Jaya Prakash, 2007). However, according to another school of researchers (Augustine et al., 2015; Absar et al., 2016) Mesoproterozoic age is also suggested. Evidences based on suspected presence of limestone xenoliths of Bhima Group within 1090 Ma Siddanpalli Kimberlite (Dongre et al., 2008) and direct radiometric age of coffinite within the faulted and brecciated Shahbad limestone from Gogi uranium deposit (TIMS U–Pb age 1266 ± 76 Ma) proved that the age of Bhima Group is Mesoproterozoic (Pandey et al., 2008). Moreover, this hydrothermal uranium ore yielded a whole rock Pb-Pb isochron age of 1308 ± 49 Ma (Pandey et al., 2009). Therefore, more direct evidence supports Mesoproterozoic age of Bhima Group. Unfortunately, there is no such age dating available from Badami Group.

In fact, the correlatable Badami and Bhima sedimentation initiated as a consequence of assembly of Supercontinent Rodinia that was built up around 1260-900Ma ago and subsequently broken up by 750-633Ma (Hoffman, 1991; Kee et al., 2019). Badami is dominantly clastic unlike the carbonate rich Bhima Group. From the age correlation and geographic proximity as well as undeformed subhorizontal dip of bedding in both the depositional areas in general, it can be justified that these were deposited within same basin at separate depocentres. Bhima sediments represent relatively deeper or distal portion of the basin unlike the fluvial to marginal marine Badami Group. Subsequent faulting affected the preserved sediments to dislocate. As it is visible that Bhima basin does not have any natural/actual basin margin but everywhere tectonic/fault contact between basement and sediments is implying rigorous disturbances after sedimentation. Thereby the southern part of Bhima basin margin was totally eroded leaving behind remnants of uppermost part of arenite and shale (i.e., clastics) in the form of Rabanpalle Formation (Goswami et al., 2021). Dominant carbonates indicate shallow marine shelf like platformal environment where detritus supply got restricted and growth of stromatolites were common.

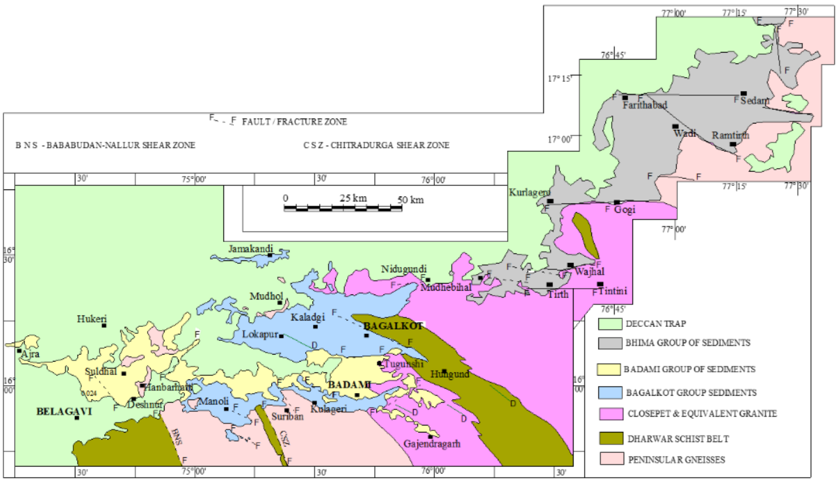

Fig 12. Combined map of KB and Bhima basin shows a broad geographic continuity and due to effects of tectonism and volcanism, present configuration is achieved.

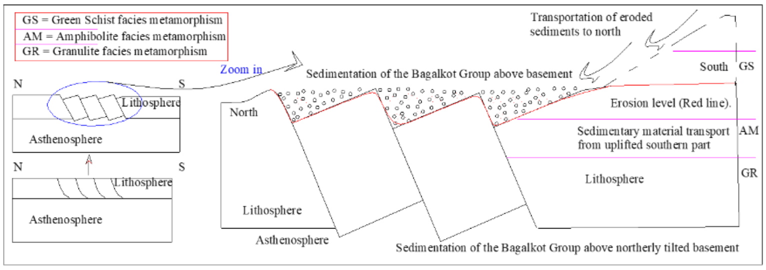

Fig 13. Northerly tilting of crustal block lead to basin creation at cratonic north and uplift with erosion along south. Exhumation lead to expose progressive deeper and higher metamorphic grade features towards south and eroded materials filled the basin in the north.

PROPOSED BASIN MODEL

Below Deccan Trap there may be Badami basinal limestone extension correlatable with the Bhima Group. However, based on the presently available data it is good enough to propose a new basin evolution model.

Initially developed block faulting due to northerly tilting of crustal block led to develop accommodation space for Bagalkot Group in proto Kaladgi basin. These normal fault arrays created passive rifting. The sediment supplied from uplifted southern basement erosion (Fig 13). Hence deeper higher-grade metamorphic rocks are exposed towards south. Along the present basin margin in the south of KB as well as Bhima basins low grade metamorphism is noted as lower greenschist facies. As we move south there is a systematic increase in metamorphic grade like upper greenschist facies followed by amphibolite facies and at very far granulite terrain also exposed along the southern extreme of Dharwar Craton. These observations are well known and thus raise the issue that where did the eroded sediment go! The answer can be explained from Figure 13. After basin filling and achieving temporary equilibrium, diagenesis of Kaladgi sediments was initiated and then Grenville orogeny affected the sediments with folding and then reactivation of faults along E-W trends. Several depocenters could be created due to this E-W fault system. Continued crustal tilting till achieving ~1.9^0 led to further sediment supply (Goswami et al., 2023) from the erosion of uplifted southern basement towards depressed northern basin. Shallow level fluvial through marginal marine to shelf environments could form to accommodate clastic and chemical sedimentation further. Systematic stages of progressive basin evolution are represented to visualize the impacts of tectonism followed by Deccan volcanism (Fig. 14).

After the diagenesis of sediments next deformation and faulting events affected sediment and E-W fault system with subsequent differential erosion again create omission of several parts of sedimentary rocks. Towards east deformation intensity increase is

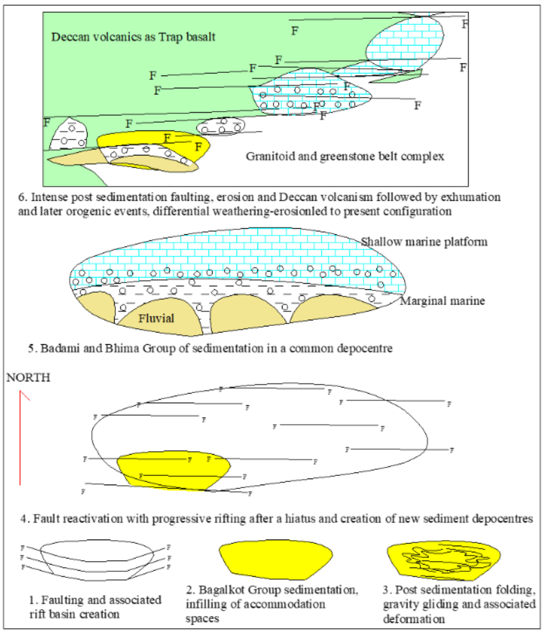

Fig 14. Progressive evolution model of KB-Bhima basin.

evidenced due to long lasting multi episodic Eastern Ghats Orogeny (EGO) and E-W compression was manifested in the form of E-W reactivated normal faults because of N-S maximum extension or minimum compression. Therefore, Bhima basinal rocks are more intensely deformed than Badami due to lesser distance from the site of main E-W compression regime of EGO.

At last profuse volcanism might have covered significant portion of the sediments in the NNW extension areas.

SCOPE OF FUTURE RESEARCH

Although the main aim of the paper is fulfilled by emphasizing few salient points regarding the stratigraphic reconstruction and basin correlation, the present work is not conclusive and there is further scope. Because, if the KB and Bhima is same basin then again Stratigraphic units of Bhima Group will have to be re-examined to fulfill the assignment criteria of Formation. Considering the KB and Bhima as a single basin all litho-units must be reassessed in terms of basin scale map. Finally, a combined comprehensive stratigraphic column will have to be prepared. In that combined Kaladgi-Badami-Bhima basin sub-basinal concepts must be introduced.

ACKNOWLEDGEMENT

Authors acknowledge the competent authority in AMD for permission and encouragement to publish this work.

REFERENCES

Absar, N., Nizamudheen, B. M., and Augustine, S. (2016). Petrography, clay mineralogy and geochemistry of clastic sediments of Proterozoic Bhima Group, Eastern Dharwar Craton, India: Implications for provenance and tectonic setting. Journal of Applied Geochemistry. 18(3), p. 237-250

Augustine, S., Nizamudheen, B. M., Absar, N., Managave, S., and Bhutani, R. (2015). Carbon and Oxygen isotopic composition of Carbonate formations of Bhima Basin, Eastern Dharwar Craton, Karnataka. Abs. in 'National Seminar on Recent Developments and challenges in Geochemistry (GEOCHEM-2015), ISAG-Annamalai Univ., p. 27-28

Awati, A. B., and Kalaswad, S. (1978). Structure of the Kaladgis around Yadwad, Belgaum district (A study based on Landsat-I); Bull. Earth Sci. 1, p. 43–47.

Bose, P. K., Sarkar, S., Mukhopadhyay, S., Saha, B., and Eriksson, P. (2008). Precambrian basin margin fan deposits: Mesoproterozoic Bagalkot Group, India. Precambrian Research, 162, p. 264–283.

Catuneanu, O. (2002). Sequence stratigraphy of clastic systems: concepts, merits, and pitfalls. Journal of African Earth Sciences, 35(1), p. 1-43. https://doi.org/10.1016/S0899-5362(02)00004-0

Chaturvedi, A. K., Kovac, P., Chawla, A. S., Wiseman, R., Markandeyulu, A., Hope, J., Sridhar, M., Carey, H., Sharp, B., and Rai, A. K. (2012). Geological Interpretation of Heliborne Geophysical Data from the Kaladgi Basin; Southern India, ASEG Extended Abstracts, 2012:1, 1-4, DOI: 10.1071/ASEG2012ab393

Dey, S. (2015). Geological history of the Kaladgi–Badami and Bhima basins, south India: sedimentation in a Proterozoic intracratonic setup. Chapter 19. In. Mazumder, R. & Eriksson, P. G. (eds) 2015. Precambrian Basins of India: Stratigraphic and Tectonic Context. Geological Society, London, Memoirs, 43, p. 283–296, http://dx.doi.org/10.1144/M43.19

Dey, S., Rai, A. K., and Chaki, A. (2009). Palaeoweathering, composition and tectonics of provenance of the Proterozoic intracratonic Kaladgi–Badami basin, Karnataka, southern India: evidence from sandstone petrography and geochemistry. Journal of Asian Earth Sciences, 34, p. 703–715.

Dongre, A., Chalapathi Rao, N.V., and Kamde, G. (2008). Limestone xenolith in Siddanpalli Kimberlite, Gadwal Granite–Greenstone Terrain, Eastern Dharwar craton, Southern India: remnant of Proterozoic platformal cover sequence of Bhima/ Kurnool age? Journal of Geology, 116, p.184– 191.

Gallagher, K., and Lambeck, K. (1989). Subsidence, sedimentation and sea-level changes in the Eromanga Basin, Australia. Basin Research, 2(2), p. 115–131.

Geological Survey of India (GSI) (1994). Generalized geological map of Dharwar Craton, adapted from project Vasundhara of Geological Survey of India Records.

Goswami, S., Mukherjee, A., Zakaulla, S., and Rai, A.K. (2016). Stress states, faulting and their effects on the Papaghni Group, Cuddapah basin, India: A study along Giddankivaripalle–Madyalabodu tract. Indian J. Geosci. 70, p. 17–33.

Goswami, S., Dey, S., Zakaulla, S., and Verma, M.B. (2020). Active rifting and bimodal volcanism in Proterozoic Papaghni sub-basin, Cuddapah basin (Andhra Pradesh), India. J. Earth Syst. Sci. 129, 21pp. https://doi.org/10.1007/s12040-019-1278-3

Goswami, S., Shrivastava, S., Das, S., and Bhattacharjee, P. (2021). Fundamentals of litho-structural mapping: Example from the SW part of the Proterozoic Bhima basin, Karnataka, India: A note on Dharwarian Crustal evolution. In S. Mukherjee (Ed.), Structural Geology and Tectonics Field Guidebook—Volume 1. Springer Nature Switzerland AG. Cham. p. 639-684. ISBN: 978-3-030-60142-3.

Goswami, S., Bhagat, S., Pande, D., Choudhury, D. K., Saravanan, B., and Sinha, D. K. (2023). Implication of deformation fabrics of schist-migmatite-gneiss and granite in understanding regional tectonics: Eastern Dharwar Craton (EDC), India. Proceedings of the Indian National Science Academy. https://doi.org/10.1007/s43538-023-00173-x

Hochstein, M. P. (2005). Heat transfer by hydrothermal systems in the east African Rifts. Proceedings World Geothermal Congress, Antalya, Turkey, p. 24–29.

Hoffman, P. F. (1991). Did the breakout of Laurentia turn Gondwanian side-out? Science, 252, p. 1409 – 1412

Jadhav, P. B. (1987). Microstructures of quartzites of Yadwad–Lokapur–Bagalkot area, Bijapur district, North Karnataka; Unpublished Ph.D. thesis, Pune University, 204pp

Jaya Prakash, A. V., Sundaram, V., Hans, S. K., and Mishra, R. N. (1987). Geology of the Kaladgi-Badami Basin. Purana Basins of Peninsular India (Middle to Late Proterozoic). Memoir Geological Society of India 6, p. 201–226.

Jaya Prakash, A. V. (2007). Purana Basins of Karnataka. Geological Survey of India, Kolkata, Memoirs, 129pp.

Joy, S., Patranabis-Deb, S., Saha, D., Jelsma, H., Maas, R., Söderlund, U., Tappe, S., van der Linde, G., Banerjee, A., and Krishnan, U. (2019). Depositional history and provenance of cratonic "Purana" basins in southern India: A multipronged geochronology approach to the Proterozoic Kaladgi and Bhima basins. Geological Journal, 54(5), p. 2957-2979

Kale, V. S., Ghunkikar, V., Paul Thomas, P., and Peshwa, V. V. (1996). Macrofacies architecture of the first transgressive suite along the southern margin of the Kaladgi basin. Journal of the Geological Society of India, 48, p. 75–92.

Kale, V. S., Nair, S., and Pillai, S. P. (1998) Testimony of intraformational limestone breccias on Lokapur–Simikeri disconformity, Kaladgi Basin; J. Geol. Soc. India, 51, p. 43–48.

Kale, V. S., and Phansalkar, V. G. (1991). Purana basins of Peninsular India: a review. Basin Research, 3, p. 1–36.

Kale, V. S., and Pillai, S. P. (2011). A reinterpretaion of two Chert breccias from the Proterozoic basins of India; J. Geol. Soc. India, 78, p. 429–445

Kandie, R. J. (2015). Eastern rift structural geology-tectonics, Volcanology and geothermal. Presented at Short Course X on Exploration for Geothermal Resources, organized by UNU-GTP, GDC and KenGen, at Lake Bogoria and Lake Naivasha, Kenya, Nov. 9–Dec. 1.

Kee Weon-Seo, Kim Sung Won, Kwon Sanghoon, Santosh, M., Ko Kyoungtae, and Jeong Youn-Joong (2019). Early Neoproterozoic (ca. 913–895 Ma) arc magmatism along the central–western Korean Peninsula: Implications for the amalgamation of Rodinia supercontinent. Precambrian Research, 335, no. 105498.

Kumar, B., Das Sharma, S., Shukla, M., and Anand Sharma, M. (1999). Chronostratigraphic implication of carbon and oxygen isotopic compositions of the Proterozoic Bhima carbonates, southern India. Journal Geological Society of India, 53, p. 593–600.

Leeder, M. R. (1995). Continental rifts and proto-oceanic troughs. In: Tectonics of Sedimentary Basins (Ed. by C. J. Busby and R. V. Ingersoll).

Maithy, P. K., and Babu, R., (1996). Carbonaceous macrofossils and organic-walled microfossils from the Halkal Formation, Bhima Group, Karnataka with remarks on age. Palaeobotanist, 45, p.1-6.

Mishra, R. N., Jaya Prakash, A. V., Hans, S. K., and Sundaram, V. (1987). Bhima Group of Upper Proterozoic – a stratigraphic puzzle. In: Purana Basins of Peninsular India (Middle to Late Proterozoic). Memoir Geological Society of India, 6, p. 227– 237

Mukherjee, M. K., Das, S., and Modak, K. (2016). Basement–cover structural relationships in the Kaladgi Basin, southwestern India:

Indications towards a Mesoproterozoic gravity gliding of the cover along a detached unconformity. Precambrian Research 281, p. 495–520

Mukhopadhyay, S., Choudhuri, A., Samanta, P., Sarkar, S., and Bose, P. K. (2013). Were the hydraulic parameters of Precambrian rivers different? Journal of Asian Earth Sciences, 91, p. 289–297.

Nagarajan, R., Sial, A. N., Armstrong-Altrin, J. S., Madhavaraju, J., and Nagendra, R. (2008). Carbon and oxygen isotope geochemistry of Neoproterozoic limestones of the Shahabad Formation, Bhima Basin, Karnataka, southern India. Revista Mexicana de Ciencias Geologicas, 25, p. 225–235.

Nair, M., and Raju, A. V. (1987). A Remote Sensing approach to basinal mapping of the Kaladgi and Badami sediments of Karnataka state; In: Purana basins of Peninsular India (Middle to Late Proterozoic) (ed.) Radhakrishna B.P, Geol. Soc. India Memoir, 6, p. 375–381

Padmakumari, V. M., Sambasiva Rao, V. V., and Srinivasan, R. (1998). Model Nd and Rb–Sr ages of shales of the Bagalkot Group, Kaladgi Supergroup, Karnataka. Abstracts: National Symposium on Late Quaternary Geology and Sea level Changes. Cochin University, Kochi, 70pp.

Pandey, B. K., Natarajan, V., Krishna, V., and Pandit, S. A., (2008). U–Pb and Sm–Nd isotope studies on uraniferous brecciated limestone from Bhima basin: evidence for a Mesoproterozoic U mineralization event in southern Peninsular India. Abs. In: Significant Milestones in the Growth of Geochemistry in India during the 50-year Period: 1958–2008. Geological Society of India and Atomic Minerals Directorate for Exploration and Research, p. 24–25.

Pandey, B. K., Krishna, V., Pandey U.K., and Sastry D.V.L.N. (2009). Radiometric dating of uranium mineralization in the Proterozoic basins of Eastern Dharwar craton, South India. In: Proceeding International Conference on peaceful use of atomic energy, New Delhi, p. 77-83

Pillai, S. P., Pande, K., and Kale, V. S. (2018). Implications of new $^{40}Ar/^{39}Ar$ age of Mallapur Intrusives on the chronology and evolution of the Kaladgi Basin, Dharwar Craton, India. Journal of Earth System Science. 127, 32pp. https://doi.org/10.1007/s12040-018-0940-5

Pillai, S. P., and Kale, V. S. (2011). Seismites in the Lokapur Subgroup of the Proterozoic Kaladgi Basin, south India: A testimony to syn-sedimentary tectonism. Sedim. Geol. 240, p. 1–13, https://doi.org/10.1016/j.sedgeo.2011.06.013.

Prothero, D. R., and Schwab, F. (2014). Sedimentary Geology: An introduction to sedimentary rocks and stratigraphy. 3rd ed. 557 pp. W. H. Freeman and Company, ISBN-13: 978-1-4292-3155-8

Rogers, J. J., and Santosh, M. (2002). Configuration of Columbia, a Mesoproterozoic supercontinent. Gondwana Research, v. 5(1), p. 5–22. doi:10.1016/S1342-937X(05)70883-2

Sathyanarayana, S. (1994). The younger Proterozoic Badami Group, Northern Karnataka. In: Ravindra, B. M. & Ranganathan, N. (eds) Geo-Karnataka. Mysore Geological Department, Bangalore, Centenary volume, p. 227–233.

Sharma, M., and Pandey, S.K. (2012). Stromatolites of the Kaladgi Basin, Karnataka,India: Their systematics, biostratigraphy and age implications. Palaeobotanist, 61, p. 103–121.

Sharma, M., and Shukla, Y. (2012). Megascopic carbonaceous compression fossils from the Neoproterozoic Bhima Basin, Karnataka, South India. In: Bhat, G. M., Craig, J., Thurow, J. W., Thusu, B. & Cozzi, A. (Eds.) Geology and Hydrocarbon Potential of Neoproterozoic– Cambrian Basins in Asia. Geological Society London, Special Publications, 366, p.277–293.

Sridhar, M., Markandeyulu, A., and Chaturvedi, A. K. (2017). Mapping subtrappean sediments and delineating structure with the aid of heliborne time domain electromagnetics: Case study from Kaladgi Basin, Karnataka. Jour. Appl. Geophy., 136, p. 9-18. http://dx.doi.org/10.1016/j.jappgeo.2016.10.024

Sridhar, M., Markandeyulu, A, Chawla, A. S., and Chaturvedi, A. K. (2018). Analyses of aeromagnetic data to delineate basement structures and reveal buried igneous bodies in Kaladgi basin, Karnataka. Journal of the Geological Society of India 91, p. 165–173. https://doi.org/10.1007/s12594-018-0830-0

Stauffer, M. (2006). Trans-Hudson Orogen. The Encyclopedia of Saskatchwen. Retrieved on 2008-02-11.

Tollo R. P., Corriveau L., McLelland, J. and Bartholomew M.J. (2004). Proterozoic tectonic evolution of the Grenville orogen in North America: An introduction. Geol. Soc. America Memoir, 197, p. 1-18. ISBN 978-0-8137-1197-3.

Varshanay, H., Samant, P., Vijaya Kumar, T., Basu, H., Prakash, B.G., Choudhury, D.K., and Saravanan, B. (2022). Sedimentary facies analysis of Badami Group of sediments and its implication on uranium mineralization in western part of Kaladgi Basin, Belagavi District, Karnataka, India. Exploration and Research for Atomic Minerals (EARFAM) 30, p. 75-96.

Received on : 15th May 2023
Revised accepted on : 09th June 2023

JOURNAL INDIAN ASSOCIATION OF SEDIMENTOLOGISTS ISSN NO 2582 – 2020
Vol. 40, Issue 1, 2023, pp. 73-80
DOI: https://doi.org/10.51710/jias.v40iI.295

Geoengineering properties of the Sandstones of Upper Murree Formation, Jammu and Kashmir: A case study

Yudhbir Singh[1], Ahsan Ul Haq[2], S K Pandita[1], Bashir Ahmad Lone[1] and Arjun Singh[1]

[1]Department of Geology, University of Jammu
[2]Department of Geology, Cluster University of Jammu
E-mail: ahsanmalik4uly@gmail.com

ABSTRACT

Sandstones play a vital role in various geotechnical and civil engineering applications. Understanding the relationship between its petrographic characteristics and geoengineering properties is crucial for reliable design and construction practices. This paper provides a concise overview of the research investigating the relation between the petrographic characteristics and corresponding geoengineering properties of upper Murree sandstone. The Murree Group consists of mudstones and sandstones, which are exposed linearly in the Outer Himalayan belt of Jammu and Kashmir. The sandstones of Murree are the only source of aggregate or building material in this region. The petrographic analysis of the samples revealed that the sandstone is of coarse to fine-grained, stably cemented, unweathered to slightly weathered and having medium strength. These rocks show fractured as well as intergranular porosity whereas, the grains are showing floating contacts, line contacts, point contacts and concavo-convex contacts. Preliminary findings of this study reveal that mineral composition, texture, fabric and the deformation of these sndstones significantly influence their geoengineering behavior. The higher concentration of quartz is an example of such behavior which generally leads to improved strength and lower deformability and on the contrary, higher concentration of clay and mica contribute to decreased strength and increased deformability. In present study, negative correlation between the porosity and compressive strength and positive correlation between cementation and strength of these rocks has been observed.

Keywords: Petrography, Geo-engineering, Upper Murree, Sandstone.

INTRODUCTION

The construction activities in the Lesser and Outer Himalayan zones pose many geological and engineering challenges to the residents living in these areas. Murree belt comprises of fragile sandstones, siltstone and mudstone, having low bearing capacity, low mechanical strength and high deformability and fracturing (Bell and Culshaw, 1998; Belland Lindsay, 1999; DeReuil et al., 2019). The physico-mechanical characteristics of the sandstones, siltstone, mudstone are the most decisive parameters in design and stability assessment of any surface and underground engineering structures (Yasar et al., 2010; Zhang et al., 2017; Sakiz, 2022). Determination of these characteristics is complicated, difficult and time consuming as well as require a great accuracy in sample preparation and testing procedure (Armaghani et al., 2014; Zhang, 2016).

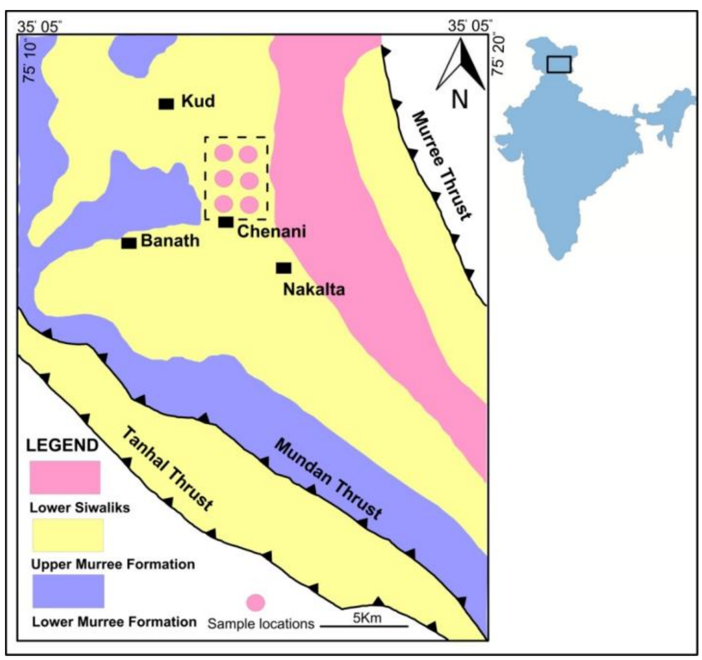

Fig. 1. The geological and structural map of the study area displays the distribution of Murree rocks (after Khan et al., 1971; Karunakaran and Ranga Rao, 1979)

To deduce the strength and class of rocks in a non-destructive and economical manner, the petrographic analysis of rocks can be significant during preliminary studies. Due to different cementation and diagenesis, geomechanical properties of sandstone and siltstone widely vary.

The variation in geomechanical properties like compressive strength, elastic modulus, shear modulus, bulk modulus and poisson's ratio have great impact on the petrographic characteristics (Bell,1978; Shakoor and Bonelli, 1991; Shahsavari and Shakiba, 2022). The petrographic characteristics of a rock are not only controlled by internal factors like environment of deposition, burial conditions, mineralogical composition, microstructure, texture, nature of grain contacts and diagenesis but also impacted by external factors like surrounding geological conditions and regional tectonic setting (Meng et al., 2006; Ulmer et al., 2014). The impact of mechanical properties on petrographic parameters of sandstone suggest a bivariant relation between strength characteristics and packing density (PD) which has no significant relationship with mineralogical composition (Bell, 1978; Tamrakar et al., 2007). Howarth and Rowlands (1986) suggested packing density in sandstone has been found to have moderate relation with several mechanical properties. Fahy and Guccione (1979) revealed that in case of calcareous sandstone, as the mean and median of grains as well as quartz content increases, the value of unconfined compressive strength (UCS) decreases. On the other hand, with increase in carbonate content and straight grain contact the value of UCS increases significantly (Fahy and Guccione, 1979). The study carried out by Doberenier and De Freitas (1986) concluded that usually the weak sandstones have low packing density and with decrease in the grain size and increase in grain contacts, the mechanical strength increases. Shakoor and Bonelli (1991) revealed that the sandstones with grain to void ratio, straight contact and grain to matrix ratio have low mechanical strength whereas, those with high density low absorption and higher values for suture contact have higher strength and Young's modulus values. Nevertheless, the textural parameters i.e. grain contacts are decisive than mineralogical composition in determining engineering parameters of sandstone (Ulusay et al., 1994). Sandstones with high percentage of angular grains and sutured contacts have relatively high strength whereas, the sandstones with significant grain to grain contacts and higher value of packing proximity, display low poisson's ratio and high young's modulus (Ulusay et al., 1994). On the contrary, point, straight, and concavo-convex grain contacts are not significant to decipher mechanical properties of sandstones (Ulusay et al., 1994). The objective of this study is to analyze the sandstones of the Upper Murree Formation to observe the relationship between petrographic characteristics and physical engineering index properties.

STUDY AREA

The Murree Formation represents Miocene molasse deposits consists of alternating beds of sandstone, siltstone, conglomerate and calcrete, deposited in tidal-fluvial dominated microtidal estuarine environment in the foredeep basin (Gansser, 1964; Singh and Singh, 1995; Singh, 2000). In the north-south traverse, these sediments are exposed for about 50 km along the Jammu-Srinagar national highway (NH-44) and for hundreds of kilometres in the southeast-northwest direction. The sandstones in the Murree Group are planar bedded, cross bedded, cross laminated and rippled, the siltstone is laminated and the conglomerates comprises of muddy pebbles (Singh, 2000). The Murree Group is sub-divided into Lower Murree and Upper Murree Formations (Wynn, 1874). Generally, lithology of Lower Murree is argillaceous whereas, the Upper Murree Formation is of arenaceous nature (Wadia, 1926, 1931). The rock sequence in the Upper Murree Formation consists of light gray, fine to medium grained, thick sandstones and brick red claystone whereas, the Lower Murrees are composed of cross-laminated, cross bedded and rippled sandstone, siltstone, conglomerate and calcrete (Karunakaran and Rao, 1979). A preliminary investigation has been carried out in Upper Murree Formation to understand the relationship among mineral composition, petrography characteristics and petrophysical properties for which six sandstone samples were collected from the study area.

MATERIAL AND METHODS

The fresh samples were collected from Upper Murree Formation (Fig. 1). Two thin sections (one horizontal and one vertical) were prepared and studied under Leica high power petrological microscope. Framework grains varying from 300 to 350 per thin section were counted. Point-counting was carried out to identify individual grains using the Gazzi-Dickinson method (Dickinson, 1970; Ingersoll *et al.*, 1984). The photomicrographs of each thin section were taken under 5X and 10X magnifications. The geomechanical properties of individual samples have been discussed following the standard methods of engineering classifications of rocks by Goodman's engineering classification (1989), classification of mineral size by Core Logging Committee (1978), classification of weathering/alteration of rocks by

RESULTS

PETROGRAPHIC AND PETROPHYSICAL ANALYSIS

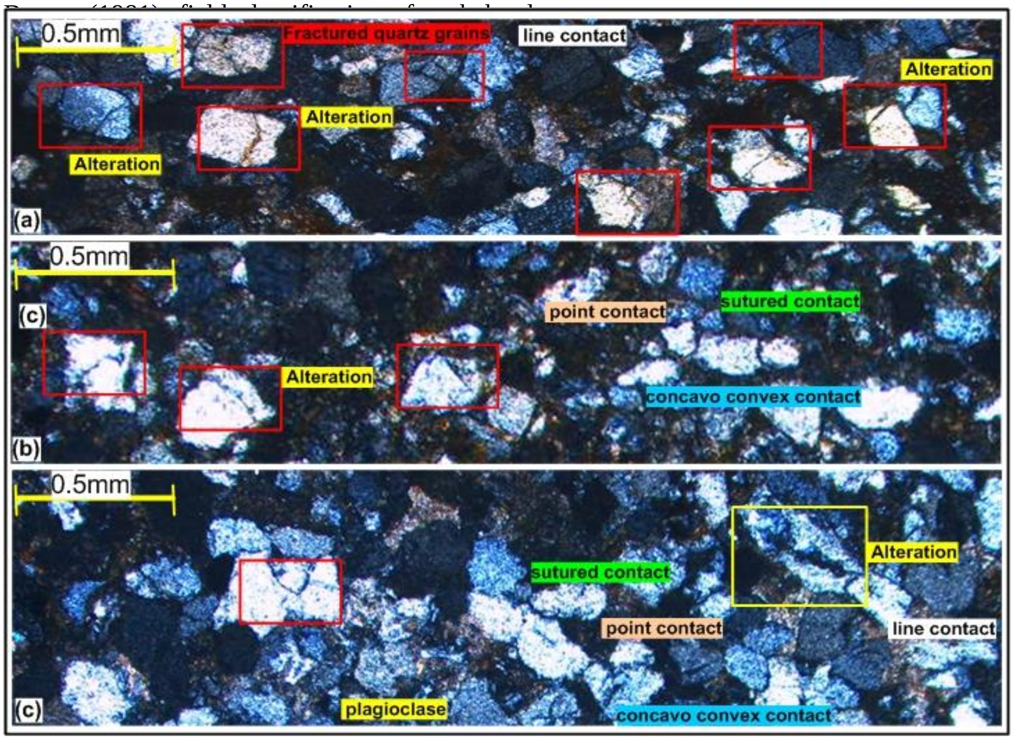

Fig. 2. Photomicrographs of the thin sections showing mineral components, microstructures, grain contacts and secondary alteration/ filling in the fractures (a) UM1 (b) UM2 (c) UM3.

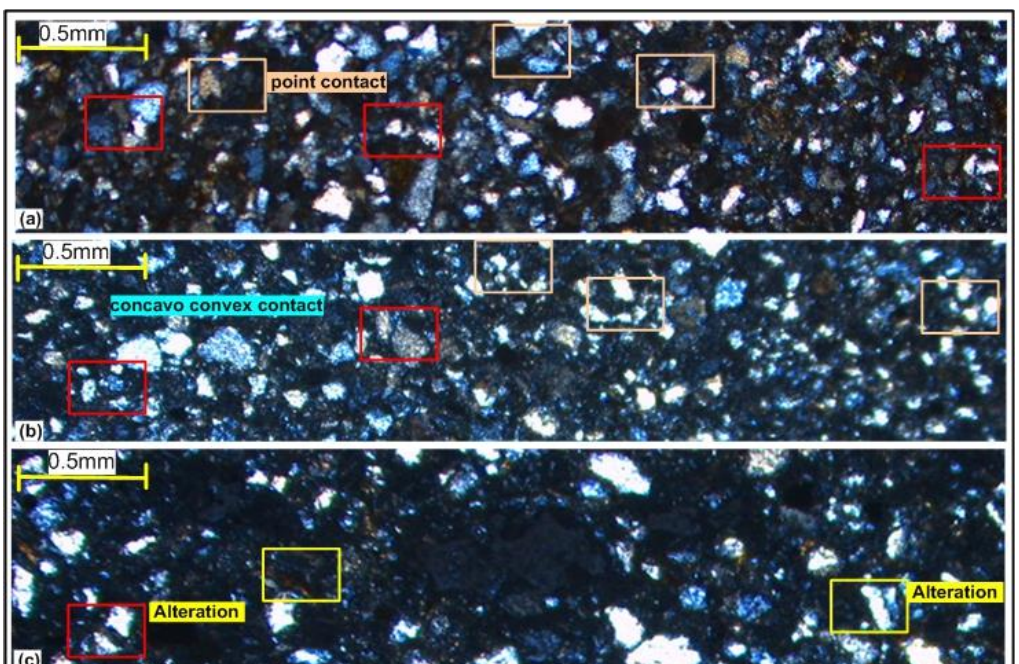

Fig. 3. Photomicrographs of the thin sections showing mineral constituents, microstructures, grain contacts and secondary alteration/ filling in the fractures (a) UM4 (b) UM5, and (c) UM6.

The modal composition and textural properties are the most important parameters that determine the maturity of sandstones. The petrographic analysis of the sandstone samples collected from the Upper Murree Formation has been carried out to estimate the model composition, textural properties, nature of matrix, fractures in the grains, and alteration or filling in the fractured grains. Thin sections of six fresh sandstone samples labelled as UM1, UM2, UM3, UM4, UM5, UM6 were analysed. The examination of thin sections revealed that the sandstones examined range in grain size from fine (UM5) to medium (UM4, UM6) and coarse grain (UM1, UM2, UM3) comprising of sub-rounded, angular to sub-angular in nature (Figs. 2 & 3). The major mineralogical constituents of all of the samples include quartz, feldspar and lithic fragments embedded

Table 1. The percentages of individual minerals identified in thin sections

Sample Constituents/Mineralogy	**UM1**	**UM2**	**UM3**	**UM4**	**UM5**	**UM6**
Quartz	65	55	70	50	62	60
Feldspar	05	04	04	05	04	05
Mica	06	06	07	07	06	08
Matrix + Cement +Clay Minerals (Smectite)	12	15	10	18	12	10
Heavy Minerals	02	02	-	-	01	-
Rock Fragments/Detrital grains	05	06	05	15	08	05
Calcite	-	-	-	-	-	-
Opaque minerals	05	12	09	05	07	12

in matrix constitutes significant proportion of the samples (10-18%). The matrix comprises of dominantly the clay minerals which are altered to montmorillonite and smectite. Mica, opaque and heavy minerals constitute the minor fraction of all the samples (Figs. 2 & 3). Quartz grains in the studied samples are monocrystalline, having undulose extinction as well polycrystalline (Figs. 2 & 3). The monocrystalline quartz grains are fractured and are filled with secondary minerals (Fig. 2a-c). The samples dominantly show aggrading neomorphism into large crystals (Fig. 3a-c). Matrix consists of very fine material, which is present within interstitial spaces between the framework grains showing variability in the packing density and packing proximity (Fig. 3c). The rock forming minerals include quartz, feldspar and rock fragments which are angular, sub-angular to sub-rounded (Fig. 2a-c). In addition, clay minerals and accessory minerals including minor amount of mica, chlorite and heavy minerals are also present (Figs. 2 & 3). The detrital fraction of the studied samples contains 40-65% quartz, 4-5% feldspars (microcline and plagioclase), lithic fragments vary between 5-10%, matrix between 10-18%, 6-8% mica and 5-12% opaque minerals (pyrite, magnetite) (Table 1). The samples show alteration of feldspar to kaolinite and fractures in quartz gains are filled with clay minerals (Fig. 2a-c). The mineralogical maturity of sandstones is determined by their quartz to feldspar ratios (Pettijohn et al., 1987). According to Prothero et al. (2004), sandstone is texturally immature if the proportion of clay size material (matrix) exceeds 50%, irrespective of the degree of sorting and roundness. Although the abundance of quartz is generally greater than other framework elements, the presence of appreciable amounts of feldspars and considerable quantity of rock fragments makes these rocks mineralogically sub mature (Table 1). Mineralogical and tectonic classifications of sandstone of Murrees were described following Folk (1974) and Dickinson, & Suczek (1979) as litharenites to sub-litharenites (Singh, 2000; Jamwal et al., 2020). The rock fragments are mostly clasts of carbonate; siltstones and shale constitute 5-10% of the samples. Quartz grains in Murree sandstone have the origin from plutonic rock (felsic in origin), older sandstones that have been recycled and also from metamorphic rocks (Saleem et al., 2018; Jamwal et al., 2020).

Five types of grain to grain contacts were observed in the thin sections. These are floating, concavo-convex, suture contact, point contact and long contact (Figs. 2 & 3). The long contact is dominating followed by concavo-convex, point contacts and suture contacts (Figs. 2 & 3). The point contacts and floating contacts of grains can be attributed to the packing during depositional process, the line contact is due to diagenesis whereas, the concavo-convex and sutured contacts may be due to notable confining and directed stresses as well as the growth of cement (Taylor, 1950). The quartz grains are fractured suggesting confining stress as well as directed stress due to the post depositional tectonic deformation as a consequence of continued India-Asia plate convergence process. The petrophysical properties of the sandstone analyzed include types and condition of porosity. The rock strength is a petrophysical property that can be deduced from the mineral composition, type of porosity and presence

Table 2: Classification of rocks samples on the basis of Petrography

Classification of mineral size (from Core Logging Committee (1978)	Fine grained (0.06 - 0.2 mm)	Medium grained (0.2 – 0.6mm)	Coarse grained (0.6 – 2.0mm)	Very Coarse Grained >2.0mm			
	UM5	UM2, UM6	UM1, UM2, and UM3				
Goodman's engineering classification of rocks (from Goodman, 1989)	Stably cemented	With slightly soluble cement	With highly soluble cement	Incompletely or weakly cemented	Un cemented		
	UM1, UM2, UM3, UM4, UM5, and UM6	-	-	-	-		
Classification of weathering/alteration is as follows: Brown (1981)	Unweathered /unaltered	Slightly weathered /altered	Medium weathered/altered	Highly weathered/ altered	Completely weathered/altered		
	UM4, UM5, and UM6	UM1, UM2, and UM3	-	-	-		
Field classification of rock hardness (Singh and Elkington, 1983)	Very soft rock (1-3 MPa)	Soft rock (3 - 10 MPa)	Medium hard rock (10 - 25 MPa)	Hard rock (25-70 MPa)	Very soft rock (1-3 MPa)	Soft rock (3 - 10 MPa)	
			UM2, UM5, and UM6,	UM1, UM3, UM4			
Classification of rock strength used by Bieniawski (1989) Intact rock strength (MPa)	extremely low (<1)	very low (1-5)	low (5-25)	moderate (25-50)	medium (50-100)	High (100-250)	Very High >250
Point load strength	-	-	-	1 - 2	2 - 4	4 - 10	> 10
	-				UM1, UM2, UM3, UM4, UM5, and UM6	-	-

of fractures in the grains. The average values of porosity of the Murree sandstone is 9.6% (Existing Optical Porosity) and 32.6% (Minus Cement Porosity) (Jamwal et al., 2020). The analysed samples show intergranular i.e. primary porosity, secondary porosity and fractured porosity (Fig. 2a-c). In all of the thin sections, the void space between the quartz grains constitutes primary porosity and is attributed to depositional processes which are having least effective porosity. The fracture porosity is dominant in the samples UM1, UM2 and UM3 and least in the sample UM6. Porosity and compressive strength are interrelated due to the fact that the strongly compact sandstone shows least porosity whereas, the weakly compact sandstone shows the highest porosity. Thus, the weakly cemented rock samples are showing low compaction and thus low porosity.

GEO-MECHANICAL PROPERTIES

The geomechanical properties of the rocks depend on the modal composition, texture, density, porosity, porewater, confining pressure, weathering and alteration, bedding plane, and joint properties (Vutukuri et al., 1978). The process of weathering is by means of either mechanical, chemical or biological action or combination of these which drastically affects the engineering properties of both the rock material and the rock mass. Some of the very important effects of weathering/alteration on rocks are the decrease in strength, density and volumetric stability and increase in deformability, porosity and weatherability. Since the rock or soil responds to different stimuli like loading-unloading, temperature disturbance, and flow of fluid, therefore, the geoengineers are mostly interested to know how beneficially the response of these materials can be controlled or modified. It is evident that in each case of construction, the geoengineer needs to know different properties of material like strength properties, volume change, fluid and gas conductivity and interaction of materials with external factors. The geotechnical property of materials also varies with depositional environment of clastic rocks. The impact of depositional environment on the mechanical properties of clastic rocks can be determined by examining the detrital quartz content (Meng et al., 2006). The textural characteristics of the sandstone/siltstone are more significant than mineralogical composition due to the fact that the mineralogical composition is independent of porosity (Heidari et al., 2013).

The increase in the quartz content and decrease in the matrix content attributed to increase in strength i.e., Uniaxial Compressive Strength (UCS) and point load index parameters (Ktena and Sabatakakis, 2013). The packing among detrital grains of sandstone can be assessed in terms of grain to grain contacts or packing proximity. The floating of detritus through cement and matrix and different types of contacts like grain to grain contact (Point, straight, concavo-convex, and sutured contact) have significant impact on the engineering properties of rocks. The nature of contact is an important parameter to determine the conditions during or post deposition. The uniaxial compressive strength of a rock material constitutes the highest strength limit of the rock mass of which it forms a part. It is determined in accordance with the standard laboratory procedures. For the purpose of rock mass classification, the use of well-known point load strength index can be useful as the index that can be determined in the field on rock core retrieved from borings and the core does not require any specimen preparation. Knowing the rock type and rock material hardness, it is possible for the experienced engineer or engineering geologist to make fairly accurate estimates on rock material strength. These can be readily verified by uniaxial compressive strength or point load tests. The samples from Upper Murree Formation show point load strength index values ranging between 2-4 MPa.

DISCUSSION AND CONCLUSIONS

Petrographic analysis of the sandstone samples of the Upper Murree Formation was carried out to know the relationship between petrographic characteristics of the samples with the geoengineering properties. The study was conducted to decipher the preliminary geomechanical properties of sandstones using petrographic analysis. This type of study is being carried out during the initial stage of any major construction project like tunnels, underground excavations, building material, road construction, railway track, etc. The thin sections were studied to know the mineral composition in terms of volume percentage, texture, fabrics and microstructures particularly focussing on the contacts of grains, fractures in the grains, infilling of fractures, alteration and matrix. The results show a wide range of textures covering fine-medium-coarse fractions (UM5-fine grained; UM4 & UM6-medium grained; UM1, UM2 & UM3-coarse grained), stably cemented (UM1, UM2, UM3, UM4, UM5, and UM6), unweathered (UM1, UM2, UM3, UM4, UM5, and UM6), two types rock hardness: medium hard rock (UM2, UM5, and UM6) and hard rock (UM1, UM3, and UM4) and having medium intact rock strength (UM1, UM2, UM3, UM4, UM5, and UM6).

The quartz grains in the studied samples are monocrystalline and polycrystalline displaying undulose extinction. The monocrystalline quartz grains are fractured and are filled with secondary minerals. The detrital fraction of the studied samples includes 40-65% quartz, 4-5% feldspars (microcline and plagioclase), lithic fragments between 5 and 10%, matrix between 10 and 18%, 6-8% mica and 5-12% opaque minerals (pyrite, magnetite). The samples show alteration of feldspar and clay minerals filled in the fractures of quartz grains but no significant relationship exists between the alteration and strength of rock. The samples of the Upper Murree sandstone have almost similar characteristics due to similar source, depositional environment, provenance, texture, weathering index, diagenetic characteristics regional and local stress conditions. This study reveals significant relationship that exist between the textures of rocks (syndepositional, diagenetic and post diagenetic) and engineering properties of the rocks (point load, strength, rock hardness and rock class). The petrographic analysis of samples from different litho-units of the Upper Murree i.e. mudstone, sandstone, siltstone can be useful to establish the relationship with geomechanical properties.

REFERENCES

Armaghani, D. J., Hajihassani, M., Bejarbaneh, B. Y., Marto, A., & Mohamad, E. T. (2014). Indirect measure of shale shear strength parameters by means of rock index tests through an optimized artificial neural network. *Measurement*, *55*, 487-498.

Bell, F. G. (1978). Petrographical factors relating to porosity and permeability in the Fell Sandstone. Quarterly journal of Engineering Geology and Hydrogeology, 11(2), 113-126.

Bell, F. G., & Culshaw, M. G. (1998). Petrographic and engineering properties of sandstones from the Sneinton Formation, Nottinghamshire, England. *Quarterly Journal of Engineering Geology*, *31*(1), 5-19.

Bell, F. G., & Lindsay, P. (1999). The petrographic and geomechanical properties of some sandstones from the Newspaper Member of the Natal Group near Durban, South Africa. Engineering geology, 53(1), 57-81.

Bieniawski, Z. T. (1989). Engineering rock mass classifications: a complete manual for engineers and geologists in mining, civil, and petroleum engineering. John Wiley & Sons.

Bieniawski, Z. T. (1989). Engineering rock mass classifications: a complete manual for engineers and geologists in mining, civil, and petroleum engineering. John Wiley & Sons.

DeReuil, A. A., Birgenheier, L. P., & McLennan, J. (2019). Effects of anisotropy and saturation on geomechanicalbehavior of mudstone. Journal of Geophysical Research: Solid Earth, 124(8), 8101-8126.

Dickinson, W. R., & Suczek, C. A. (1979). Plate tectonics and sandstone compositions. Aapg Bulletin, 63(12), 2164-2182.

Dickinson, W.R. (1970). Interpreting detrital modes of graywacke and arkose. J. Sediment. Petrol. 40, 695–707.

Dobereiner, L., & Freitas, M. D. (1986). Geotechnical properties of weak sandstones. Geotechnique, 36(1), 79-94.

Fahy, M. P., & Guccione, M. J. (1979). Estimating strength of sandstone using petrographic thin-section data. Bulletin of the Association of Engineering Geologists, 16(4), 467-485.

Folk, R. L.(1974) Petrology of Sedimentary Rocks: Austin, TX, Hemphill Press, second edition, 182 p.

Gansser, A. (1964). Geology of the Himalayas.

Goodman, R. E. (1989). Introduction to rock mechanics. John Wiley & Sons.

Howarth D.F, Rowlands J.C (1986) Development of an index to quantify rock texture for qualitative assessment of intact rockproperties. Geotech Testing J 9:169–179

Ingersoll, R. V., Bullard, T. F., Ford, R. L., Grimm, J. P., Pickle, J. D., &Sares, S. W. (1984). The effect of grain size on detrital modes: a test of the Gazzi-Dickinson point-counting method. Journal of Sedimentary Research, 54(1), 103-116.

ISRM. 1981. Rock characterization, testing and monitoring – ISRM suggested methods. In Brown E.T. (ed), International Society of Rock Mechanics, Pergamon, Oxford.

Jamwal, M., Pandita, S. K., Sharma, M., & Bhat, G. M. (2020). Petrography, provenance and diagenesis of Murree Group of rocks exposed along Basohli–Bani road, Kathua, Jammu. Journal Indian Association of Sedimentologists, 37, 15-26.

Karunakaran. C. and Ranga Rao, A. (1979). Status of exploration for hydrocarbons in the Himalayan Region. Him. Geol. Sem., New Delhi 1976, Geol. Sur. India, Misc. Publ.v.41 (V). pp. I-66.

Khan, A., Raghavendra Rao, V., Ganju, J. L., & Sankaran, R. V. (1971). Discovery of invertebrate and vertebrate fossils from Upper Murree Formation of Palkhai Syncline near Udhampur, Jammu and Kashmir State, India. *Journal of the Paleontological Society of India*, *16*, 16-20.

Ktena S. T and Sabatakakis, N. (2013). Correlation between mechanical and petrographic parameters of sandstones. Bulletin of the Geological Society of Greece, 47(4), 1726-1730.

Meng, Z., Zhang, J., & Peng, S. (2006). Influence of sedimentary environments on mechanical properties of clastic rocks. Environmental geology, 51, 113-120.

Mughal, M. S., Zhang, C., Du, D., Zhang, L., Mustafa, S., Hameed, F., ... & Blaise, D.

(2018). Petrography and provenance of the Early Miocene Murree Formation, Himalayan Foreland Basin, Muzaffarabad, Pakistan. Journal of Asian Earth Sciences, 162, 25-40.

Sakız, U. (2022). Predicting the brittleness of sandstones from the Leeb hardness test. *Petroleum Science and Technology*, 1-25.

Shahsavari, M. H., & Shakiba, M. (2022). An experimental insight into the influence of sand grain size distribution on the petrophysical and geomechanical properties of artificially made sandstones. *Journal of Petroleum Science and Engineering*, *215*, 110632.

Shakoor, A., & Bonelli, R. E. (1991). Relationship between petrographic characteristics, engineering index properties, and mechanical properties of selected sandstones. *Bulletin of the Association of Engineering Geologists*, *28*(1), 55-71.

Singh, B. P. (2000). Sediment dispersal pattern in the Murree Group of the Jammu area, NW Himalaya, India. Himalayan Geology, 21, 189-200.

Singh, B. P., & Singh, H. (1995). Evidence of tidal influence in the Murree Group of rocks of the Jammu Himalaya, India. Tidal signatures in modern and ancient sediments, 343-351.

Singh, R., Hassani, F. P., & Elkington, P. A. S. (1983). The application of strength and deformation index testing to the stability assessment of coal measures excavations. In The 24th US Symposium on Rock Mechanics (USRMS). One Petro.

Tamrakar, N. K., Yokota, S., & Shrestha, S. D. (2007). Relationships among mechanical, physical and petrographic properties of Siwalik sandstones, Central Nepal Sub-Himalayas. *Engineering Geology*, *90*(3-4), 105-123.

Taylor, J. M. (1950). Pore-space reduction in sandstones. AAPG bulletin, 34(4), 701-716.

Ulmer-Scholle, D. S., Scholle, P. A., Schieber, J., & Raine, R. J. (2014). *A color guide to the petrography of sandstones, siltstones, shales and associated rocks* (Vol. 109). Tulsa, OK, USA: American Association of Petroleum Geologists.

Ulusay, R., Türeli, K., & Ider, M. H. (1994). Prediction of engineering properties of a selected litharenite sandstone from its petrographic characteristics using correlation and multivariate statistical techniques. Engineering Geology, 38(1-2), 135-157.

Vutukuri V. S., Lama R. D. (1978). Handbook on Mechanical Properties of Rock, Clausthal, Trans Tech Publications, vol. 2.

Wadia, D. N. (1928). Geology of India, London, 1926. The geology of Poonch State (Kashmir) and adjacent portions of the Punjab: India Geol. Survey Mem, 51, 185-370.

Wadia, D. N. (1931). The syntaxis of the northwest Himalaya: its rocks, tectonics and orogeny. Rec. Geol. Surv. India, 65(2), 189-220.

Wynne, A. B. (1874). Observations on some features in the physical geology of the Outer Himalayan Region of the Upper Punjâb, India. Quarterly Journal of the Geological Society, 30(1-4), 61-80.

Yaşar, E., Ranjith, P. G., & Perera, M. S. A. (2010). Physico-mechanical behaviour of southeastern Melbourne sedimentary rocks. *International Journal of Rock Mechanics and Mining Sciences*, *47*(3), 481-487.

Zhang, H., Adoko, A. C., Meng, Z., Wang, H., & Jiao, Y. (2017). Mechanism of the mudstone tunnel failures induced by expansive clay minerals. *Geotechnical and Geological Engineering*, *35*, 263-275.

Zhang, L. (2016). *Engineering properties of rocks*. Butterworth-Heinemann.

Received on : 09th June 2023
Revised accepted on : 16th June 2023